SECURITY CLASSIFICATION OF THIS PAGE

FILE COPY

UNCLASSIFIED

REPORT DOCUMENTATION PAGE

AD-A225 762

DTIC ELECTE AUG 27 1990

1a. REPORT SECURITY CLASSIFICATION	1b. RESTRICTIVE MARKINGS
	3. DISTRIBUTION/AVAILABILITY OF REPORT Approved for public release; distribution unlimited.
4. PERFORMING ORGANIZATION REPORT NUMBER(S)	5. MONITORING ORGANIZATION REPORT NUMBER(S) AFOSR-TR- 90 0872
6a. NAME OF PERFORMING ORGANIZATION Jacek Lagowski	6b. OFFICE SYMBOL (If applicable)
7a. NAME OF MONITORING ORGANIZATION Air Force Office of Scientific Research	
6c. ADDRESS (City, State, and ZIP Code) Massachusetts Institute of Technology 77 Massaschusette Ave. Cambridge, MA 02139	7b. ADDRESS (City, State, and ZIP Code) Bolling Air Force Base, DC 20332-6448
8a. NAME OF FUNDING/SPONSORING ORGANIZATION AFOSR	8b. OFFICE SYMBOL (If applicable) NE
9. PROCUREMENT INSTRUMENT IDENTIFICATION NUMBER AFOSR-86-0342	
8c. ADDRESS (City, State, and ZIP Code) AFOSR/NE Bldg. 410 Bolling AFB, DC 20332	10. SOURCE OF FUNDING NUMBERS PROGRAM ELEMENT NO: 61102F; PROJECT NO: 2306; TASK NO: B1; WORK UNIT ACCESSION NO:

11. TITLE (Include Security Classification)
Investigation of New Semiinsulating Behavior of III-V Compounds

12. PERSONAL AUTHOR(S)
Dr. Jacek Lagowski

13a. TYPE OF REPORT	13b. TIME COVERED	14. DATE OF REPORT (Year, Month, Day)	15. PAGE COUNT
Final	FROM 8/16/88 TO 2/23/90		

16. SUPPLEMENTARY NOTATION

17. COSATI CODES			18. SUBJECT TERMS (Continue on reverse if necessary and identify by block number)
FIELD	GROUP	SUB-GROUP	

19. ABSTRACT (Continue on reverse if necessary and identify by block number)

Our investigation of defect interactions and properties related to semiinsulating behavior of III-V semiconductors resulted in about twenty original publications, six doctoral thesis, one masters thesis and numerous conference presentations.

The studies of new compensation mechanisms involving transition metal impurities have defined direct effects associated with deep donor/acceptor levels acting as compensating centers. Electrical and optical properties of vanadium and titanium levels were determined in GaAs, InP and also in ternary compounds InGaAs. The experimental data provided basis for the verification of chemical trends and the VRBE method. They also defined compositional range for III-V mixed crystals whereby semiinsulating behavior can be achieved using transition elements deep levels and a suitable codoping with shallow donor/acceptor impurities.

20. DISTRIBUTION/AVAILABILITY OF ABSTRACT ☑ UNCLASSIFIED/UNLIMITED ☐ SAME AS RPT ☐ DTIC USERS	21. ABSTRACT SECURITY CLASSIFICATION UNCLASSIFIED
22a. NAME OF RESPONSIBLE INDIVIDUAL Alan Pontinen	22b. TELEPHONE (Include Area Code) 202-767-4931
	22c. OFFICE SYMBOL NE

DD FORM 1473, 84 MAR 83 APR edition may be used until exhausted
All other editions are obsolete

SECURITY CLASSIFICATION OF THIS PAGE

Our discovery of the indirect effect of V-doping on semiinsulating property of GaAs has clarified the long standing controversy on the role of V. Our study showed that vanadium is

capable of gettering donor impurities in the crystal growth melts. Its role is therefore similar to that of oxygen which is known to reduce the concentration of Si donors in melt grown GaAs crystals.

In order to resolve the question of oxygen related electronic centers in GaAs we have prepared a series of crystals intentionally doped with the low natural abundance oxygen 18 isotope. This enhanced a detection of oxygen by SIMS and also facilitated the unique identification of the infrared local vibration mode spectrum of oxygen based on the isotope shift. This work was realized in collaboration with IR Spectroscopic Groups in the Fraunhofer Institut and in the J.J.Thomson Phys.Lab.

Our investigation of native defects introduced by excessive stress and nonstoichiometry has shown that the midgap donor EL2 is not formed during plastic deformation of GaAs up to 3% i.e. within the range typical for the crystal growth from the melt. On the other hand we established that the EL2 defect is formed during postsolidification cooling of the crystal in the temperature zone 1100 C to 700 C. We have also studied the stoichiometry dependance of native acceptors. Empirical data on EL2 and acceptor formation were used in a quantitative compensation model which successfully explained resistivity dependance of SI GaAs on the melt stoichiometry and the cooling rate of the grown ingot.

Reprints of selected publications are enclosed with the final report.

FINAL TECHNICAL REPORT

to

Air Force Office of Scientific Research
Bolling Air Force Base, D.C. 20332

on

INVESTIGATION OF NEW SEMIINSULATING BEHAVIOR OF III-V COMPOUNDS

(AFOSR-86-0342)

For Period

August 16, 1986 to February 28, 1990

Submitted by

Dr. Jacek Lagowski
Department of Materials Science and Engineering*
Massachusetts Institute of Technology
Cambridge, Massachusetts 02139

* Present Address: Center for Microelectronics Research, College of Engineering, University of South Florida, Tampa, Florida 33620-5350

SUMMARY

Our investigation of defect interactions and properties related to semiinsulating behavior of III-V semiconductors resulted in about twenty original publications, six doctoral thesis, one masters thesis and numerous conference presentations.

The studies of new compensation mechanisms involving transition metal impurities have defined direct effects associated with deep donor/acceptor levels acting as compensating centers. Electrical and optical properties of vanadium and titanium levels were determined in GaAs, InP and also in ternary compounds InGaAs. The experimental data provided basis for the verification of chemical trends and the VRBE method. They also defined compositional range for III-V mixed crystals whereby semiinsulating behavior can be achieved using transition elements deep levels and a suitable codoping with shallow donor/acceptor impurities.

Our discovery of the indirect effect of V-doping on semiinsulating property of GaAs has clarified the long standing controversy on the role of V. Our study showed that vanadium is capable of gettering donor impurities in the crystal growth melts. Its role is therefore similar to that of oxygen which is known to reduce the concentration of Si donors in melt grown GaAs crystals.

In order to resolve the question of oxygen related electronic centers in GaAs we have prepared a series of crystals intentionally doped with the low natural abundance oxygen 18 isotope. This enhanced a detection of oxygen by SIMS and also facilitated the unique identification of the infrared local vibration mode spectrum of oxygen based on the isotope shift. This work was realized in collaboration with IR Spectroscopic Groups in the Fraunhofer Institute and in the J.J.Thornson Phys.Lab.

Our investigation of native defects introduced by excessive stress and nonstoichiometry has shown that the midgap donor EL2 is not formed during plastic deformation of GaAs up to 3% i.e. within the range typical for the crystal growth from the melt. On the other hand we established that the EL2 defect is formed during postsolidification cooling of the crystal in the temperature zone 1100 C to 700 C. We have also studied the stoichiometry dependance of native acceptors. Empirical data on EL2 and

acceptor formation were used in a quantitative compensation model which successfully explained resistivity dependance of SI GaAs on the melt stoichiometry and the cooling rate of the grown ingot.

Reprints of selected publications are enclosed with the final report.

Thesis Supported by the AFOSR Grant

Doctoral Thesis:

1. Charles D. Brandt, "A Study of Energy Levels Introduced by 3rd Transition Elements in II-V Compound Semiconductors", Ph.D. Thesis, MIT, 1987.

2. Der-Gao Lin, "Effects of Doping on the Defect Structure and Electronic Properties of GaAs", Ph.D. Thesis, MIT, 1987.

3. Leszek M. Pawlowicz, "Studies of Point Defect Control in LEC Growth of GaAs", Ph.D. Thesis, MIT, 1987.

4. Chan H. Kang, "Surface Morphology and Defect Interactions Upon Heat Treatment of GaAs", Ph.D. Thesis, MIT, 1988.

5. Kyung Hyun Ko, "Engineering of Defects in LEC GaAs by Nonstoichiometric Growth", Ph.D. Thesis, MIT, 1988.

6. Kei-Yu Ko, "Impurity Gettering by Transition Elements in GaAs; Growth of Semi-Insulating GaAs Crystals", Ph.D. Thesis, MIT, 1988.

Master's Thesis:

7. Ann C. Westerheim, "Growth and Characterization of Titanium-Doped GaAs and InGaAs Grown by Liquid Phase Electroepitoxy", M.S., MIT, 1989.

List of Selected Publications Supported by AFOSR Grant

A.M. Hennel, C.D. Brandt, K.Y. Ko, J. Lagowski, and H.C. Gatos, "Optical and electronic properties of vanadium in gallium arsenide", J. Appl. Phys. 62, 163 (1987)

J. Lagowski, M. Bugajski, M. Matsui, and H.C. Gatos, "Optical characterization of semi-insulating GaAs: Determination of the Fermi energy, the concentration of the midgap EL2 level and its occupancy", Appl. Phys. Lett., 51, 511 (1987)

M. Skowronski, J. Lagowski, M. Milshtein, C.H. Kang, F.P. Dabkowski, A. Hennel, and H.C. Gatos, "Effect of plastic deformation on electronic properties of GaAs", J. Appl. Phys. 62, 3791 (1987)

T. Bryskiewicz, M. Bugajski, B. Bryskiewicz, J. Lagowski and H.C. Gatos, "LPEE growth and characterization of $In_{1-X}Ga_XAs$ bulk crystals", Inst. Phys. Conf. Ser. 91, 259 (1988)

M. Bugajski, K.H. Ko, J. Lagowski, and H.C. Gatos, "Native acceptor levels in Ga-rich GaAs", J. Appl. Phys. 65, 596 (1989)

M. Hoinkis, E.R. Weber, W. Walukiewicz, J. Lagowski, M. Matsui, H.C. Gatos, B.K. Meyer and J.M. Spaeth, "Unification of the properties of the EL2 defect in GaAs", Physical Review B, 39, 5538 (1989)

J. Schneider, B. Dischier, H. Seelewind, P.M. Mooney, J. Lagowski, M. Matsui, D.R. Beard and R.C. Newman, "Assessment of oxygen in gallium arsenide by infrared local vibrational mode spectroscopy", Appl. Phys. Lett. 54, 1442 (1989)

K.Y. Ko, J. Lagowski, and H.C. Gatos, "Gettering of donor impurities by V in GaAs and the growth of semi-insulating crystals", J. Appl. Phys. 66, 3309 (1989)

Optical and electronic properties of vanadium in gallium arsenide

A. M. Hennel,[a] C. D. Brandt, K. Y. Ko, J. Lagowski, and H. C. Gatos
Massachusetts Institute of Technology, Cambridge, Massachusetts 02139

(Received 15 January 1987; accepted for publication 10 March 1987)

The effects of vanadium doping on the electrical and optical properties of GaAs were systematically studied in melt-grown crystals prepared by the liquid-encapsulated Czochralski and horizontal Bridgman techniques and in epitaxial crystals prepared by liquid-phase electroepitaxy. By employing deep-level transient spectroscopy, Hall-effect measurements and the $V^{2+}(3d^3)$ and $V^{3+}(3d^2)$ intracenter optical-absorption spectra, one vanadium-related level was identified in all crystals, i.e., the substitutional-vanadium acceptor level (V^{3+}/V^{2+}) at 0.15 ± 0.01 eV below the bottom of the conduction band. From the absorption measurements we conclude that the vanadium (V^{4+}/V^{3+}) donor level must be located within the valence band. Because of its energy position, the above level cannot account for the reported semi-insulating properties of V-doped GaAs. We observed no midgap levels resulting from vanadium-impurity (defect) complexes. The high resistivity reported for certain V-doped GaAs crystals must result from indirect effects of vanadium, such as the gettering of shallow-level impurities.

I. INTRODUCTION

In the last few years several laboratories have reported the successful growth of semi-insulating (SI) V-doped GaAs, emphasizing its potential for improving device-processing characteristics relative to Cr-doped GaAs.[1] SI V-doped GaAs crystals have been grown by liquid-encapsulated Czochralski (LEC),[2–5] vapor-phase epitaxy (VPE),[6] and metallo-organic chemical vapor deposition (MOCVD)[7,8] techniques. The growth of low-resistivity V-doped GaAs crystals by LEC[9,10] and horizontal Bridgman (HB)[5,11] techniques has also been reported. In the above studies the positions of the energy levels tentatively attributed to vanadium range from near the conduction band edge[9–12] to midgap.[2,6,7]

It has also been shown[13,14] that the diffusivity of vanadium in GaAs is about one order of magnitude lower than that of chromium. On the basis of this finding and the report of a level at $E_v + 0.58$ eV in V-doped VPE GaAs,[6] a compensation mechanism for V-doped SI GaAs was proposed.[13,14] These reports also concluded that V-doped SI GaAs would be superior in quality to all other commercially available types of SI GaAs crystals.

In this paper we discuss the effects of vanadium on the properties of GaAs based on the results of studies carried out on a series of V-doped melt- and solution-grown GaAs crystals using different growth and doping conditions. We show that the only vanadium-related level within the GaAs energy gap is an acceptor level at 0.15 eV below the conduction band. Some preliminary results have already been presented.[15–17]

II. EXPERIMENTAL PROCEDURES

Vanadium-doped melt-grown GaAs crystals were prepared by the LEC and HB techniques by using both pyrolytic boron nitride (PBN) and quartz crucibles. Two different types of crucibles were used in order to test the hypothesis that inconsistencies in the reported data resulted from interactions of vanadium with impurities originating in the crucible. (For example, SI LEC GaAs crystals were grown by Wacker-Chemictronic with the use of quartz crucibles.[4,13]) Doping with vanadium at concentrations reaching a level of 3×10^{19} cm^{-3} in the melt was realized by adding ultrapure elemental vanadium (99.9995%) or vanadium pentoxide V_2O_5 (99.995%) to the GaAs melt. The use of V_2O_5 was motivated by the speculation that vanadium-oxygen complexes could be responsible for deep levels in GaAs.[6,7]

Some of the crystals were additionally doped with either shallow donors (Se,Si) or shallow acceptors (Zn) in order to vary the Fermi-level position across the entire band gap.

A key element in this study was the investigation of low-temperature solution-grown *n*-type V-doped crystals prepared by liquid-phase electroepitaxy (LPEE).[18] Without intentional doping, this technique yields electron-trap–free GaAs crystals,[19] providing a unique means for the unambiguous identification of levels introduced by vanadium.

In our investigation we also employed melt-grown inverted thermal conversion (ITC) V-doped GaAs crystals.[20] This new type of GaAs crystal contains virtually no native midgap levels (EL2), allowing the study of V-related optical-absorption spectra without interference from the well-known EL2 absorption.

Hall-effect measurements were conducted by using the standard Van der Pauw configuration. Ohmic contacts were fabricated by using an In/Sn alloy for *n*-type samples and an In/Zn alloy for *p*-type samples. Typically, measurements were carried out at 300 and 77 K. For several samples, carrier concentration as a function of temperature was measured over the range of 170–465 K.

The features of our transient capacitance system pertinent to this study include (a) precise temperature control and monitoring in the range 15–420 K, (b) direct emission-rate measurements over a range 10^{-3}–10^{4} s^{-1} from capacitance relaxation recorded with a signal averager, (c) stan-

[a] On leave from the Institute of Experimental Physics, Warsaw University, Warsaw, Poland.

 0021-8979/87/130163-08$02.40

dard deep-level transient spectroscopy (DLTS) mode operation with the use of a boxcar averager, and (d) optical deep-level spectroscopy (ODLTS) operation with the use of 1.06-μm excitation from a YAG laser. Schottky diodes were fabricated by evaporating Au onto n-type samples and Al onto p-type material.

Optical-absorption measurements were performed at 300, 77, and 5 K on a Cary model 17 spectrophotometer using a helium-gas–flow cryostat. Samples were typically from 0.5 to 1.0 cm thick. All of the absorption measurements performed at 5 K were preceded by a period of white light illumination in order to photoquench the well-known absorption due to EL2. All of the photoconductivity measurements were performed at 77 K on a simple LiF prism-based optical system.

III. EXPERIMENTAL RESULTS AND DISCUSSION

A. Hall-effect measurements

Doping with vanadium increased the resistivity of n-type GaAs and had no effect on the resistivity of p-type crystals. Standard Hall-effect measurements on low-resistivity n-type V-doped GaAs crystals yielded low-temperature free-electron mobility (μ) values that were systematically smaller than those obtained at room temperature. Typical results for crystals with free-electron concentrations (n) equal to a few times 10^{16} cm^{-3} were the following: $\mu = 2800$–3100 cm^2/V s at 77 K and $\mu = 3400$–3700 cm^2/V s at 300 K. These results, indicative of a high degree of ionized impurity scattering at low temperature due to the presence of vanadium, can be tentatively explained by assuming that vanadium acts as an acceptor in this material.

From systematic Hall-effect measurements as a function of temperature between 170 and 465 K, the free-carrier concentration (n) can be plotted as a function of reciprocal temperature, as shown in Fig. 1. From these data the energy (E_A) of a compensating vanadium level was found to be

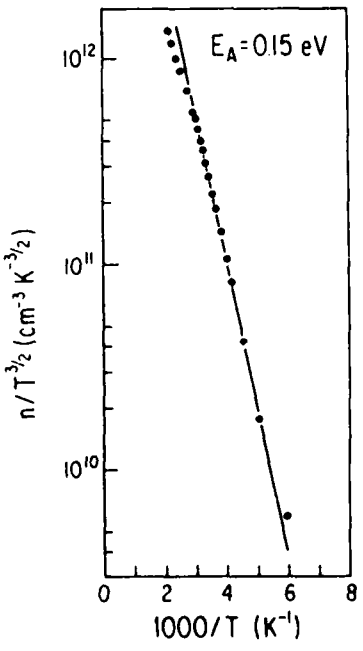

FIG. 1. Activation plot $n/T^{3/2}$ vs $1000/T$ of the free-electron concentration in high-resistivity LEC V-doped n-type GaAs ($N_V > N_D$).

0.15 $\pm$ 0.01 eV below the conduction band.[16] In this analysis we have assumed the Hall-scattering factor (r_n) to be equal to 1.1 ($\pm$ 10%) throughout the measured temperature range.

Further analysis of the Hall data can provide an estimate of the concentration of vanadium centers by using the charge-balance expression given by Look[21]:

$$n + \frac{N_V}{1 + \Phi_{AC}/n} = N_D^+ - N_A^- ,$$

where $\Phi_{AC} = (g_{A0}/g_{A1})N_C' T^{3/2} e^{-E_A/kT}$ is a "modified" density-of-states function, $N_C' = 2(2\pi m_e^* k)^{3/2}/h^3 = 8.1\times 10^{13}$ cm^{-3} K$^{-3/2}$, N_V is the concentration of vanadium-related centers (assumed to be acceptors in this case), g_{A0} (g_{A1}) is the degeneracy of the unoccupied (occupied) state, E_A is the level energy measured from the bottom of the conduction band (a positive value), n is the concentration of free electrons, and N_D^+ and N_A^- are the concentrations of all ionized donors and acceptors (excluding vanadium), respectively. By curve fitting to the $n(T)$ data, the concentration of vanadium-related centers (N_V) can be estimated to be a few times 10^{16} cm^{-3} with an occupation fraction of these centers (N_V^-/N_V) between 0.4 and 0.6 at 200 K. With use of the free-electron mobility values in compensated GaAs calculated by Walukiewicz *et al.*[22,23] for 77 and 300 K, the degree of shallow-donor compensation in these crystals (N_D^+/N_D) falls between 0.5 and 0.8. Combination of these results gives an upper limit for the concentration of vanadium-related acceptors of about 5×10^{16} cm^{-3}.

B. DLTS measurements

DLTS and capacitance transient experiments were performed on low-resistivity GaAs:V,Se crystals where the selenium-donor concentration (N_D) exceeded the concentration of vanadium-related centers. The free-electron concentration in these crystals is weakly dependent on temperature, making it possible to carry out capacitance transient measurements to well below 77 K. Typical DLTS spectra in the range 100–440 K for a reference LEC GaAs:Se crystal, a LEC GaAs:V,Se crystal, a reference HB GaAs:Si crystal, and a HB GaAs:V,Si crystal are shown in Figs. 2(a), 2(b) and Figs. 3(a),3(b), respectively. The dominant midgap level EL2 is clearly visible in all LEC and HB spectra at about 390 K. No other midgap levels could be detected. However, in V-doped crystals a new peak at about 100 K appears, indicating the presence of a new electron trap. In the n-type LPEE GaAs:V crystals this same electron trap is present, as shown in Fig. 2(c). These crystals are electron-trap free without vanadium doping; thus the presence of this new electron trap in this material provides proof that it is related to vanadium.

Capacitance transients caused by electron emission from this trap were measured as a function of temperature in order to obtain values of the activation energy and electron-capture cross section. From the thermal activation plot of the emission rate ($T^2 e_n^{-1}$ vs $1000/T$), which is presented in Fig. 4, we have found[15] an activation energy for this vanadium-related trap of 0.15 $\pm$ 0.01 eV and an electron-capture cross section σ_∞ of about 2×10^{-14} cm^2. We were unable to

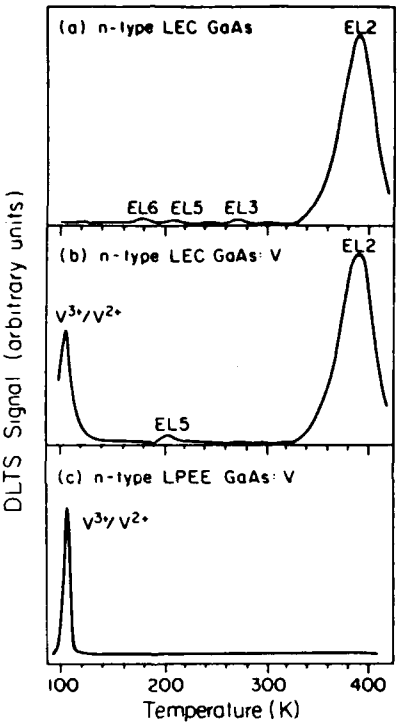

FIG. 2. DLTS spectra of (a) *n*-type LEC GaAs, (b) low-resistivity V-doped LEC GaAs ($N_V < N_D$), and (c) V-doped *n*-type LPEE GaAs. $t_1/t_2 = 5$ ms/10 ms.

measure the temperature dependence of this cross section. However, for the case of Ti-doped GaAs having an acceptor level of $E_c - 0.23$ eV,[24] the activation energy of the electron-capture cross section was found to be smaller than 0.01 eV,

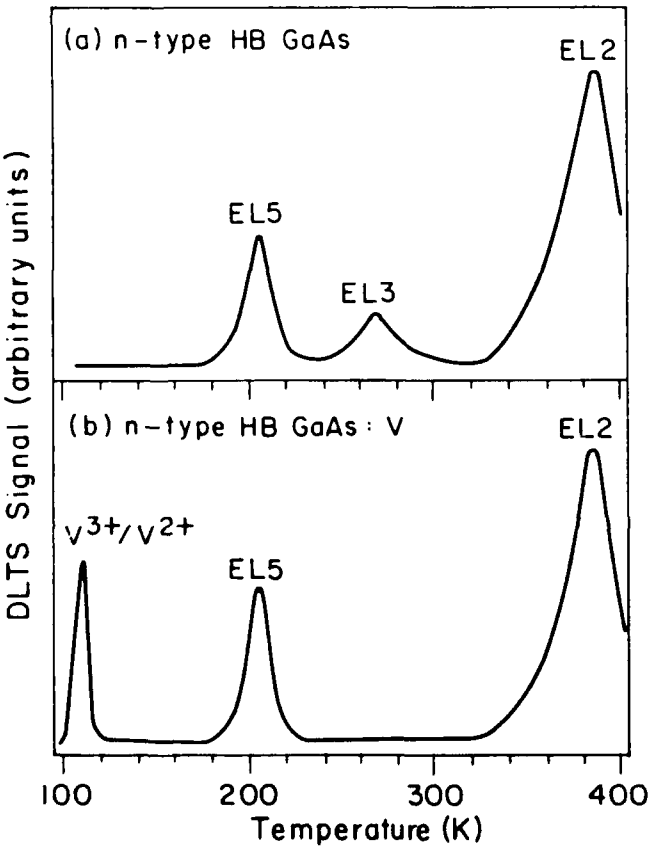

FIG. 3. DLTS spectra of (a) *n*-type HB GaAs and (b) low-resistivity V-doped HB GaAs ($N_V < N_D$). $t_1/t_2 = 5$ ms/10 ms.

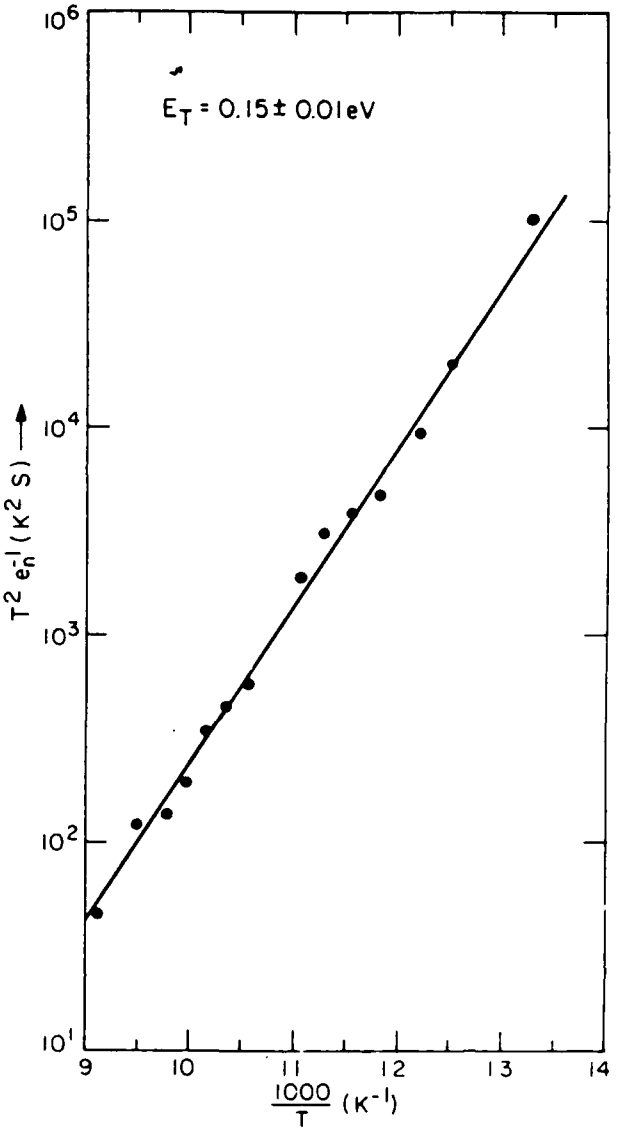

FIG. 4. Emission-rate thermal activation plot $T^2 e_n^{-1}$ vs $1000/T$ for V-related electron trap in LEC GaAs.

i.e., our experimental error. Thus, taking into account the agreement between the DLTS and Hall-effect data concerning the level energy, we can assume that the activation energy for electron capture for vanadium is also negligible.

The concentration of vanadium centers calculated from the DLTS data was found to be approximately 10^{16} cm^{-3}, in agreement with the value obtained from Hall measurements.

DLTS measurements on *p*-type V-doped GaAs did not reveal any hole trap that could be related to vanadium. Typical DLTS spectra in the range 100–440 K for a reference HB GaAs:Zn crystal and a HB GaAs:V,Zn crystal are shown in Figs. 5(a) and 5(b), respectively. In addition, optical DLTS measurements on *n*-type crystals did not show any minority carrier traps that could be related to vanadium.

In view of the results presented thus far, several conclusions regarding the behavior of vanadium in GaAs can be drawn. Regardless of the dopant form (V or V_2O_5), crucible material (SiO_2 or PBN), or growth technique (LEC, HB, or LPEE), vanadium introduces one electron trap into the en-

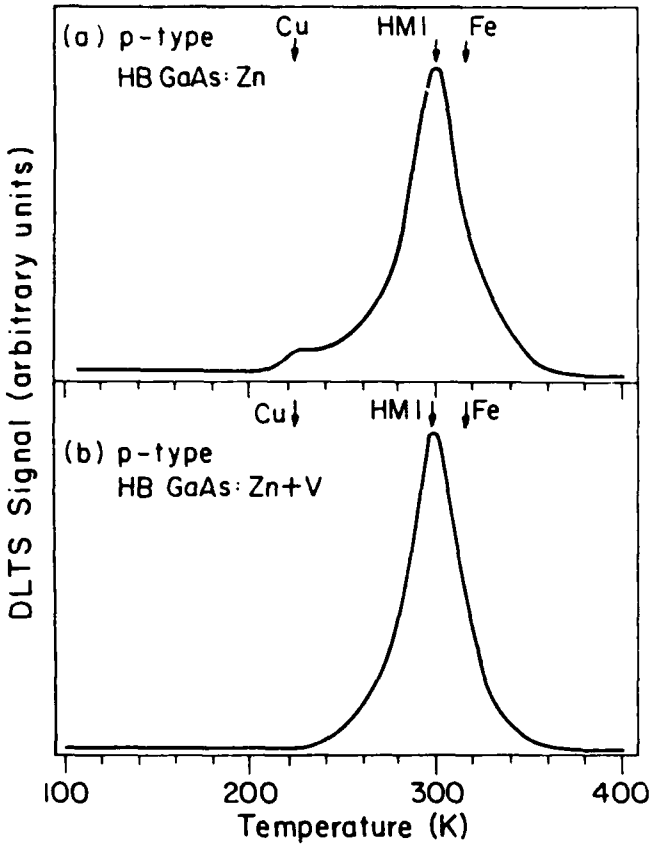

FIG. 5. DLTS spectra of (a) p-type HB GaAs and (b) V-doped HB GaAs. $t_1/t_2 = 5$ ms/10 ms.

ergy gap at 0.15 eV below the bottom of the conduction band. No evidence of any midgap level related to vanadium was found, which directly draws into question the utility of vanadium in producing semi-insulating GaAs. The identification of this 0.15-eV vanadium level as an acceptor will be more fully discussed in the following section.

It should be noted that results obtained in some other laboratories did indicate the presence of a vanadium-related acceptor level in the vicinity of the conduction band edge. Thus Clerjaud *et al.*[12] reported electron traps at $E_c - 0.14$ eV and $E_c - 0.23$ eV from DLTS measurements of HB GaAs:V, while Ulrici *et al.*[10] reported an acceptor level in LEC GaAs:V at $E_c - 0.14$ eV. We think that the levels reported at $E_c - 0.14$ eV are undoubtedly related to vanadium, with the difference between our results and those quoted above lying within the experimental error.

C. Absorption and photoconductivity spectra

Having identified the level at $E_c - 0.15$ eV as being introduced by vanadium, we employed optical measurements to obtain information concerning its microscopic nature.

Optical-absorption measurements were performed on both n- and p-type, V-doped GaAs crystals. In this way, spectra were obtained for Fermi-level positions spanning the entire energy gap. The absorption spectra obtained fell into two primary groups:

(a) For all high-resistivity GaAs:V crystals and p-type GaAs:V, Zn crystals (independent of the zinc-doping level), a characteristic double-peak absorption band was observed between 1.0 and 1.2 eV, preceded at 5 K by a weak zero-phonon line (ZPL) at 1.008 eV and a single absorption line at 0.909 eV. An additional absorption band starting at about 1.35 eV and superimposed on the fundamental absorption edge was also observed. All of these absorption features are shown in Fig. 6(a).

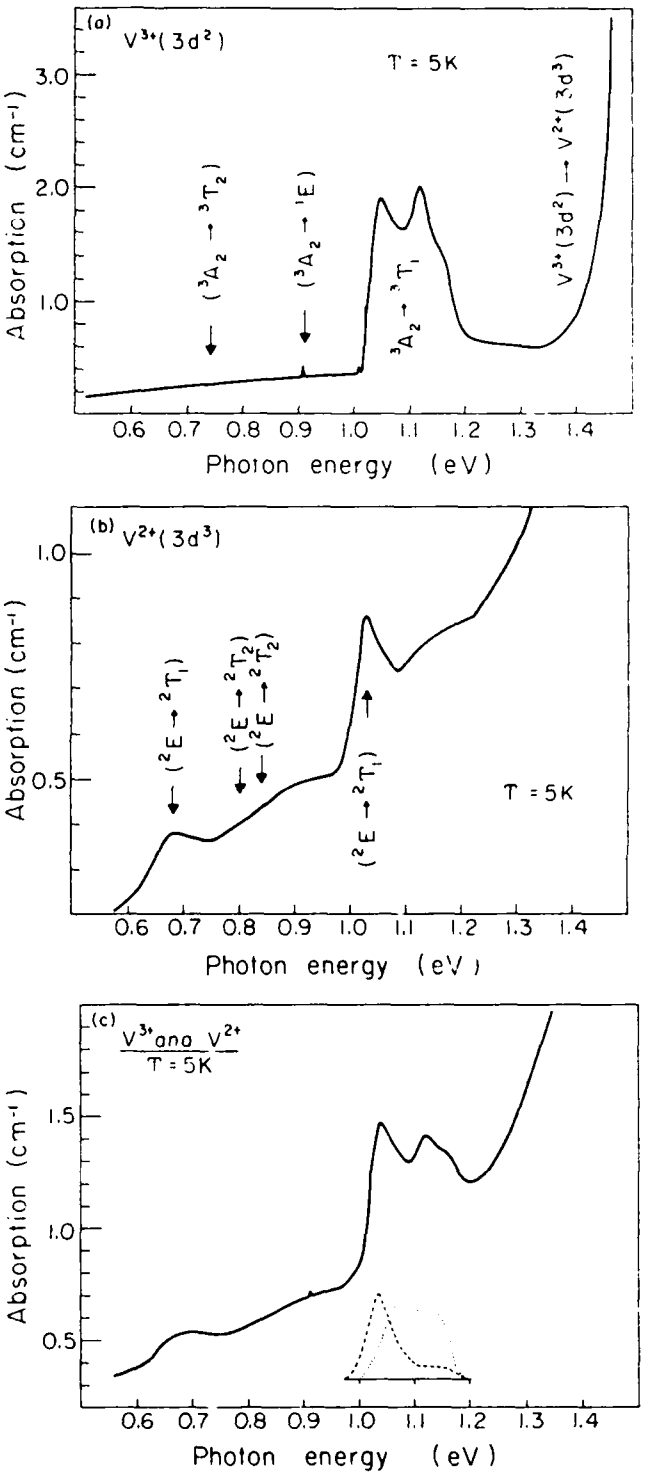

FIG. 6. Optical-absorption spectra of (a) p-type and high-resistivity, (b) n-type ($N_V < N_D$), and (c) n-type ($N_V > N_D$) V-doped GaAs obtained at 5 K. In (a) and (b) assignments of vanadium intracenter transitions according to Ref. 25 are indicated. The inset of (c) shows the relative contribution of the V^{2+} and V^{3+} charge states.

(b) For n-type GaAs:V,Se, heavily doped with selenium ($N_D > 10^{17}\,cm^{-3}$), two absorption bands at 0.68 eV and 1.03 eV without any ZPL were observed, as shown in Fig. 6(b). These bands are superimposed on an absorption background that begins at about 0.3 eV.

For lightly doped n-type GaAs:V crystals, a mixed absorption spectrum, composed of both (a) and (b)-type absorption features, was observed. Figure 6(c) shows an example of such a mixed absorption spectrum.

The nature of the characteristic absorption band shown in Fig. 6(a) has already been studied and is discussed in detail in the review paper by Clerjaud.[1] This band constitutes an intracenter transition within neutral, substitutional [$V^{3+}(3d^2)$] vanadium between the ground $^3A_2$ and the excited $^3T_1$ state. Furthermore, the luminescence spectrum[1] (ZPLs at 0.74 eV), involving the excited $^3T_2$ and ground $^3A_2$ states of this $V^{3+}(3d^2)$ configuration, was also observed in these same samples.[26] Therefore, the vanadium in all of our p-type and high-resistivity n-type crystals is in the neutral $V^{3+}(3d^2)$ charge state. This assignment is further supported by the results of Clerjaud *et al.*[12] who correlated observation of the EPR spectrum of the neutral $V^{3+}(3d^2)$ with the absorption spectrum in Fig. 6(a).

The absorption line at 0.909 eV in Fig. 6(a) has also been observed by Clerjaud *et al.*[12] and recently interpreted by Caldas *et al.*[25] as being due to the $^3A_2 \rightarrow {}^1E$ spin-forbidden transition of the $V^{3+}(3d^2)$ charge state.

Figure 6(a) also shows an absorption band starting at 1.35 eV whose intensity correlated with that of the main V^{3+} intracenter absorption. This result is in agreement with the existing assignment[10,12] of this absorption to the optical transition:

$$V^{3+}(3d^2) + e^-(\mathrm{VB}) \Rightarrow V^{2+}(3d^3)\,.$$

The second type of absorption spectrum shown in Fig. 6(b) is, in our opinion, due to intracenter transitions of the singly ionized $V^{2+}(3d^3)$ charge state. This spectrum is observed in all low-resistivity n-type GaAs:V crystals, and its intensity follows that of the DLTS vanadium peak. Furthermore, Fig. 6(c) illustrates the smooth transition between the two different vanadium spectra when the Fermi level is located at the $E_c - 0.15$-eV vanadium level. The band at 1.03 eV had been observed by Clerjaud *et al.*[12] and interpreted in terms of the $V^{2+}(3d^3)$ intracenter transition. However, they did not observe the band at 0.68 eV because of a rising low-energy absorption background. Ulrici *et al.*[10] did observe both of these bands, but did not interpret them as being connected with the $V^{2+}(3d^3)$ charge state or correlate them together. We can explain the reason for this omission as the observation by Ulrici *et al.* of a mixed V^{3+} and V^{2+} absorption spectrum similar to that presented in Fig. 6(c).

At this time we are unable to make a definite identification of the $V^{2+}(3d^3)$ electron states responsible for the absorption bands presented in Fig. 6(b), because with the lack of a positive identification of any V^{2+} EPR spectra, the ground-state symmetry remains uncertain. However, Katayama-Yoshida and Zunger[27] and also Caldas *et al.*[25] have predicted that the ground state of the $V^{2+}(3a^1)$ configuration in GaAs crystals should be the low-spin ^2E state, rather than the normally expected (according to Hund's rule) high-spin $^4T_1$ state. Within this model Caldas *et al.* have interpreted the entire $V^{2+}(3d^3)$ absorption spectrum, as indicated in Fig. 6(b).

From our identification one can further conclude that the absorption background observed in Figs. 6(b) and 6(c) probably corresponds to the transition

$$V^{2+}(3d^3) \Rightarrow \rightarrow V^{3+}(3d^2) + e^-(\mathrm{CB})\,,$$

which is complementary to the 1.35-eV absorption observed in the V^{3+} spectrum.

The results of photoconductivity measurements on these low-resistivity n-type samples are shown in Fig. 7. The presence of the same two maxima of the $V^{2+}(3d^3)$ charge state at 0.68 and 1.03 eV in the photoconductivity spectrum is a well-known property of excited states of a many-electron impurity. These states are therefore degenerate with the GaAs conduction band and undergo an autoionization effect,[1,28] making them observable under these experimental conditions.

All of the aforementioned assignments are further supported by electron-paramagnetic-resonance (EPR) measurements of our samples.[29] The characteristic substitutional $V^{3+}(3d^2)$ spectrum[4] was observed for all p-type and high-resistivity n-type V-doped GaAs samples. In the case of samples with the Fermi-level position above the $E_c - 0.15$-eV level, no EPR spectrum was found, which can be attributed to the high conductivity of such samples.

To conclude this discussion, we can state unequivocally that the optical and electrical properties of V-doped GaAs are self-consistent. Identification of the substitutional noncomplexed-vanadium optical spectra enables us to identify the $E_c - 0.15$ eV level as the $V^{3+}(3d^2)/V^{2+}(3d^3)$ single acceptor. Furthermore, the observation of the intracenter

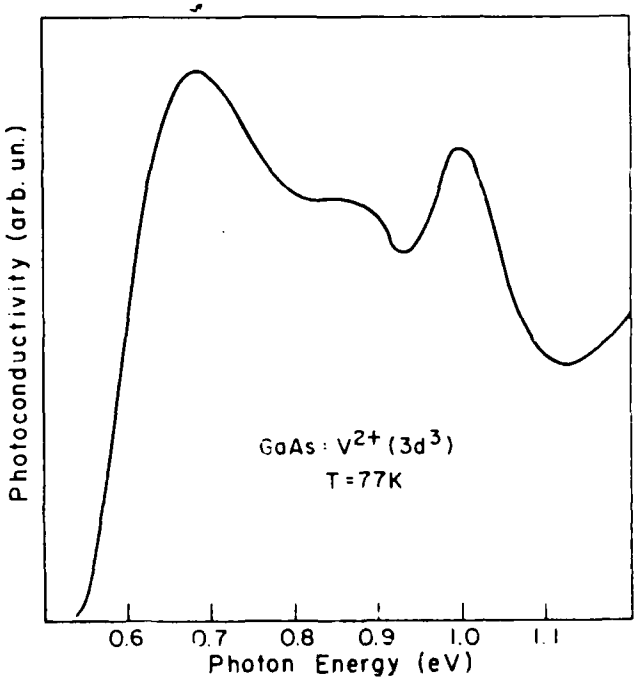

FIG. 7. Photoconductivity spectrum of n-type V-doped GaAs obtained at 77 K.

V^{3+} absorption spectrum for all positions of the Fermi level between the V^{3+}/V^{2+} acceptor level and the valence band proves that there is no other substitutional-vanadium level within the GaAs energy gap, i.e., that the $V^{4+}(3d^1)/V^{3+}(3d^2)$ donor level must be located within the valence band. Figure 8 schematically presents all of the substitutional-vanadium levels in GaAs.

D. Calibration of the optical spectra

The DLTS and optical-absorption spectra obtained from low-resistivity V-doped GaAs samples provide the data necessary to calculate the optical-absorption cross sections (σ) of the $V^{2+}(3d^3)$ intracenter transitions [Fig. 6(b)]. At liquid-helium temperature their values are the following:

$$\sigma(1.03\ \text{eV}) = \frac{\alpha(1.03\ \text{eV}) - \alpha(0.95\ \text{eV})}{N(\text{DLTS})} = 3.5\times10^{-17}\ \text{cm}^2\ (\pm 20\%),$$

$$\sigma(0.68\ \text{eV}) = \frac{\alpha(0.68\ \text{eV}) - \alpha(0.60\ \text{eV})}{N(\text{DLTS})} = 1.5\times10^{-17}\ \text{cm}^2\ (\pm 20\%),$$

where $\alpha(E)$ is the absorption coefficient for the photon energy E, and $N(\text{DLTS})$ is the concentration of vanadium centers obtained from DLTS measurements.

Our as-grown LEC GaAs crystal have a native defect acting as a deep acceptor, which disappears after a standard 850 °C anneal.[30] This native defect provides compensation in as-grown material sufficient to position the Fermi level at or slightly below the 0.15-eV vanadium level, resulting in a V^{3+} or mixed absorption spectrum; after annealing, only a pure V^{2+} spectrum is observed. We have used this phenomenon to extend our calibration to the $V^{3+}(3d^2)$ main intracenter transition. Comparing the as-grown and annealed spectra of the same n-type V-doped samples, we were able to use the above calibration to find the $V^{3+}(3d^2)$ absorption cross section at liquid-helium temperature as

$$\sigma(1.04\ \text{eV}) = \frac{\alpha(1.04\ \text{eV}) - \alpha(0.97\ \text{eV})}{N(\text{DLTS})} = 1\times10^{-16}\ \text{cm}^2\ (\pm 40\%),$$

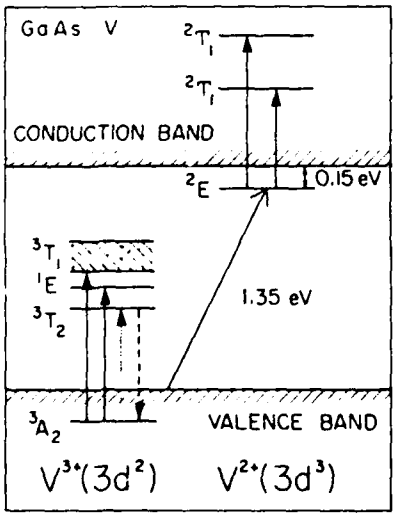

FIG. 8. Energy levels of the $V^{3+}(3d^2)$ and $V^{2+}(3d^3)$ charge states in GaAs. Vertical arrows represent intracenter transitions and the slanted arrow represents the charge transfer $V_1^{3+}(3d^2) + e^- \Rightarrow V^{2+}(3d^3)$. The indicated level symmetries have been taken from Ref. 25.

E. Theoretical considerations and comparison with other III–V compounds

In addition to all of the technological and experimental studies of V-doped GaAs, some theoretical calculations have also been performed.[25,27] These calculations were not only directed toward an identification of a vanadium spin state (as was mentioned before), but also strove to provide positions of the energy levels within the band gap. The V^{3+}/V^{2+} acceptor level has been calculated to be at $E_v + 1.35$ eV (Ref. 25) and $E_v + 1.34$ eV (Ref. 27), respectively. The V^{4+}/V^{3+} donor level in both cases has been predicted to be inside the valence band; in one case its position could be estimated as -0.03 eV (Ref. 25) below the top of the valence band. All of these predictions are in a very good agreement with our experimental findings.

Furthermore, based on the findings of Ledebo and Ridley[31] and also of Caldas *et al.*,[32] that the vacuum-referred binding energies (VRBE) of transition-metal impurities remain nearly constant within a given class of semiconducting compounds (i.e., III–V crystals), we can present the available data about substitutional-vanadium levels in the III–V semiconductors. In the case of indium phosphide, the $V^{4+}(3d^1)/V^{3+}(3d^2)$ donor level has been found at $E_v + 0.21$ eV (Refs. 33 and 34) or $E_v + 0.24$ eV (Ref. 35), and the $V^{3+}(3d^2)/V^{2+}(3d^3)$ acceptor level is proposed by Lambert *et al.*[36] to lie in the conduction band. For n-type gallium phosphide, the vanadium-acceptor level has only recently been identified at $E_c - 0.58$ eV (Ref. 37). Measurements on p-type GaP should reveal the vanadium-donor level as well.

All of these experimental results are presented in Fig. 9 with the use of the electron-affinity data from Ref. 32. One

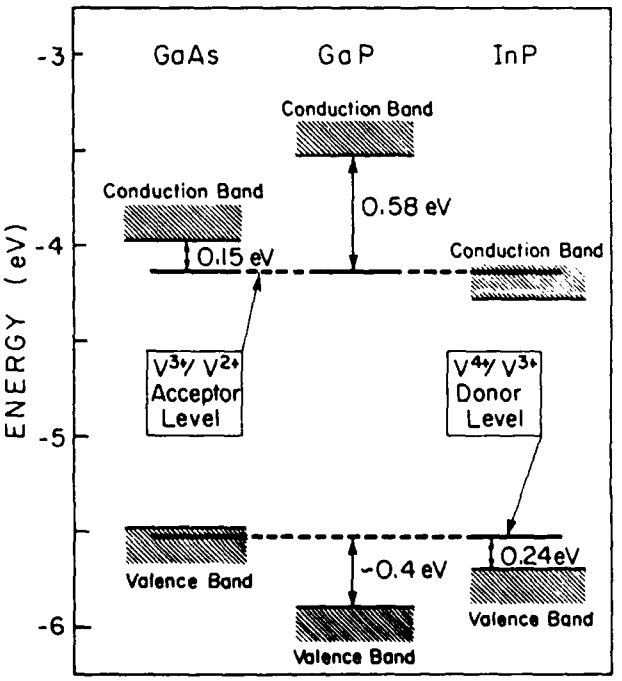

FIG. 9. Vacuum-related binding energies of the vanadium-donor and -acceptor levels in some III–V compounds. The vanadium-donor level in GaP has not yet been observed, but is predicted to lie at $E_v + 0.4$ eV.

can see excellent agreement between the reported vanadium VRBEs and also predict that the vanadium-donor levels are located at about $E_v + 0.4$ eV in GaP and very close to the top of the valence band in GaAs.

It is also evident from this figure that none of the substitutional-vanadium levels in GaAs or InP can act as centers for producing SI material.

F. Implications for SI GaAs

All of the above experimental and theoretical results prove that the substitutional $V^{3+}(3d^2)/V^{2+}(3d^3)$ acceptor level at $E_c - 0.15$ eV is the only vanadium-related level found within the GaAs energy gap. However, several authors have suggested the existence of electrically active vanadium-related complexes in GaAs[5-8,10,37-39] as possibly providing a midgap level. Models invoking a vanadium-oxygen complex[6,7] or a vanadium-arsenic vacancy complex[10,38] have been put forth. We did not detect any optical or electronic evidence of a vanadium-related midgap level in our n-type LEC, HB, and LPEE V-doped crystals.

For the case of a vanadium-arsenic vacancy complex model,[10,38] it should be mentioned that although an analogy with a chromium trigonal center Cr^{2+}-X (see, for example, Ref. 1) is used, there is no experimental evidence (analogous to the known properties of the chromium complex) that such a vanadium complex exists. There is also no definite proof that the acoustic-paramagnetic-resonance (APR) spectra[38] and the thermally detected electron-paramagnetic-resonance (TDEPR) spectra[39] are vanadium related. The reported crystals contain several other transition-metal impurities, and the APR and TDEPR measurements give no information about the concentration of investigated anisotropic centers. Last, the authors of this model[10] failed to grow any SI V-doped material.

During the course of our study, several HB SI V-doped crystals were successfully grown and characterized. We have found, however, that the Fermi-level position in these crystals is controlled by the deep donor EL2, which is present in concentrations greater than that of substitutional vanadium as determined from optical-absorption measurements. Furthermore, the absorption and EPR data from these SI samples are identical to those discussed in Sec. C.

All of these arguments lead quite clearly to the conclusion that vanadium does not play an electronic role in the formulation of SI GaAs. The results do suggest, however, that vanadium could play a more subtle chemical role (e.g., as a gettering agent), thus aiding in the growth of normal EL2-compensated SI material, rather than being directly responsible for its electrical properties. In Table I we have collected all of the published data on the energy levels in V-doped GaAs crystals as of this writing. Comments as to the actual origin of the dominant deep level in each case (e.g., V^{3+}/V^{2+} or EL2), in view of the results presented in this study, are also included.

TABLE I. Deep levels observed in V-doped GaAs.

Energy position (eV)	Crystal growth method[a]	Relation to vanadium	Possible origin
$E_c - 0.15$[b]	LEC, HB, LPEE	V^{3+}/V^{2+} acceptor	
$E_c - 0.14$[c]	LEC	V^{3+}/V^{2+} acceptor	
$E_c - 0.14$[d]	HB	V^{3+}/V^{2+} acceptor	
$E_c - 0.22$[e]	LEC	not related to V	EL14 or Ti[f]
$E_c - 0.23$[d]	HB	not related to V	EL14 or Ti[f]
$E_c - 0.5$[g]	MOCVD	not related to V	?
$E_c - 0.77$[h]	LEC	not related to V	EL2
$E_v + 0.58$[i]	VPE	not related to V	HM1[j,k]

[a] (LEC) liquid-encapsulated Czochralski, (HB) horizontal Bridgman, (LPEE) liquid-phase electroepitaxy, (MOCVD) metallo-organic chemical vapor deposition, (VPE) vapor-phase epitaxy.
[b] References 15, 16, and this study.
[c] Reference 10.
[d] References 11, 12, and 40.
[e] Reference 9.
[f] Reference 24.
[g] Reference 7.
[h] References 2 and 3.
[i] Reference 6.
[j] J. Lagowski, D. G. Lin, T.-P. Chen, M. Skowronski, and H. C. Gatos, Appl. Phys. Lett. **47**, 929 (1985).
[k] J. Osaka, H. Okamoto, and K. Kobayashi, in *Semi-Insulating III-V Materials, Hakone, 1986*, edited by H. Kukimoto and S. Miyazawa (North-Holland/OHMSHA, Tokyo, 1986), p. 421.

IV. CONCLUSIONS

Through the use of DLTS, Hall-effect, and optical-absorption measurements, we have identified the substitutional-vanadium V^{3+}/V^{2+} acceptor level in GaAs at 0.15 eV below the bottom of the conduction band. The substitutional-vanadium V^{4+}/V^{3+} donor level was found to be located within the valence band. In addition, no evidence of any midgap level due to vanadium-impurity (defect) complexes was observed. These results confirm the fact that vanadium cannot provide the compensation necessary for producing SI GaAs. The high resistivity of some SI V-doped GaAs crystals can be readily explained by the overwhelming presence of the native defect EL2. We believe that vanadium can, however, play an important chemical role by removing or reacting with residual shallow donors during the growth of high-resistivity material.

ACKNOWLEDGMENTS

We are deeply indebted to Dr. T. Bryskiewicz for growing the V-doped LPEE GaAs crystals. We are very grateful to Dr. B. Clerjaud (Université Paris VI) for the EPR measurements of our crystals and many helpful discussions, to Dr. P. W. Yu for the luminescence measurements of our crystals, to Dr. P. Becla for his help in our photoconductivity measurements, and to L. Pawlowicz and F. Dabkowski for growing some of the V-doped LEC GaAs crystals used in this study. We are also grateful to the Air Force Office of Scientific Research and the Office of Naval Research for financial support and the IBM Corporation for C. D. Brandt's graduate fellowship.

[1] For a review, see B. Clerjaud, J. Phys. C **18**, 3615 (1985).
[2] A. V. Vasil'ev, G. K. Ippolitowa, E. M. Omel'yanovskii, and A. M. Ryskin, Sov. Phys. Semicond. **10**, 341 (1976).
[3] V. S. Vavilov and V. A. Morozova, Sov. Phys. Semicond. **20**, 226 (1986).
[4] U. Kaufmann, H. Ennen, J. Schneider, R. Worner, J. Weber, and F. Kohl, Phys. Rev. B **25**, 5598 (1982).
[5] P. S. Gladkov and K. B. Ozanyan, J. Phys. C **18**, L915 (1985).

[6]H. Terao, H. Sunakawa, K. Ohata, and H. Watanabe, in *Semi-Insulating III-V Materials, Evian, 1982*, edited by S. Makram-Ebeid and B. Tuck (Shiva, Nantwich, England, 1982), p. 54.
[7]M. Akiyama, Y. Karawada, and K. Kaminishi, J. Cryst. Growth **68**, 39 (1984).
[8]Y. Kawarada, M. Akiyama, and K. Kaminishi, in *Semi-Insulating III-V Materials, Hakone, 1986*, edited by H. Kukimoto and S. Miyazawa (North Holland/OHMSHA, Tokyo, 1986), p. 509.
[9]R. W. Haisty and G. R. Cronin, in *Physics of Semiconductors*, edited by M. Hulin (Dunod, Paris, 1964), p. 1161.
[10]W. Ulrici, K. Friedland, L. Eaves, and D. P. Halliday, Phys. Status Solidi B **131**, 719 (1985).
[11]A. Mircea-Russel, G. M. Martin, and J. Lowther, Solid State Commun. **36**, 171 (1980).
[12]B. Clerjaud C. Naud, B. Deveaud, B. Lambert, B. Plot-Chan, G. Bremond, C. Benjeddou, G. Guillot, and A. Nouailhat, J. Appl. Phys. **58**, 4207 (1985).
[13]W. Kutt, D. Bimberg, M. Maier, H. Krautle, F. Kohl, and E. Bauser, Appl. Phys. Lett. **44**, 1078 (1984).
[14]W. Kutt, D. Bimberg, M. Maier, H. Krautle, F. Kohl, and E. Tomzig, Appl. Phys. Lett. **46**, 489 (1985).
[15]C. D. Brandt, A. M. Hennel, L. M. Pawlowicz, F. P. Dabkowski, J. Lagowski, and H. C. Gatos, Appl. Phys. Lett. **47**, 607 (1985).
[16]A. M. Hennel, C. D. Brandt, H. Hsiaw, L. M. Pawlowicz, F. P. Dabkowski, and J. Lagowski, *Gallium Arsenide and Related Compounds 1985*, Institute of Physics Conference Service No. 79) (Hilger, Bristol, 1986), pp. 43–48.
[17]A. M. Hennel, C. D. Brandt, L. M. Pawlowicz, and K. Y. Ko, in *Semi-Insulating III-V Materials, Hakone, 1986*, edited by H. Kukimoto and S. Miyazawa (North Holland/OHMSHA, Tokyo, 1986), p. 465.
[18]T. Bryskiewicz, in *Semiconductor Optoelectronics*, edited by M. A. Herman (PWN-Polish Scientific, Warsaw, 1980), pp. 187–212; in *Progress in Crystal Growth and Characterization*, edited by B. Pamplin (Pergamon, Oxford, in press).
[19]T. Bryskiewicz, C. F. Boucher, Jr., J. Lagowski, and H. C. Gatos, J. Cryst. Growth (to be published).
[20]J. Lagowski, H. C. Gatos, C. H. Kang, M. Skowronski, K. Y. Ko, and D. G. Lin, Appl. Phys. Lett. **49**, 892 (1986).
[21]D. C. Look, in *Semiconductors and Semimetals*, edited by R. K. Willardson and A. C. Beer (Academic, New York, 1983), Vol. 19, p. 75.
[22]W. Walukiewicz, J. Lagowski, L. Jastrzebski, M. Lichtensteiger, and H. C. Gatos, J. Appl. Phys. **50**, 899 (1979).
[23]W. Walukiewicz, J. Lagowski, and H. C. Gatos, J. Appl. Phys. **53**, 769 (1982).
[24]C. D. Brandt, A. M. Hennel, L. M. Pawlowicz, Y.-T. Wu, T. Bryskiewicz, J. Lagowski, and H. C. Gatos, Appl. Phys. Lett. **48**, 1162 (1986).
[25]M. Caldas, S. K. Figueiredo, and A. Fazzio, Phys. Rev. B **33**, 7102 (1986).
[26]P. W. Yu (private communication).
[27]H. Katayama-Yoshida and A. Zunger, Phys. Rev. B **33**, 2961 (1986).
[28]See, for example, K. Kocot and J. M. Baranowski, Phys. Status Solidi B **81**, 629 (1977); A. P. Radlinski, Phys. Status Solidi B **84**, 503 (1977).
[29]B. Clerjaud (private communication).
[30]C. D. Brandt (unpublished).
[31]L. A. Ledebo and B. K. Ridley, J. Phys. C **15**, L961 (1982).
[32]M. J. Caldas, A. Fazzio, and A. Zunger, Appl. Phys. Lett **45**, 671 (1984).
[33]G. Bremond, A. Nouailhat, G. Guillot, B. Deveaud, B. Lambert, Y. Toudic, B. Clerjaud, and C. Naud, in *Microscopic Identification of Electronic Defects in Semiconductors*, Materials Research Society Symposia Proceedings, edited by N. M. Johnson, S. G. Bishop, and G. D. Watkins, (Materials Research Society, Pittsburgh, 1985), Vol. 46, p. 359.
[34]B. Deveaud, B. Plot, B. Lambert, G. Bremond, G. Guillot, A. Nouailhat, B. Clerjaud, and C. Naud, J. Appl. Phys. **59**, 3126 (1986).
[35]C. D. Brandt, A. M. Hennel, J. Lagowski, and H. C. Gatos (unpublished).
[36]B. Lambert, B. Deveaud, Y. Toudic, G. Pelous, J. C. Paris, and G. Grandpierre, Solid State Commun. **47**, 337 (1983).
[37]W. Ulrici, L. Eaves, K. Friedland, D. P. Halliday, and J. Kreibl, in Proceedings of the 14th International Conference on Defects in Semiconductors, Paris, 1986 (to be published).
[38]V. W. Rampton, M. K. Saker, and W. Ulrici, J. Phys. C **19**, 1037 (1986).
[39]A.-M. Vasson, A. Vasson, C. A. Bates, and A. F. Labadz, J. Phys. C **17**, L837 (1984).
[40]E. Litty, P. Leyral, S. Loualiche, A. Nouailhat, G. Guillot, and M. Lannoo, Physica B **117/118**, 182 (1983).

Optical characterization of semi-insulating GaAs: Determination of the Fermi energy, the concentration of the midgap EL2 level and its occupancy

J. Lagowski, M Bugajski,[a] M. Matsui,[b] and H. C. Gatos
Massachusetts Institute of Technology, Cambridge, Massachusetts 02139

(Received 6 April 1987; accepted for publication 17 June 1987)

The key electronic characteristics of semi-insulating GaAs, i.e., the Fermi energy, concentration, and occupancy of the midgap donor EL2, and the net concentration of ionized acceptors can all be determined from high-resolution measurements of the EL2 intracenter absorption. The procedure is based on the measurement of zero-phonon line intensity before and after the complete transfer of EL2 to its metastable state followed by thermal recovery. The procedure is quantitative, involves no fitting parameters, and unlike existing methods, is applicable even when a significant part of the EL2 is ionized.

Electronic parameters of semi-insulating (SI) GaAs and its behavior during device processing depend on the concentration of the native deep donor EL2 and the net concentration of ionized acceptors.[1] Currently, the evaluation of such pertinent parameters is carried out employing a combination of optical and electrical measurements.[1–4] The concentration of EL2 is evaluated from the near-infrared optical absorption, while Hall effect and electrical conductivity measurements yield the Fermi energy from which the EL2 occupancy can be calculated. The concentration of ionized EL2 provides, of course, a measure of the net ionized acceptor concentration. The knowledge of the Fermi energy is crucial, since optical absorption measurements alone cannot differentiate between changes in EL2 occupancy and EL2 concentration. Thus, the reliability of the optical absorption procedure for the determination of the EL2 concentration, as commonly employed, is decreased as the fraction of the ionized EL2 becomes significant, i.e., in *n*-type SI GaAs with resistivities exceeding 10^8 Ω cm and in *p*-type SI GaAs.

In this letter we discuss a characterization approach which is based on measurements of optical absorption, but it is applicable to both *n*- and *p*-type SI GaAs.

The difference between the present approach and earlier approaches is twofold. Firstly, we utilize the EL2 intracenter absorption rather than the total EL2 absorption band. The intracenter absorption is uniquely related to the neutral (occupied) state of EL2 in contrast to the total absorption, in which the photoionization transitions from the occupied EL2 state to the conduction band are involved as well as those from the valence band to the ionized EL2 state.[4,5] Secondly, we utilize the optical excitation of EL2 to its metastable state[6] in order to transfer the entire concentration of EL2 into the neutral state. In the standard approaches the metastable state is used to determine the background absorption which is not related to EL2.[3]

The proposed procedure involves three steps: (1) the SI GaAs sample is cooled in the dark from room temperature to 6 K; (2) EL2 is optically bleached (with white light); and (3) the sample is annealed at 120–140 K and cooled back to 6 K. The optical absorption spectrum is measured after each step and the corresponding intensities of the zero-phonon line (α^1_{ZPL}, α^2_{ZPL}, and α^3_{ZPL}, respectively) are used for the quantitative analysis. It is essential that the energy range from 1.037 and 1.041 eV, corresponding to the zero-phonon line,[4,5] is recorded with enhanced resolution and sensitivity.

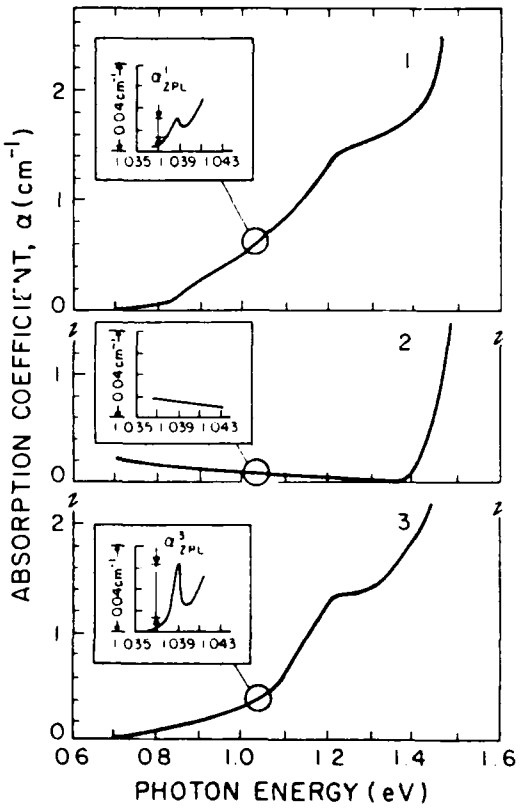

FIG. 1. 6 K optical absorption spectra of GaAs with the EL2 occupancy fraction $f \simeq 0.3$ at 300 K: 1—after cooling from 300 K; 2—after absorption bleaching; and 3—after subsequent annealing at 140 K for 5 min. Inserts show the zero-phonon line absorption.

[a] On leave from Institute of Electron Technology, Warsaw, Poland.
[b] On leave from Sumitomo Metal Mining Co., Ltd., Tokyo, Japan.

 0003-6951/87/330511-03$01.00

Furthermore, the measurements must be carried out with very low intensity incident light in order to prevent any measurable transfer of EL2 into its metastable state during the measurements following steps (1) and (2).

In order to demonstrate the new procedure we take an example of undoped SI GaAs with a relatively low value of Hall effect mobility at 300 K (about 3000 cm^2/V s) and very high resistivity (about 5×10^8 Ω cm). In such material a significant fraction of EL2 is expected to be ionized[2] and thus the standard optical method based on Ref. 3 is not readily applicable. The optical spectra taken after steps (1), (2), and (3), and denoted as (1), (2), and (3), respectively, are shown in Fig. 1. Spectrum (1) reflects the ionized state of EL2 frozen from room temperature. This spectrum is different from the EL2 absorption band characteristic of *n*-type conducting GaAs where EL2 is completely neutral. On the other hand, the zero-phonon line (see insert) is clearly observed and provides a measure of the concentration of neutral EL2. Illumination with strong white light [step (2)] eliminates the entire spectrum, including the zero-phonon line (see spectrum 2). EL2 is entirely in its metastable state which is neutral, and optically inactive. Annealing at 140 K for 5 min transforms EL2 back to its normal, optically active, state, without changing its occupancy. As a result, spectrum (3) corresponds to EL2, which is entirely neutral. As can be seen, about a threefold increase in the zero-phonon line intensity is observed in comparison to spectrum (1). The whole absorption band also changes its shape becoming similar to the characteristic absorption of conducting *n*-type GaAs.

The zero-phonon line intensity ratio $\alpha^1_{ZPL}/\alpha^3_{ZPL}=f_n$ provides a direct measure of the EL2 occupancy factor $f_n=n^0_{EL2}/N_{EL2}$ (where n^0_{EL2} and N_{EL2} represent neutral and total EL2 concentration, respectively). The Fermi energy with respect to the bottom of the conduction band becomes $E_c-E_F=kT\ln(f_n^{-1}-1)+E'_{EL2}$, where $E'_{EL2}=0.759-0.237\times10^{-4}T^{7/8}$ is "effective" EL2 energy which includes a contribution from the degeneracy factor. It must be emphasized that the occupancy factor f_n or the Fermi energy E_F can be used to determine the conductivity type and the free electron and hole concentrations.[1,2] If prior to cooling [step (1)], the sample is equilibrated in the dark at 300 K, the f_n and E_F values can be taken as representive of this temperature. From existing calculations in Refs. 2 and 9, f_n and E_F at 300 K can be related to values of resistivity (or conductivity), free-carrier concentration, and Hall effect mobility.

A recent high-resolution optical and transient capacitance study[4] of EL2 provided a quantitative relation between α_{ZPL} and n^0_{EL2}, i.e., $\alpha_{ZPL}/n^0_{EL2}=1.1\times10^{-18}$ cm^2. This ratio is insensitive to temperature between 2 to 10 K. The total EL2 concentration estimated form α^1_{ZPL} becomes $N_{EL2}=0.9\times10^{18}\alpha^1_{ZPL}$. The concentration of ionized EL2 is given by $n^+_{EL2}=0.9\times10^{18}(\alpha^1_{ZPL}-\alpha^3_{ZPL})$. Considering electrical neutrality, the net concentration of ionized acceptors we have is $N_A-N_D=n^+_{EL2}$ (where N_D refers to ionized donors other than EL2).

For example, the set of electrical parameters evaluated from optical measurements for the crystal analyzed in Fig. 1 is as follows: $N_{EL2}=1.5\times10^{16}$ cm^{-3}, $n^0_{EL2}=5\times10^{15}$ cm^{-3}, $N_A-N_D=1.0\times10^{16}$ cm^{-3}, $f_n=0.3$, $E_c-E_F=0.73$ eV, $\rho(300\text{ K})\simeq7\times10^3$ Ω cm, $\mu_H\sim3500$ cm^2/V s, $p(300\text{ K})\simeq5\times10^6$ cm^{-3}. We should point out that conductivity and Hall effect measurements yielded resistivity and Hall effect mobility values within 20% from above estimates.

Application of the present approach to different SI GaAs with high Hall effect mobility ($\mu_H>5000$ cm^2/V s) and relatively low resistivity (300 K resistivity below 10^8 Ω cm) is illustrated in Fig. 2. In such material the majority of EL2 is expected to be neutral. Indeed, only a very small enhancement of the zero-phonon line intensity was observed after step (3). Actually, the ratio $f_n=\alpha^1_{ZPL}/\alpha^3_{ZPL}=0.98$ implies that only 2% of EL2 is ionized. Quantitative analysis yields the following values of the other parameters: $E_c-E_F=0.64$ eV; $N_{EL2}=3.6\times10^{16}$ cm^{-3}, $n^+_{EL2}=N_A-N_D=1.6\times10^{15}$ cm^{-3}. In this case the standard

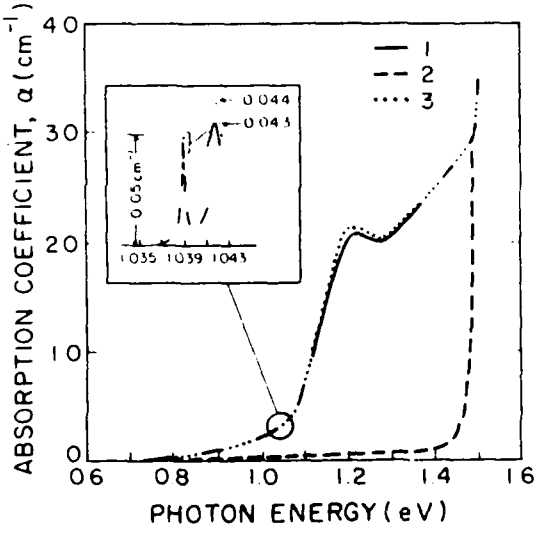

FIG. 2. 6 K optical absorption spectra of standard SI GaAs with majority of EL2 occupied at 300 K. 1, 2, and 3 correspond to the same conditions as in Fig. 1.

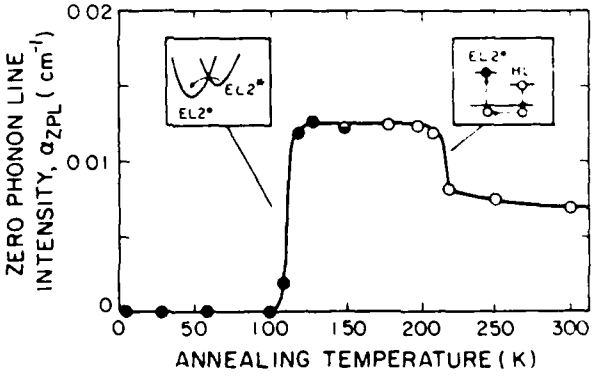

FIG. 3. Zero-phonon line intensity vs the annealing temperature of step (3) used to recover the EL2 from the metastable state. Filled and open circles correspond to annealing time of 10 and 15 min, respectively.

method for the determination of EL2 concentration from the total optical absorption at $\lambda = 1.06\,\mu$m can be conveniently employed. Indeed, this standard method yielded $N_{EL2} = 3.4 \times 10^{16}\,\text{cm}^{-3}$ (using the revised calibration factor after Ref. 4) in very good agreement with the present approach.

It should be pointed out that EL2 is the dominant midgap level in GaAs crystals grown by the standard methods from As-rich melts.[7] Other midgap levels are present, but at concentrations about one magnitude smaller than that of EL2. Since the zero-phonon line employed here is uniquely related to EL2 with a specific signature,[5] our approach for the determination of the EL2 concentration remains valid, even in the presence of other midgap levels at concentrations comparable to those of EL2. In such a case, however, the concentration of ionized EL2 cannot be taken as an exact measure of concentration of the net ionized acceptors but rather as the lower limit of $N_A^+ - N_D^+$.

In the course of this investigation we found that the intensity of the zero-phonon line, α^1_{ZPL}, reaches a constant value for annealing temperatures $T_A > 120$ K, consistent with the established EL2 behavior in SI GaAs. Beyond 220 K, however, α^1_{ZPL} decreases significantly, as shown in Fig. 3. Measurements of thermally stimulated current (TSC) showed that this decrease is associated with the thermal emission of holes (trapped during illumination at low temperatures by hole traps HL3, HL9, and HL10)[10] and their recombination with EL2 electrons. Thus, if relatively shallow hole traps are present at high densities, a decrease of α^1_{ZPL} can in general take place. This potentially interfering process can be recognized (using additional TSC measurements) and minimized by adjusting the annealing conditions, i.e., temperature and annealing time.

In summary, we have shown that high-resolution measurements of the 1.039 eV zero-phonon line can be very effectively applied for the optical characterization of SI GaAs. This approach has fundamental advantages over the standard optical method for the determination of the EL2 concentration in the characterization of materials in which EL2 is partially ionized. It should prove particularly useful in the characterization of a new type of GaAs crystal exhibiting inverted thermal conversion (ITC) in which very high resistivity is achieved by thermal annealing.[11] The standard optical method is not suitable for ITC GaAs because in this material a significant fraction of EL2 is ionized.

The authors are grateful to the National Aeronautics and Space Administration and to the Air Force Office of Scientific Research for financial support.

[1] G. M. Martin, J. P. Farges, G. Jacob, and J. P. Hallais, J. Appl. Phys. **51**, 2840 (1980).
[2] W. Walukiewicz, J. Lagowski, and H. C. Gatos, Appl. Phys. Lett. **43**, 192 (1983).
[3] G. M. Martin, Appl. Phys. Lett. **39**, 747 (1981).
[4] M. Skowronski, J. Lagowski, and H. C. Gatos, J. Appl. Phys. **59**, 2451 (1986).
[5] M. Kaminska, M. Skowronski, and W. Kuszko, Phys. Rev. Lett. **55**, 2204 (1985).
[6] G. Vincent, D. Bois, and A. Chantre, J. Appl. Phys. **53**, 3643 (1982).
H. C. Gatos and J. Lagowski, Mater. Res. Soc. Symp. Proc. **46**, 153 (1985).
[8] The revised value of the EL2 electron emission activation energy is used after Ref. 7. This value is slightly lower (by 10 meV) than the value used in Ref. 1.
[9] J. S. Blakemore, J. Appl. Phys. **53**, R123 (1982).
[10] G. M. Martin, in *Semi-Insulating III-V Materials*, edited by G. J. Rees (Shiva, Orpington, U.K., 1980), p. 13.
[11] J. Lagowski, H. C. Gatos, C. H. Kang, M. Skowronski, K. Y. Ko, and D. G. Lin, Appl. Phys. Lett. **49**, 892 (1986).

Effect of plastic deformation on electronic properties of GaAs

M. Skowronski,[a] J. Lagowski, M. Milshtein,[b] C. H. Kang, F. P. Dabkowski,[c]
A. Hennel,[d] and H. C. Gatos
Massachusetts Institute of Technology, Cambridge, Massachusetts 02139

(Received 8 May 1987; accepted for publication 26 June 1987)

A systematic study of plastically deformed (in compression) GaAs was carried out employing deep-level spectroscopies, optical absorption, and electronic transport measurements. Deformation-induced changes in the free-carrier concentration, the mobility, and occupation of deep levels were associated with a deep acceptor defect. Changes of the optical absorption in deformed samples were found to be due to a localized stress field of dislocations rather than transitions via localized levels. No evidence was found of any meaningful increase ($>2\times10^{15}$ cm^{-3}) of the concentration of EL2 or other midgap donors for deformation up to about 3%. Thus, it is evident that the enhancement of the electron paramagnetic resonance signal of the arsenic antisite As_{Ga} in deformed semi-insulating GaAs must be due to the increased ionization of As_{Ga} rather than the generation of new antisite defects.

I. INTRODUCTION

The relatively low mechanical strength of GaAs (the critical resolved sheer stress about one order of magnitude smaller than that of silicon) causes melt-grown crystals to be very susceptible to plastic deformation induced by thermal gradients.[1,2] The magnitude of thermal stresses can be particularly large in crystals grown by liquid encapsulated Czochralski (LEC). The dislocation density,[1-3] the electrical resistivity,[4] and the optical transmissivity[5,6] in such crystals exhibit spatial variations which often resemble the characteristic pattern of thermal stress. Similar patterns were also found in the leakage current[7,8] and the threshold voltage variations of the enhancement mode field-effect transistors[9] produced on semi-insulating (SI) LEC wafers. The understanding of these practically and fundamentally important results is at present very limited. In most instances it is not clear whether they reflect real cause to effect relations or coincidental processes only.

A number of investigations carried out in recent years was devoted to the effects of plastic deformation on electronic properties of GaAs.[10-22] Deformation-induced deep levels, and especially the main native deep donor EL2 and the related antisite defect As_{Ga}, were focal points in these studies.[10-15] Early results obtained with deep-level transient spectroscopy (DLTS) seemed to indicate an increase of EL2 concentration during plastic deformation.[13] Electron paramagnetic resonance (EPR) measurements on deformed SI GaAs crystals also showed an enhancement of the characteristic quadruplet line assigned to the singly ionized state of the arsenic antisite As_{Ga}.[11,12,17] The similarity between the photoquenching of the EPR signal and the EL2-related photocapacitance spectra was taken as evidence of the common deformation related origin of the arsenic antisite and EL2.[12] More recent results of DLTS[18,19] and of the optical absorption[20] imply that the EL2 concentration increases only very little (if at all) after plastic deformation. This finding contrasted with the behavior of the EPR signal and led to a hypothesis of different antisite complexes, all of which contribute to the EPR quadruplet, but only some to EL2.[21] However, it has been pointed out that the enhancement of the EPR signal may be caused by deformation-induced acceptors which increase the concentration of ionized antisite As_{Ga}.[22]

The present study addresses the question of deformation-induced midgap donors, the acceptors, and their effects on deep donor occupation. Optical and electronic properties of plastically deformed GaAs were investigated employing a series of *n*-type, SI, and *p*-type crystals, which enables the separation between the creation of new deep levels and the changes in population of the levels already present prior to deformation. Our experimental approach combined the measurements of DLTS (or thermally stimulated current for SI samples), Hall effect, and optical absorption performed on the same samples. In addition, deformed samples were subsequently subjected to thermal annealing in order to evaluate the stability of deformation-induced defects.

II. EXPERIMENT

A. Sample preparation

Conducting *n*- and *p*-type crystals used in this study were grown from the melt in this laboratory. For *n*-type samples selenium was used as a dopant, and the resulting net carrier concentration was $5\text{–}10\times10^{16}$ cm^{-3}. The mobility was in excess of 3000 cm^2/V s. *p*-type crystals were doped with zinc. Two sets of samples were used with 300-K hole concentration of 5×10^{15} and 5×10^{16} cm^{-3}, respectively. The dopant concentration in all cases was low enough to prevent the effects of impurity hardening and to avoid changes in the mechanical properties of the crystals. Prior to deformation, whole ingots were annealed for 12 h at 850 °C under As overpressure to assure thermal stability of the starting material and to relieve any residual built-in stress. The ingots were subsequently cut in the form of rectangular slabs $4\times4\times7$ mm^3 with the long axis (111), (110), or

[a] Present address: Cabot Corporation, Billerica, MA 01821.
[b] Present address: 781 Hamilton St., Somerset, NJ 08873.
[c] Present address: Polaroid Corporation, Cambridge, MA 02139.
[d] Present address: Institute of Experimental Physics, Warsaw University, Warsaw, Poland.

 0021-8979/87/213791-08$02.40

(100) being in the direction of applied stress. Each sample used in the experiment had its own reference sample cut in the immediate vicinity from the same crystal. The reference samples have undergone the same thermal treatment as the deformed specimens to precisely determine the effects of deformation.

The samples for capacitance measurements were lapped and chemically polished, and immediately afterward were placed in the evaporator. For n- and p-type GaAs the metal-semiconductor Schottky diodes were formed by evaporation of gold and aluminum, respectively. All diodes were carefully tested for the leakage current density and the breakdown voltage.

B. Plastic deformation

Deformation, in a compression mode, was performed at 400 °C in an "Instron" tensile machine equipped with a load cell. The sample with the length l_0 of 7 mm, was placed between two alumina cylinders located inside the resistance furance which controlled the sample temperature within 5 °C. Deformation was realized by compressing the sample at a constant rate dl/dt of 0.05 mm/min. The load cell was used to monitor the applied force. All samples used in this study showed a gradual increase in the compression stress and a monotonic decrease of the length. The samples with irregular response to deformation were rejected from further study since they might have contained internal cracks. The degree of deformation $\Delta l/l_0$ was determined by careful measurements of sample length l_0 before and l_1 after deformation. For easy comparison a deformation was realized in all three directions, (100), (110), and (111), employed in previous studies.[10–22] The degree of deformation $\Delta l/l_0$ was varied between 0% and 4%.

C. Characterization

Plastically deformed and reference samples were subjected to identical electrical and optical characterization. Thus, the electrical conductivity and Hall-effect measurements were performed using van der Pauw configuration. Optical absorption measurements were done with a near-infrared high-resolution spectrometer. The sample was placed on a cold finger in a variable temperature liquid-He cryostat. Absorption spectra were measured using very low-intensity incident light in order to prevent EL2 transfer into the metastable state. Deep-level characterization was carried out with standard deep-level transient capacitance measurements using a box-car averager. Optical deep-level transient capacitance spectroscopy was also employed for the hole trap determination in n-type GaAs. Deep levels in semi-insulating GaAs were analyzed by the thermally stimulated current technique. Low-temperature photoluminescence measurements were carried out on deformed and reference samples. They showed no detectable contamination with common transition-metal impurity acceptors Cu and Mn after the heat treatment involved in a plastic deformation.

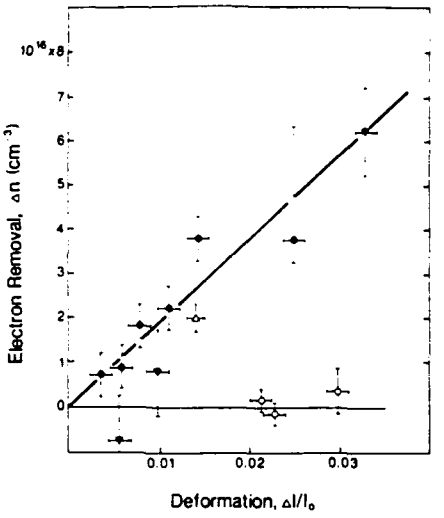

FIG. 1. Electron removal Δn vs the degree of deformation $\Delta l/l_0$. Full circles and full triangles correspond to n-type samples deformed along (111) and (110) directions, respectively. Open circles correspond to p-type samples deformed in the (111) direction. Open triangle denotes the magnitude of electron removal from EL2 in the (100) direction.

III. RESULTS AND DISCUSSION

A. Free-carrier concentration

Plastic deformation results in a significant decrease of the free-electron concentration n in n-type samples; however, it has only a minor effect on the free-carrier concentration in semi-insulating GaAs and practically no effect on the free-hole concentration p in p-type GaAs. The net decrease in the majority-carrier concentration determined at 300 K from Hall-effect and conductivity measurements is given in Fig. 1 as a function of the deformation $\Delta l/l_0$.

For n-type samples electron concentration decreases linearly with deformation. The same qualitative trend was observed previously for GaAs plastically deformed[14] or irradiated with electrons.[23] It was tentatively interpreted as a result of the creation of new acceptor-type defects. These stress-induced acceptors N_A would compensate shallow donors N_D, causing a decrease in the electron concentration, $n = N_D - N_A$. In addition, the negatively charged, filled acceptors should increase the ionized impurity scattering, leading to a decrease in the electron mobility. Indeed, in deformed samples a large decrease of electron mobility, μ_n, was observed. For example, for $\Delta l/l_0 = 0.014$ the 300-K mobility μ_n dropped to 1900 cm^2 V s from 3800 cm^2/V s prior to deformation (Table I). According to the GaAs mobility table from Ref. 24, this would correspond to an increase of the total concentration of the ionized centers by about

TABLE I. Effect of plastic deformation on 300-K free-carrier concentration and mobility.

	Before deformation	After deformation	$\Delta l/l_0$(%)
n (cm^{-3})	5.0×10^{16}	3.1×10^{16}	1.5
μ_n (cm^2/V s)	3800 ± 200	1900 ± 200	
p (cm^{-3})	3.1×10^{16}	3.5×10^{16}	2.9
μ_p (cm^2/V s)	160 ± 40	190 ± 40	

5×10^{17} cm^{-3}. This concentration appears much too high, and the low mobilities in deformed crystals must result from inhomogeneous distribution of stress-induced scattering centers, and possibly also from the scattering of free carriers by dislocations. The profound effect of macroscale inhomogeneities on the Hall-effect mobility in GaAs was recently demonstrated in Ref. 25. The mobility increase in deformed samples after thermal annealing (which eliminates deformation-induced acceptors) implies that mobility-limiting inhomogeneities are due to nonuniform distribution of stress-induced acceptors.

For p-type samples (open circles in Fig. 1) no significant change in hole concentration was observed. This behavior is consistent with the interpretation for n-type samples providing that the stress-induced acceptors are sufficiently deep not to be ionized in p-type material. From the Fermi energy $E_F - E_v \simeq 0.2$ eV in our samples we conclude that the acceptors must be located at energy exceeding 0.2 eV above the valence band. As electrically neutral these acceptors have no effect on the hole concentration, $p = N_A - N_D$. From the results for p-type GaAs we also conclude that no donor-type defects are introduced by plastic deformation in the same energy range ($\gtrsim 0.2$ eV above the valence band). In p-type material such donors would be ionized, causing a decrease in the free-hole concentration $\Delta p \simeq -\Delta N_D$, in contrast with an experimental observation that $\Delta p \simeq 0$.

Electronic transport in SI GaAs is by far more sensitive to electrical inhomogeneities than that in conducting crystals (due to the lack of free-carrier screening of localized potentials). Accordingly, the deformation-induced changes in electronic characteristics of SI GaAs were determined employing the optical method[26] for determination of the Fermi energy and free-carrier concentration from low-temperature measurements of the zero phonon line of the EL2 intracenter absorption.[27,28] Detailed results are discussed in the subsequent section. We conclude from them that as a result of plastic deformation, the Fermi energy in SI GaAs drops down below the middle of the energy gap. Electron concentration decreases and for a higher degree of deformation the material becomes lightly p type. However, in absolute scale Δp and Δn are only of the order of 10^7 cm^{-3}. However, in SI GaAs the deformation-induced acceptors are ionized; they are expected to be compensated by an increased degree of ionization of the midgap EL2 donor ($\Delta n_{EL2} \simeq N_A$) rather than by a change in the free-carrier concentration.

Thus, it is seen that the effects of plastic deformation on the free-carrier concentration are all consistently explained in terms of deformation-induced deep acceptors. They also strongly imply that no donor levels (including the arsenic antisite As_{Ga} defect expected to act as a double donor) are introduced in GaAs by plastic deformation.

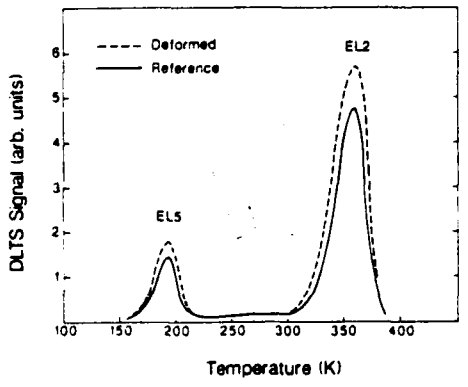

FIG. 2. DLTS spectra corresponding to electron traps in deformed and reference samples of n-type GaAs. Gate settings $t_1/t_2 = 20$ ms/40 ms.

B. Deep-level transient spectroscopy

Typical DLTS spectra of deformed and reference samples are presented in Fig. 2. They show EL2 and EL5 electron traps typical for melt-grown GaAs. However, no new electron traps were detected in deformed samples under the same experimental conditions; the DLTS peak heights in deformed samples were larger than in reference samples. Total capacitance values of the diodes were also changed after deformation. Both of these changes were caused by a decrease in the net concentration of ionized centers ($N_D - N_A$). When the correction factors[28] for the conversion of DLTS peak heights to the trap concentration were taken into account, the same values of EL2 and EL5 concentrations were found in deformed and reference samples. Identical behavior was observed for all three deformation directions, (100), (110), and (111). An estimated 10% uncertainty in DLTS measurements of EL2 concentration yielded an experimental error $\Delta N_{EL2} \simeq \pm 2\times10^{15}$ cm^{-3}. The deformation-induced EL2 concentration changes previously reported for deformed epitaxial layers[14] and horizontal Bridgmann crystals[10] fall within this range. Therefore, one can safely estimate the upper limit for changes in EL2 concentration upon plastic deformation $\Delta l/l_0$ up to 3% to be $\Delta N_{EL2} < 2\times10^{15}$ cm^{-3}. To our knowledge, the results in Ref. 13 (clearly inconsistent with all other published data) are the only exception to this rule.

C. Optical DLTS measurements

Hole traps located in the lower half of the energy gap were studied employing optical DLTS (ODLTS). Optical pulses filling the traps with photoexcited minority carriers were provided by the chopped light from a YAG cw laser. The main limitation of this method is that the light does not fill the traps completely. The equilibrium occupation of the trap in the depletion region under intense illumination is $p_t = N_t\sigma_n/(\sigma_n + \sigma_p)$, where σ_p and σ_n are photoionization cross sections for holes and electrons, respectively. Since $\sigma_n/(\sigma_p + \sigma_n) < 1$, the peak heights in ODLTS spectra underestimate the absolute value of the trap concentration, N_t. However, the peak height can be reliably used to measure a relative change in the concentration of a given trap and to estimate the lower limit of trap concentration.

The typical ODLTS spectra of deformed and reference n-type samples are shown in Fig. 3. Both electron and hole traps were observed as positive and negative peaks, respectively. The position of the major electron trap coincides with the EL2 peak in the DLTS spectrum measured at the same gate setting $t_1/t_2 = 20$ ms/40 ms. The hole trap spectrum for

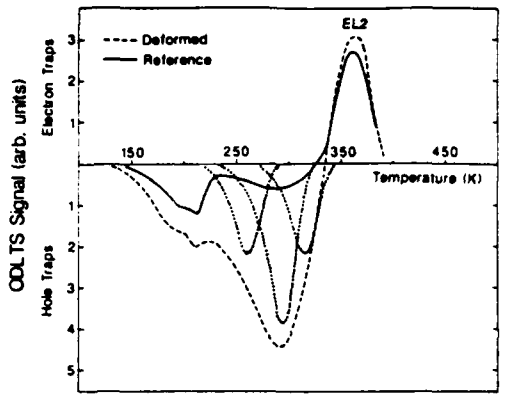

FIG. 3. Optical DLTS spectra in deformed and reference samples of n-type GaAs. Components of deconvoluted hole trap ODLTS peak are shown with dotted curves. Gate settings $t_1/t_2 = 20$ ms/40 ms.

the reference sample shows only two bands from 150 to 220 K and between 250 and 330 K, respectively. The spectrum of the deformed crystal is dominated by a large wide band peaked at about 290 K (gate setting 20 and 40 ms). As shown in Fig. 3, the total ODLTS band between 200 and 350 K can be deconvoluted into three components with peaks at 320, 290, and 260 K. The corresponding emission rate activation energy could be estimated only for a dominant 290-K peak. This estimation, $E_A \simeq 0.45$ eV, carries a large error of about ± 0.1 eV due to overlapping of the peaks which limits a temperature range useful for construction of individual Arhennius plots. This trap is similar to the deformation-induced hole trap H_B reported in Ref. 10. The slight difference in DLTS peak position is due to a different gate setting ($t_1/t_2 = 1.95$ ms/7.8 ms) used in Ref. 10.

As shown in Fig. 4, the concentration of this trap increases linearly with deformation. As pointed out above, ODLTS does not give the absolute value of the trap concentration, but only its lower limit. For the 0.45-eV trap this limit is about 1×10^{16} cm^{-3} for $\Delta l/l_0 = 2\%$. A similar estimation for the combined concentration of other deformation-induced traps (i.e., the components of the deconvoluted spectrum in Fig. 3) yields the value $> 1.5\times10^{16}$ cm^{-3}. Total hole trap concentration $\gtrsim 2.5\times10^{16}$ cm^{-3} at $\Delta l/l_0 = 2\%$ is in good agreement with the total acceptor concentration $N_A \simeq 4\times10^{16}$ cm^{-3} required to account for the electron removal data shown in Fig. 1.

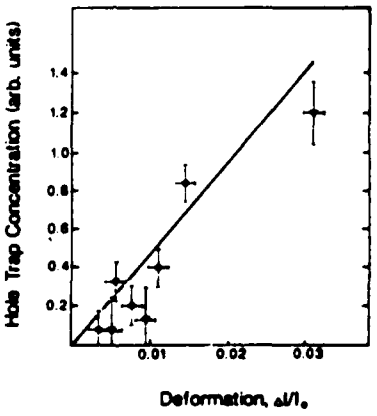

FIG. 4. Concentration of the dominant deformation-induced hole trap (ODLTS peak at about 290 K) vs the deformation $\Delta l/l_0$.

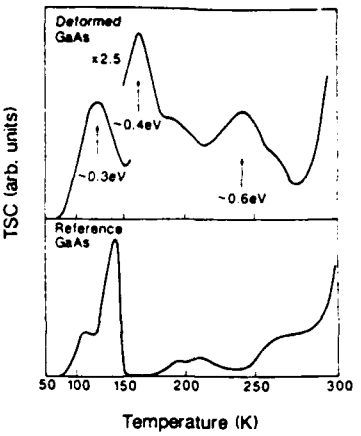

FIG. 5. Thermally stimulated current spectra of deformed (upper spectrum) and reference (lower spectrum) samples of SI GaAs.

D. Thermally stimulated current

The thermally stimulated current (TSC) method is especially useful for the study of electron and hole traps in high-resistivity materials[29] where standard DLTS and capacitance ODLTS are not readily applicable. The method employs optical excitation of excess carriers at low temperature. Subsequent continuous temperature increase in the dark leads to a release of carriers from traps and creates peaks of the electric current versus temperature.

TSC spectra of the deformed and reference samples are shown in Fig. 5. The presence of three new deformation-induced traps is evidenced by TSC peaks at 125, 160, and 240 K. These temperatures correspond roughly to trap energies of 0.3, 0.4, and 0.6 eV,[29] which is in good agreement with hole traps observed by the optical DLTS in deformed samples of n-type GaAs.

E. Optical absorption

Optical absorption spectra measured at 77 K on n-type GaAs samples undeformed and plastically deformed to different $\Delta l/l_0$ values are shown in Fig. 6. The spectrum of the reference sample is a typical EL2-related absorption observed in the melt-grown GaAs.[27,28,30] The near-infrared part of this spectrum originates from EL2 photoionization with the onset at about 0.8 eV. Intracenter EL2 transitions (shadowed area) for $1.0 < h\nu < 1.3$ eV superimposed on the photoionization background produce an absorption bulge around 1.2 eV. It is evident from Fig. 6 that the plastic defor-

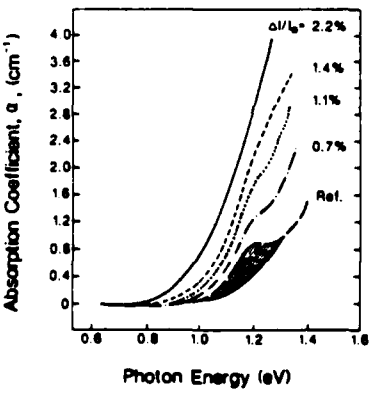

FIG. 6. 77-K optical absorption spectra of n-type GaAs for different deformation $\Delta l/l_0$. Dashed area on the spectrum of undeformed reference samples denotes the EL2 intracenter absorption.

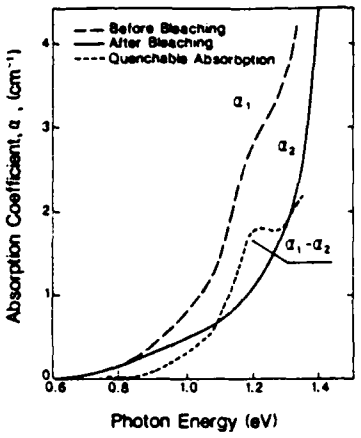

FIG. 7. Low-temperature (6 K) optical absorption spectra of n-type GaAs deformed to $\Delta l/l_0 = 2.2\%$.

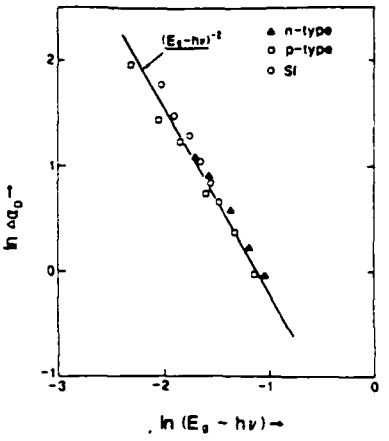

FIG. 9. Energy dependence of the deformation-induced unquenchable change in the optical absorption coefficient. Points, experimental; line, theoretical dependence for optical absorption due to dislocations.

mation significantly changes an overall shape of the absorption spectrum, introducing a featureless absorption background which increases monotonically toward the energy gap. The EL2 contribution to absorption in deformed samples can still be separated using optical quenching at low temperature which transfers the EL2 into an optically inactive metastable state. The quenchable absorption (i.e., $\alpha_1 - \alpha_2$, in Fig. 7) corresponds to EL2 while the unquenchable part (α_2 in Fig. 7) corresponds to other absorption processes. Employing optical quenching by a strong white light illumination for 10 min at 6 K we have found that for all plastically deformed n-type samples, the spectral shape and the intensity of the quenchable part ($\alpha_1 - \alpha_2$) were the same as that for the reference sample. The monotonically increasing (with $h\nu$) absorption component (α_2 in Fig. 7) became clearly visible after quenching of the absorption.

The magnitude of quenchable absorption and total absorption change $\Delta\alpha = \alpha(1.2\,\text{eV}) - \alpha(0.7\,\text{eV})$ are shown in Fig. 8. The quenchable absorption remains constant over the entire deformation range. However, the total absorption change, $\Delta\alpha$, increases linearly with the deformation $\Delta l/l_0$. Without spectral measurements combined with optical quenching, the increase of $\Delta\alpha$ could easily be taken as apparent proof of the increase in EL2 concentration. [Note that it is a standard practice in GaAs to assume that the entire sub-band-gap absorption originates from EL2. Thus, the difference in absorption for two photon energies $\Delta\alpha = \alpha(1.2\,\text{eV}) - \alpha(0.7\,\text{eV})$ is treated as a measure of the EL2 concentration.] In fact, the deformation-induced absorption change has nothing to do with either EL2 or any other localized deep level. First of all, the same unquenchable absorption was observed in deformed samples—n type, semi-insulating, and p type, i.e., irrespective of the Fermi energy shift from the bottom of the conduction band to the top of the valence band. It is very unlikely that the spectral shape and the intensity of any photoionization in GaAs could remain the same when the level involved undergoes a change from occupied to empty. Secondly, as shown in Fig. 9, the deformation-induced absorption satisfies a specific spectral dependence $\Delta\alpha_D = K \times (E_g - h\nu)^{-2}$, incompatible with standard deep-level transitions.[31] However, this dependence was previously observed in plastically deformed direct band-gap semiconductors (GaAs and CdSe) and was explained in terms of a deformation potential model which considered a decrease in the energy gap E_g in the stress field of dislocations.[32]

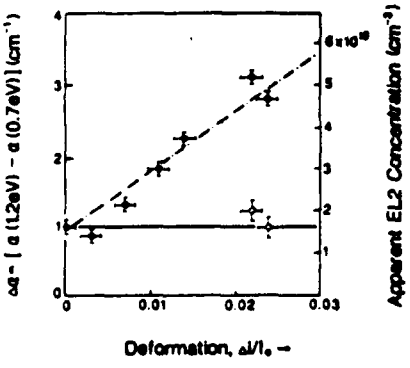

FIG. 8. Deformation-induced change in the absorption coefficient; total change, dark circle and broken line; EL2-related quenchable absorption, light circles and solid line. Measurements at 6 K.

F. 1.039-eV zero phonon line

Low-temperature high-resolution measurements of optical absorption have shown that the plastic deformation changes the shape and the intensity of the characteristic 1.039-eV zero phonon line (ZPL) located at the onset of the EL2 intracenter transition.[27] The results presented in Fig. 10 were obtained with semi-insulating GaAs deformed in the (100) direction with $\Delta l/l_0 = 0.013$. With respect to the undeformed sample the peak position is shifted to a slightly higher energy. In addition, the line broadens and it can be deconvoluted into three components. This behavior is consistent with the splitting pattern of the line under applied stress.[33] Thus, for the stress applied in the (100) direction

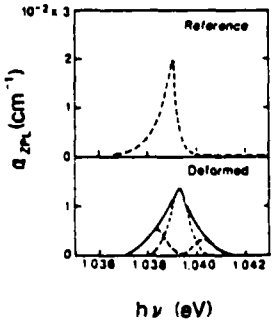

FIG. 10. High-resolution 6-K spectra of the zero phonon line of the EL2 intracenter absorption in SI GaAs. Upper spectrum, before deformation; lower spectrum, after deformation to $\Delta l/l_0 = 1.4\%$.

one expects a slight shift of the line to higher energy resulting from two unresolvable line components moving upwards in energy. The additional two components must result from stresses in the (111) and (110) directions (both of which split the line into high- and low-energy components) associated with the not exactly uniaxial character of plastic deformation. Residual stresses present in the sample after deformation may be associated with stress fields around dislocations discussed in conjunction with a deformation-induced optical absorption tail.

It should be noted that the presently observed behavior of the zero phonon line may account for an apparent complex character of the line in some of the crystals in terms of the stress-induced effects.

In n-type GaAs the broadening of ZPL is the only stress-induced effect. However, in semi-insulating crystals an additional phenomenon is observed which proves the importance of the deformation-induced shift of the Fermi energy. As discussed in detail elsewhere,[26] the liquid-He measurements of the zero phonon line in GaAs directly after cooling, α^1_{ZPL}, and after optical bleaching followed by 10-min annealing at 140 K, α^2_{ZPL}, yield the EL2 occupancy fraction $\eta \simeq \alpha^1_{\mathrm{ZPL}}/\alpha^2_{\mathrm{ZPL}}$. (This approach is based on the fact that the ZPL measures the concentration of occupied EL2 and that the complete transition to a metastable state leaves all EL2 in an occupied state.) As shown in Table II, the EL2 occupancy fraction in reference crystal is $\eta \simeq 0.95$, while after plastic deformation it drops down to about 0.45. The increase in ionized EL2 concentration, ΔN_{EL2}, must be equal to a net concentration of the ionized acceptors ΔN_A introduced by a deformation. The experimental point marked in Fig. 1 with an open triangle corresponds to this value.

It is of importance to note that the presently proven downward shift of the Fermi energy in deformed SI GaAs (caused by deformation-induced acceptors in the lower half of the energy gap) provides a missing link in explanation of the apparently conflicting findings: i.e., the lack of increase of the EL2 concentration and an increase in EPR signal of an ionized antisite defect As_{Ga} clearly related to EL2.[17,21,22] It is now evident that an increase of EPR signal results from an increase in the fraction of ionized As_{Ga} defects rather than the increase of the total antisite concentration.

G. Annealing

Plastically deformed samples, after characterization, were annealed at several temperatures between 600 and 900 °C. The annealing was performed in a closed quartz ampul with a controlled arsenic pressure, corresponding to equilibrium conditions. After annealing the samples were repolished and characterized again.

We found that prolonged annealing at 800 or 850 °C eliminated all deformation-induced changes in electrical properties. The most important effect of annealing was perhaps the total disappearance of the 0.45-eV hole trap. The ODLTS spectrum of the deformed and subsequently annealed sample (10 h at 850 °C) was virtually identical to the reference sample shown in Fig. 2(b). According to the discussion in Sec. III A and III B, this acceptor clearly contributes to free-electron removal and possibly also to a decrease in electron mobility. In fact, after annealing, the carrier concentration and the mobility recovered to their predeformation values.

DLTS and optical absorption measurements have led to a new observation of a decrease in the EL2 concentration during annealing of deformed samples. Figure 11 presents the results of optical absorption measurements on deformed and annealed samples. All spectra show a consistent trend, namely, the EL2 absorption band steadily decreases with increasing deformation $\Delta l/l_0$. For samples deformed by 1.4%, only half of the original EL2 absorption is preserved. The samples used in those measurements were all n type after annealing with carrier concentration in the 10^{16}-cm^{-3} range. Therefore, all EL2 centers were filled with electrons, and consequently the decrease of the absorption band was a direct measure of the decrease in the EL2 concentration.

Similar results were also obtained with DLTS. They are summarized in Fig. 12 together with the results from optical measurements. It is clear that although deformation itself does not change the EL2 concentration, subsequent annealing of deformed samples leads to partial EL2 annihilation. Because in undeformed samples the EL2 defect was stable up to 900 °C, this annihilation must result from the interaction of EL2 with stress-induced defects, dislocations, and/or native defects. The exact nature of this interaction is not known at present.

IV. SUMMARY AND CONCLUSIONS

The introduction of deep acceptors is the most important primary effect which is responsible for most of the deformation-induced changes in electronic properties of GaAs. In n-type GaAs the acceptors are ionized. They compensate shallow donors causing the free-electron removal. The presence of ionized acceptors decreases the electron mobility value due in part to increased ionized impurity scattering and in part to inhomogeneities associated with nonuniform distribution of the acceptors. As long as the deformed GaAs remains conducting n type, the midgap EL2 donor is completely occupied. Accordingly, no change in the characteristic quenchable EL2 absorption band is observed after deformation of n-type GaAs. However, the deformation

TABLE II. Effect of deformation on EL2 occupation in SI GaAs deduced from the zero phonon line absorption.

Sample	Deformation $\Delta l/l_0$(%)	EL2 occupancy fraction $\eta = \alpha^1_{\mathrm{ZPL}}/\alpha^2_{\mathrm{ZPL}}$	Fraction of EL2 ionized $(1-\eta)$	Net concentration of ionized acceptors (cm^{-3})
As-grown	0	0.95	0.05	2.0×10^{15}
Deformed	1.4	0.45	0.55	2.0×10^{16}

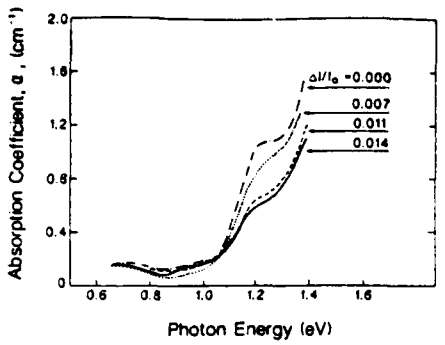

FIG. 11. 77-K optical absorption spectra of deformed n-type samples annealed at 850 °C for 10 h.

produces a featureless unquenchable absorption tail $\Delta\alpha_D$, which extends well into the subband-gap region. In Refs. 17 and 21 this absorption tail was considered to be due to transitions via localized levels of the arsenic antisite As_{Ga} defect introduced by deformation. We found no evidence supporting this interpretation. On the contrary, the characteristic spectral dependence $\Delta\alpha_D \sim (E_g - h\nu)^{-2}$ is consistent with "the dislocation absorption" which is due to energy gap changes in the stress field of dislocations.

In p-type GaAs the deformation causes no change in the concentration of free holes and had no effect on the free-carrier mobility. Results obtained with p-type GaAs also prove that no donors are produced by plastic deformation at energies higher than 0.2 eV above the valence band. This conclusion received further support from DLTS data which showed no new electron traps and no appreciable change in concentration of any electron traps present prior to the deformation. Therefore, we must reject the hypothesis of Refs. 17 and 21 that the donor-type arsenic antisite defect As_{Ga} is created during the plastic deformation. For similar reasons, we also reject the hypothesis of Refs. 18 and 19 of the creation of the arsenic interstitial As_I donor with energy level about 0.77 eV below the conduction band. Both of these hypotheses were postulated to explain the increase in the EPR quadruplet signal in plastically deformed GaAs. Present results fully support the very recent explanation of this effect by Bray in Ref. 22 in terms of the increased ionization of As_{Ga} brought about by the compensating action of the deformation-induced acceptors. Our measurement of the zero phonon line in SI GaAs provided the first direct evidence of the increased ionization of the midgap donor EL2 (related to the antisite defect As_{Ga}) in deformed crystals.

Thermal annealing experiments showed that the deformation-induced acceptors fully anneal out at temperatures of about 800 °C. However, the annealing also takes place at lower temperatures > 600 °C. The EL2 concentration in deformed samples was found to decrease during annealing. The unique mechanism of this process cannot be formulated at present. We are also unable to identify the origin of the native acceptors induced by deformation. However, it is possible that the EL2 annihilation may result from the interaction of As_{Ga} with native defects containing a gallium vacancy. An acceptor-type gallium vacancy may also be a constituent of defects responsible for the deformation-induced native acceptors. Further studies are obviously needed to identify the pertinent defects and their interaction.

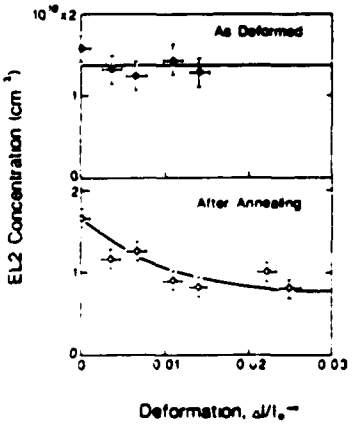

FIG. 12. EL2 concentration vs the degree of deformation $\Delta l/l_0$ for as-deformed samples (upper figure) and after 850 °C annealing for 10 h (lower figure).

ACKNOWLEDGMENTS

The authors are grateful to Dr. W. Walukiewicz for valuable discussions. They are also grateful to the U.S. Air Force Office of Scientific Research and to Sumitomo Electric Industries, Ltd. for financial support.

[1] A. S. Jordan, R. Caruso, A. R. Von Neida, and J. W. Nielsen, J. Appl. Phys. 52, 3331 (1981).
[2] A. S. Jordan, A. R. Von Neida, and R. Caruso, J. Cryst. Growth 70, 555 (1984).
[3] A. S. Jordan, R. Caruso, and A. R. Von Neida, Bell Sys. Tech. J. 59, 593 (1980).
[4] T. Obokata, T. Matsumura, K. Terashima, F. Orito, T. Kikuta, and T. Fukuda, Jpn. J. Appl. Phys. 23, L602 (1984).
[5] M. R. Brozel, I. Grant, R. M. Ware, and D. J. Stirland, Appl. Phys. Lett. 42, 610 (1983).
[6] D. E. Holmes and R. T. Chen, J. Appl. Phys. 55, 3588 (1984).
[7] Y. Matsumoto and H. Watanabe, Jpn. J. Appl. Phys. 21, L515 (1982).
[8] S. Miyazawa, T. Mizutani, and H. Yamazaki, Jpn. J. Appl. Phys. 21, L542 (1982).
[9] Y. Nanishi, S. Ishida, T. Honda, H. Yamazaki, and S. Miyazawa, Jpn. J. Appl. Phys. 21, L335 (1982).
[10] T. Isida, K. Maeda, and S. Takeuchi, Appl. Phys. 21, 257 (1980).
[11] T. Wosinski, Phys. Status Solidi A 60, K149 (1980).
[12] W. E. Weber, H. Ennen, U. Kaufman, J. Windscheif, J. Scheider, and T. Wosinski, J. Appl. Phys. 53, 6140 (1982).
[13] T. Wosinski, A. Morawski, and T. Figielski, Appl. Phys. A 30, 233 (1983).
[14] F. Hasegawa, N. Yamamoto, and Y. Nannichi, Extended Abstracts of the 16th Conference on Solid State Devices and Materials, Kobe, Japan, 1984, p. 169.
[15] S. Benakki, A. Goltzene, C. Schwab, Wang Guangyu, and Zou Yuanxi, Phys. Status Solidi B 138, 143 (1986).
[16] D. Gerthsen, Phys. Status Solidi A 97, 527 (1986).
[17] E. R. Weber, in *Semi-insulating III-V Materials*, edited by D. C. Look and J. S. Blakemore (Shiva, Nantwich, England, 1984), p. 296.
[18] K. Sumino, in *Defects and Properties of Semiconductors*, edited by J. Chikawa, K. Sumino, and K. Wada (KTK Scientific, Tokyo, Japan, 1987), Chap. 1.
[19] M. Suezawa and K. Sumino, Jpn. J. Appl. Phys. 25, 533 (1986).
[20] L. Samuelson, P. Omling, E. R. Weber, and H. G. Grimmeis, in *Semi-insulating III-V Materials*, edited by D. C. Look and J. S. Blakemore (Shiva, Nantwich, England, 1984), p. 268.
[21] P. Omling, E. R. Weber, and L. Samuelson, Phys. Rev. B 33, 5880 (1986).
[22] R. Bray, Solid State Commun. 60, 867 (1986); E. R. Weber, Solid State Commun. 60, 871 (1986).
[23] F. Yamaguchi and C. Ventura, J. Appl. Phys. 57, 604 (1985).
[24] W. Walukiewicz, J. Lagowski, L. Jastrzebski, M. Lichtensteiger, and H. C. Gatos, J. Appl. Phys. 50, 899 (1979).

[25]W. Walukiewicz, Le Wang, L. M. Pawlowicz, J. Lagowski, and H. C. Gatos, J. Appl. Phys. **59**, 3144 (1986).
[26]J. Lagowski, M. Bugajski, M. Matsui, and H. C. Gatos, Appl. Phys. Lett. **51**, 511 (1987).
[27]M. Kaminska, M. Skowronski, J. Lagowski, J. M. Parsey, and H. C. Gatos, Appl. Phys. Lett. **43**, 302 (1983).
[28]M. Skowronski, J. Lagowski, and H. C. Gatos, J. Appl. Phys. **59**, 2451 (1986).
[29]G. M. Martin, in *Semi-Insulating III-V Materials*, edited by G. J. Rees (Shiva, Orpington, UK, 1980), p. 13, and references therein.
[30]G. M. Martin, Appl. Phys. Lett. **39**, 747 (1981).
[31]G. Lucovsky, Solid State Commun. **3**, 209 (1965).
[32]A. V. Bazhenov and L. L. Krasil'nikova, Sov. Phys. Solid State **26**, 356 (1984).
[33]M. Kaminska, M. Skowronski, and W. Kuszko, Phys. Rev. Lett. **55**, 2204 (1985).

Inst. Phys. Conf. Ser. No. 91: Chapter 3
Paper presented at Int. Symp. GaAs and Related Compounds, Heraklion, Greece, 1987

LPEE growth and characterization of $In_{1-x}Ga_xAs$ bulk crystals

T. Bryskiewicz,* M. Bugajski,** B. Bryskiewicz, J. Lagowski and H.C. Gatos

Massachusetts Institute of Technology, Cambridge, MA 02139, USA

ABSTRACT: A novel procedure for liquid phase electroepitaxial (LPEE) growth of highly uniform multicomponent bulk crystals has been developed and successfully applied to the growth of high quality bulk $In_{1-x}Ga_xAs$ crystals. $In_{1-x}Ga_xAs$ ingots 14 mm in diameter and up to 3 mm thick were grown on (100) InP substrates. In terms of homogeneity, electrical characteristics, and defect structure they are comparable to high quality thin LPE layers.

1. INTRODUCTION

Liquid phase electroepitaxy is a solution growth technique in which the growth process is induced and sustained solely by passing a direct electric current across the solution-substrate interface while the temperature of the overall system is maintained constant (Bryskiewicz 1986 and references therein). It has been found that after initial stages of growth the solute electrotransport towards the interface becomes the dominant driving force for the growth (Bryskiewicz 1978, Jastrzebski et al 1978, Bryskiewicz et al 1980). Therefore, within a few minutes after an electric current is turned on the growth proceeds under isothermal and steady-state conditions. These features of electroepitaxy have proven (both experimentally and theoretically) to be uniquely suited for the growth of ternary and quaternary semiconductor compounds with constant composition (Daniele 1981 Bryskiewicz et al 1980). $Ga_{1-x}Al_xAs$ wafers as thick as 600 μm (Daniele et al 1981), $GaAs_{1-x}Sb_x$ (Biryulin et al 1983), $In_{1-x}Ga_xP$ (Daniele et al 1983), and $Hg_xCd_{1-x}Te$ (Vanier et al 1980) epilayers up to 200 μm, 120 μm, and 500 μm, respectively, grown by LPEE showed a remarkable uniformity of composition, varying by Δx=0.01-0.03 over their entire thickness. However, the growth procedures proposed thus far (Daniele et al 1981, Nakajima 1987) are suitable for the growth of uniform wafers a few hundred microns thick.

In this paper a novel procedure, useful for electroepitaxial growth of bulk crystals (several millimeters thick) of ternary and quaternary semiconductors is proposed. This novel procedure is successfully applied to the growth of high quality $In_{1-x}Ga_xAs$ bulk crystals.

2. NOVEL LPEE GROWTH PROCEDURE

The growth of highly uniform $In_{1-x}Ga_xAs$ bulk crystals was carried out in a novel vertical LPEE apparatus (Bryskiewicz et al 1987a), employed recently

*On leave from Microgravity Research Associates, Inc., Midland, TX 79701, USA.
**On leave from Institute of Electron Technology, 02-668 Warsaw, Poland.

to the growth of epitaxial quality GaAs bulk crystals (Bryskiewicz et al 1987b). A schematic diagram of the growth cell used in our growth experiments is shown in Fig. 1. During electroepitaxial growth solution is contacted by the substrate at the bottom and the source material at the top. Thus, the crystallizing material driven by the electric current is deposited onto the substrate while the solution is being continuously saturated with the source material. A very important characteristic of the growth cell seen in Fig. 1 is the shape of a graphite source holder which allows the current to bypass the source material. This results in a minimization of the Joule heating for an arbitrary form (monocrystal, polycrystal, or chunks) of the source material. The requirements for the source are thus limited to the compositional homogeneity and the chemical composition fitted to the composition of the crystal to be grown. In order to achieve these source characteristics, a procedure for the preparation of a macroscopically homogeneous source material had to be developed.

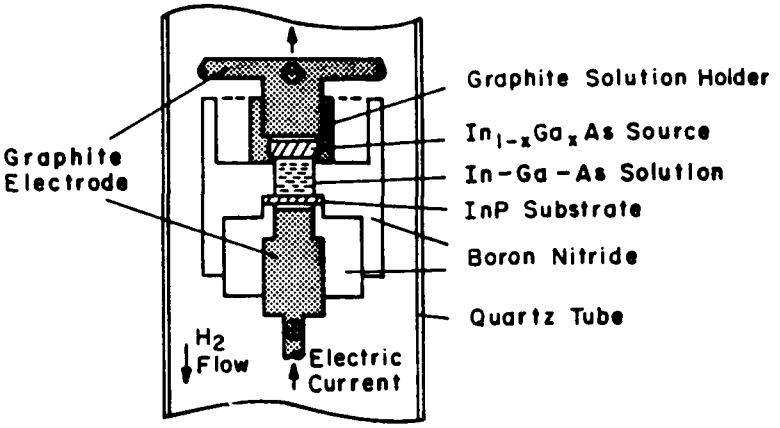

Fig. 1. Schematic diagram of the growth cell used for LPEE growth of $In_{1-x}Ga_xAs$ bulk crystals.

In this study the source material required for the growth of highly uniform $In_{1-x}Ga_xAs$ bulk crystals was prepared in a sealed quartz ampoule evacuated to 10^{-6} Tr. The inner wall of the quartz ampoule was covered with a pyrolytic carbon in order to prevent wetting. A semiconductor grade InAs-GaAs quasibinary mixture and a small amount of a high purity arsenic were sealed in the ampoule, heated up to about 20-30°C above the liquidus temperature and kept molten for one hour. High compositional homogeneity of the $In_{1-x}Ga_xAs$ source material was assured by rapid cooling of the ampoule. $In_{1-x}Ga_xAs$ bulk crystals with compositions between x=0.46 and x=0.48 were grown at 650°C on (100)-oriented, Sn-doped InP substrates. The grown ingots were 14 mm in diameter and up to 3 mm thick, i.e., suitable for slicing up to five wafers.

3. CRYSTAL CHARACTERIZATION

A microphotograph of the etch pits revealed on the (100)-oriented InP substrate and on the $In_{.52}Ga_{.48}As$ bulk crystal is seen in Fig. 2. Although the dislocation loops generation process is very likely to occur in this case near the surface, we did not observe any significant increase in the etch pit density between the InP substrate (EPD$\sim$.5-2x10^5cm^{-2}) and $In_{1-x}Ga_xAs$ crystals.

Electrical parameters of the $In_{1-x}Ga_xAs$ bulk crystals grown from unbaked In-rich solutions are shown in Table I. It is expected that the free electron concentration in the low 10^{16}cm^{-3} range can be reduced considerably by using higher purity solution components and/or by baking the solution prior to each run (Bhattacharya et al 1983). The 300°K mobility as high as 8000 cm^2/Vs and the 77°K mobility of about 13,000 cm^2/Vs is

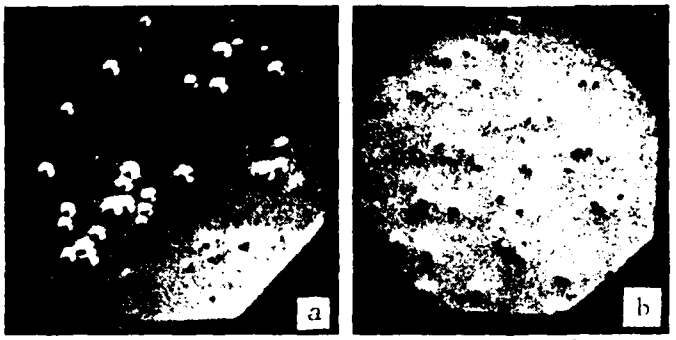

Fig. 2. Optical micrographs showing the typical etch pit pattern observed on (a) (100)-oriented InP substrate; (b) $In_{.52}Ga_{.48}As$ bulk crystal.

high homogeneity and structural perfection of the $In_{1-x}Ga_xAs$ ingots.

Table I. Electrical characteristics of LPEE $In_{1-x}Ga_xAs$ bulk crystals.

Composition (at.%)	Conductivity Type	Carrier Concentration (cm^{-3}) 300°K	77°K	Mobility (cm^2/Vs) 300°K	77°K
46	n	2.7×10^{16}	2.4×10^{16}	6240	13620
47	n	4.5×10^{16}	4.1×10^{16}	7780	11750
48	n	4.6×10^{16}	4.0×10^{16}	7640	13140

In addition, DLTS measurements did not reveal any measurable electron traps in these crystals.

Structural perfection as well as high compositional homogeneity of the $In_{1-x}Ga_xAs$ bulk crystals, comparable in quality with thin LPE layers, is documented by a high resolution photoluminescence (PL) spectrum shown in Fig. 3. This spectrum was recorded at 5°K for a nominally undoped n-type

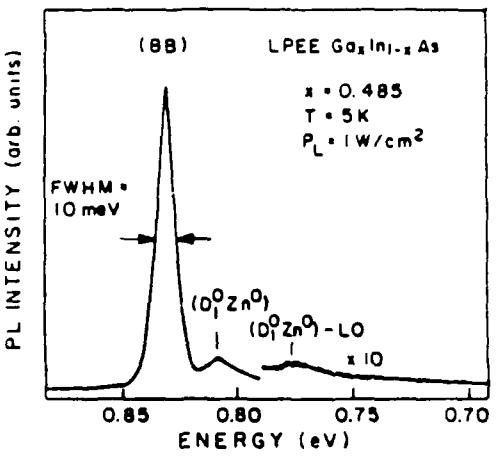

Fig. 3. 5°K PL spectrum of n-type $In_{.52}Ga_{.48}As$ grown on (100) InP substrate; $n = 4\times10^{16}cm^{-3}$.

LPEE $Ga_{.52}Ga_{.48}As$ crystal. The dominant line at 0.8303 eV corresponds to the band-to-band transitions (BB). The above assignment was made on the basis of the line shape and the luminescence intensity vs. excitation density dependence (which appeared to be nearly quadratic). As seen in Fig. 3, the full width at half maximum (FWHM) of the (BB) line is equal to 10 meV. This value can be understood in terms of alloy broadening due to the random distribution of the In and Ga cations. From the model developed for $Al_xGa_{1-x}As$ (Schubert et al 1984) the alloy broadening of the BB transitions in $In_{1-x}Ga_xAs$ has been estimated to be in the 9.2-13.7 meV range. The spread in the calculated FWHMs results mainly from the uncertainties of the values of the heavy hole mass and band discontinuity at the $In_{1-x}Ga_xAs$/InP heterointerface. Nevertheless, an overall agreement between theory and experiment is satisfactory.

The second line in Fig. 3 located 20.4 meV below the (BB) peak is due to the presence of the residual Zn acceptor, and it corresponds to the donor-

acceptor (DA) type of transitions. The binding energy E_A of the Zn acceptor estimated from the line position in different samples is E_A=20.6-21.5 meV, in close agreement with E_A=22±1 meV reported by Goetz et al (1983).

The measurements of the (BB) peak position were used to determine the compositional variations vs. a distance from the substrate and along the crystal surface. The results are shown in Fig. 4a and b, respectively. An excellent compositional homogeneity of the $In_{1-x}Ga_xAs$ ingots, both perpendicular and parallel to the growth direction, is evident. In both cases the composition fluctuations do not exceed 1%.

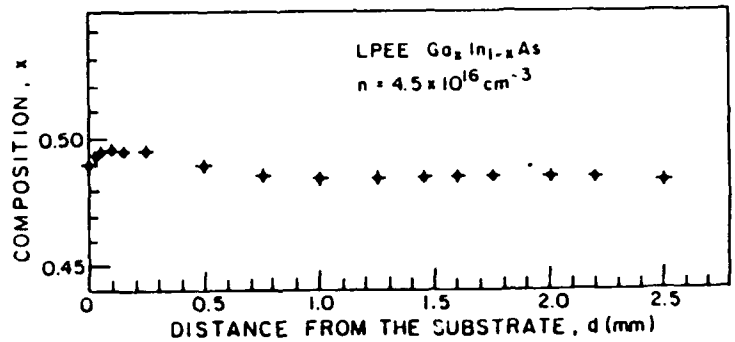

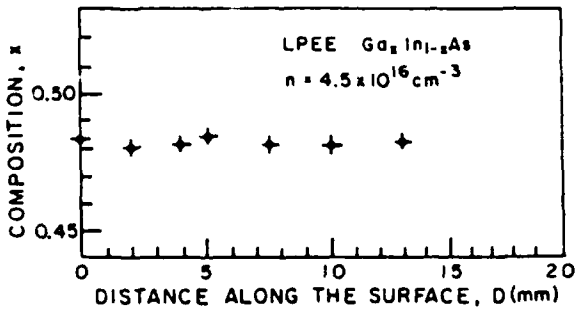

Fig. 4. Composition profile of $In_{.52}Ga_{.48}As$ obtained from PL measurements:

(a) along the growth direction

(b) perpendicular to the growth direction.

The authors are grateful to Microgravity Research Associates, Inc., and to the Air Force Office of Scientific Research for financial support.

4. REFERENCES

Bhattacharya P K, Rao M V and Tsai M-J 1983 J. Appl. Phys. 54, 5096

Biryulin Y F, Golubev L V, Novikov S V and Shmartsev Yu V 1983 Sov. Tech. Phys. 9, 68 (Pis'ma Zh. Tekh. Fiz. 9, 155)

Bryskiewicz T 1978 J. Cryst. Growth 43, 567

Bryskiewicz T, Lagowski J and Gatos H C 1980 J. Appl. Phys. 51, 988

Bryskiewicz T 1986 Prog. Crystal Growth and Charact. 12, 29 (Pergamon)

Bryskiewicz T, Boucher Jr C F, Lagowski J and Gatos H C 1987a J. Cryst. Growth 82, 279

Bryskiewicz T, Bugajski M, Lagowski J and Gatos H C 1987b J. Cryst. Growth (to be published)

Daniele J J and Hebling A J 1981 J. Appl. Phys. 52, 4325

Daniele J J and Lewis A 1983 J. Electron. Mat. 12, 1015

Goetz K H, Bimberg D, Jurgensen H, Selders J, Solomonov A V, Glinski G F and Razeghi M 1983 J. Appl. Phys. 54, 4543

Jastrzebski L, Lagowski J, Gatos H C and Witt A F 1978 J. Appl. Phys. 49, 5909; 50, 7269 (1979)

Nakajima K 1987 J. Appl. Phys. 61, 4626

Schubert E F, Gobel E O, Horikoshi Y, Ploog K and Queisser H J 1984 Phys. Rev. B 30, 813

Vanier P A, Pollak F H and Raccah P M 1980 J. Electron. Mat. 9, 153

Native acceptor levels in Ga-rich GaAs

M. Bugajski,[a] K. H. Ko, J. Lagowski, and H. C. Gatos
Massachusetts Institute of Technology, Cambridge, Massachusetts 02139

(Received 25 July 1988; accepted for publication 30 September 1988)

A photoluminescence, photocapacitance, and thermal annealing study of Ga-rich GaAs has revealed the complex behavior of acceptor levels at 68–77 and 200 meV above the valence band. The concentration of all levels is enhanced by Ga-rich growth conditions, however, only the 77- and 200-meV levels formed preferably in *n*-type GaAs are consistent with a double-acceptor model of the gallium antisite defect. In *p*-type GaAs the 68-meV level associated with a different single-acceptor defect is dominant. It is argued that the inhibited formation of double-acceptor Ga_{As} defects in *p*-type crystals is caused by the Fermi-energy control of the defect formation.

INTRODUCTION

Two energy levels at 77 and 200 meV above the valence band are commonly found in GaAs grown from Ga-rich melts.[1–10] They were attributed to a double acceptor and extensively studied in conjunction with luminescence lines at 1.443, 1.32, and 1.283 eV. The 1.443- and 1.23-eV lines are of primary interest in this work. The 1.443-eV lines originated from free electron to neutral acceptor transition (e,A^0), while the 1.32-eV line involves transition to the ionized acceptor (e,A^-).[4–7] As discussed in Refs. 11 and 12, the origin of the third line (1.283 eV) is different. This line will not be discussed further. These levels also attracted a lot of attention as native acceptors potentially involved in a compensation scheme in semi-insulating (SI) GaAs. It has been suggested that the concentration ratio between the native donor EL2 (formed under As-rich conditions) and the acceptors (favored by gallium-rich conditions) determines the SI behavior of undoped GaAs grown from As-rich melt and the *p*-type behavior of crystals grown from Ga-rich melts. The isolated gallium antisite, Ga_{As}, double-acceptor defect was proposed to account for the presence of the levels. This interpretation appears to be the most widely accepted at present, however, the identification of the levels with Ga_{As} cannot be taken as unambiguously proven. Another origin of the shallower acceptor has also been suggested.[13,14] The present work was undertaken in order to clarify further the properties and the origin of native levels in Ga-rich GaAs. The results of combined measurements of photoluminescence (PL), photocapacitance spectroscopy, and standard deep-level transient spectroscopy (DLTS), exposed a serious interpretational conflict between photoluminescence data alone and results of transient capacitance spectroscopy.

EXPERIMENTAL RESULTS

The crystals were grown by the liquid-encapsulated Czochralski (LEC) method from nonstoichiometric melts with the aresenic atom fraction $\delta \equiv [As]/([As]+[Ga])$ ranging from 0.42 to 0.48. The value of δ changes during the growth process, and different segments of the ingot correspond to different δ values. A quantitative relation between the distance along the growth ingot, x (or the solidified fraction of the melt, f), and δ was calculated considering the normal freeze process of the binary compound and taking into account that the weight loss during the growth of GaAs is due to the loss of volatile arsenic (see Ref. 15). Undoped crystals grown from Ga-rich melts were slightly *p* type, consistent with previous results.[16] Crystals intentionally doped with Zn (*p* type) and Se (*n* type) were grown in order to vary the Fermi-level position in the energy gap.

For photoluminescence measurements samples were mounted on the cold finger of a variable temperature continuous flow liquid-helium cryostat. Luminescence was excited with the 514-nm line of an argon Ar^+ laser. The spectral resolution was in all cases better than 0.5 meV. Capacitance and photocapacitance transient measurements were performed on metal-semiconductor Schottky diodes prepared by evaporation of Au and Al on *n*- and *p*-type samples, respectively. For optical deep-level transient spectroscopy (ODLTS) the filling of traps with minority carriers was realized using 0.9-μm (1.31 eV) incident light. Measurements were carried out at temperatures 12–300 K. Standard DLTS spectra were also measured at temperatures between 4 and 400 K. Figure 1 shows the intensity [normalized to the bound exciton (BE) line] of characteristic PL lines: A 1 to 1.443 eV and A 2 to 1.320 eV [see the insert in Fig. 1(a)] plotted versus δ in *n*- and *p*-type crystals. Assuming that the A 1 and A 2 lines are due to free electron to acceptor transitions, the ionization energies of corresponding levels become 77 and 200 meV. Both peaks 1.443 and 1.320 eV are followed by equally spaced longitudinal optical (LO) phonon replicas. A 1 and A 2 lines are present in the spectra of all Ga-rich crystals, undoped *p* type and intentionally doped *n* and *p* type. Also, in all crystals the intensity of both lines increases with decreasing arsenic atom fraction in the melt. However, large systematic differences in the integrated (including phonon replicas) line intensity ratio $A\,1/A\,2$ are seen in *n*- and *p*-type crystals. As shown in Fig. 1(a), the ratio $A\,1/A\,2$ roughly equals 1 in the whole melt stoichiometry range studied. In *p*-type crystals the $A\,1/A\,2$ intensity ratio increases with decreasing δ and reaches a large value of about 10 for δ lower than 0.45 [see Fig. 1(b)].

A transient capacitance spectroscopy study showed two energy levels with the hole emission thermal activation energies of 70–80 and 200 meV, respectively, in all Ga-rich crystals. Similar to photoluminescence data, the concentration

[a] On leave from Institute of Electron Technology, Warsaw, Poland.

 0021-8979/89/020596-04$02.40

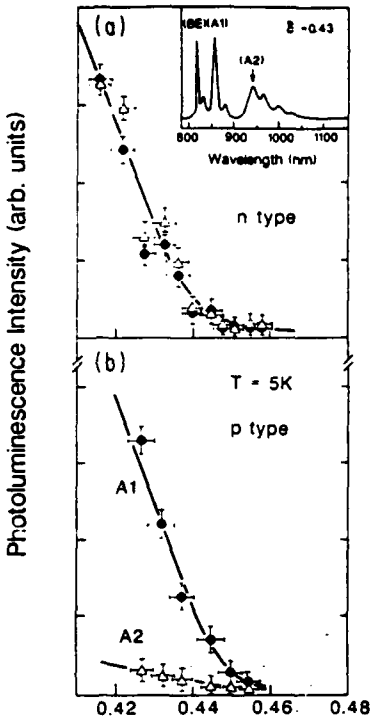

FIG. 1. Stoichiometry dependence of the intensity of characteristic PL lines: A 1 at 1.443 eV and A 2 at 1.320 eV in (a) n-type and (b) p-type crystals. Insert in (a) shows the typical low-temperature PL spectrum. The free-carrier concentration for all the samples was of the order of 10^{16} cm^{-3}.

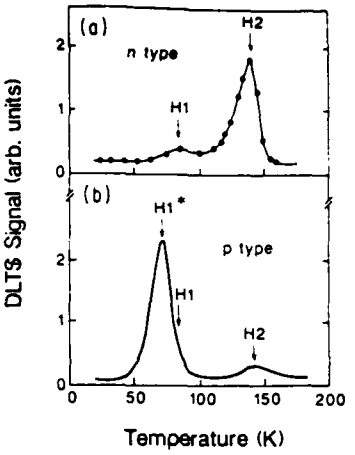

FIG. 2. ODLTS spectrum of (a) Ga-rich n-type crystal and DLTS spectrum of (b) Ga-rich p-type crystal. In both cases $\delta = 0.43$; $n,p \approx 10^{16}$ cm^{-3}.

of both levels increased with decreasing arsenic atom fraction in the growth melt. In n-type GaAs the levels were observed by optical deep-level transient capacitance spectroscopy using a minority-carrier optical filling pulse [see Fig. 2(a)]. In p-type GaAs the levels were observed as majority-carrier traps employing standard deep-level transient capacitance measurements [see Fig. 2(b)]. Transient capacitance spectra shown in Fig. 2 prove again a profound difference in the relative concentrations of the two hole traps in n- and p-type GaAs. Thus, the concentration ratio between the deep (200 meV) and the shallow traps (70–80 meV) in p-type crystals is significantly smaller than in n-type crystals. Transient spectroscopy data also indicate systematic differences in the lower temperature peak positions in n- and p-type GaAs. The hole emission rate, e_p, thermal activation plots ($e_p^{-1}T^2$ vs $1000/T$) yielded the values of activation energies of 68 ± 3 and 77 ± 3 meV in p- and n-type crystals, respectively.

This result and the differences in the concentrations of shallow and deep levels observed by transient capacitance and photoluminescence imply very strongly that the defect giving rise to the shallow trap and the A 1 photoluminescence line in n-type GaAs is not the same as the defect giving rise to corresponding features in p-type GaAs.

DISCUSSION

Before any futher analysis of the origin of the level we will once again address the question of photoluminescence characteristics. It should be emphasized that the photoluminescence data alone (i.e., without the DLTS data) can be explained very well in terms of a model assuming a common origin of the A 1 and A 2 lines and their association with two charge states of one and the same double-acceptor defect [i.e., $(-/0)$ and $(--/-)$ charge states, respectively]. Accordingly, the high-intensity ratios $A\,1/A\,2$ in p-type crystals can be attributed to the predominant presence of the defect in the neutral A^0 state, while the much higher intensity of the A 2 line in n-type crystals is readily explained by an increased fraction of the singly ionized A^- acceptor level.

The photoluminescence experiment which could differentiate between the case of identical and the case of different defects in n- and p-type GaAs is the dependence of A 1 and A 2 line intensities on the excitation density. It was found that in the n-type sample the A 1 line intensity depends quadratically on the excitation intensity, and the A 2 line intensity depends linearly on excitation. At very high excitation the A 1 line intensity becomes linear with excitation, and the ratio of $I_{(A2)}/I_{(A1)}$ becomes constant. In p type both lines A 1 and A 2 increase linearly with the excitation intensity. The excitation dependence of PL intensity in n-type samples is consistent with the double-acceptor model, while the behavior observed in p-type samples contradicts this model. In n-type GaAs the Fermi level is above both acceptor levels, and in thermal equilibrium (without excitation) acceptors are doubly ionized, i.e., in the A^{--} state. Thus for the (e,A^0) transition to occur, the center must trap two photoexcited holes. That gives a quadratic dependence of the (e,A^0)-A 1 line intensity on excitation as opposed to linear for the (e,A^-)-A 2 line, which requires trapping of only one photoexcited hole by the center. In p-type material presently investigated, the Fermi level was situated below the 77-meV level, and all centers were in the neutral, A^0, state. Thus, to facilitate the radiative transition (e,A^-) one would expect two photogenerated electrons would be needed. For the double-acceptor model the (e,A^-)-A 2 line intensity should depend quadratically on excitation, which is in contradiction to the experimental results the double-acceptor model must also be rejected in p-type GaAs based on the quantitative DLTS data. For two charge states of a double acceptor one would expect the concentration of the corresponding traps to be equal. As can be seen from Fig. 2(b), the magnitudes of the two DLTS peaks are significantly different. This result is in accord with the observation of Yu *et al.*,[3] who reported only one hole trap in p-type GaAs grown under Ga-rich conditions with energy of about 77 meV. We are unaware of any other DLTS study

indicating the presence of the deeper (200 meV) trap at concentrations comparable to that of the shallower trap (70–80 meV).

A completely different situation is observed in the ODLTS spectra of n-type samples. The spectrum shows two peaks, but the dominant one is the higher-temperature peak $H2$. Its position coincides exactly with the $H2$ peak position in p-type samples, whereas the $H1$ peak position is clearly shifted towards higher energies, compared to the $H1^*$ peak position in p-type samples. The much smaller height of the $H1$ peak which (assuming that the levels are due to two charge states of the double acceptor center, would correspond to the neutral charge state of the defect) does not reflect the actual concentration of the trap, but rather the smaller probability of removing the second electron from the center by means of optical illumination. Thus, one can conclude that ODLTS measurements on n-type material do not rule out the possibility that the defect in question is a gallium antisite double acceptor. We have also observed a different behavior of both levels in n- and p-type crystals subjected to thermal annealing. The experiments were carried out in a closed two-zone apparatus containing the samples and elemental arsenic in the hot and cold zones, respectively. All annealing experiments were carried out under equilibrium arsenic ambient pressure to prevent degradation of GaAs surface morphology caused by preferential arsenic evaporation. Two-step annealing was performed: (1) annealing at 1200 °C for 16 h followed by rapid (completed within several seconds) quenching to room temperature and (2) subsequent annealing at 800 °C for 4 h. The procedure was essentially the same as the one previously reported in Ref. 17. The properties of the crystals were reexamined after each annealing step. Photoluminescence spectra of n-type crystals, shown in Fig. 3(a), provide the evidence of almost complete elimination of the defect responsible for the 1.443- and 1.320-eV lines by 1200 °C annealing followed by rapid quenching. Subsequent annealing at 800 °C restores the characteristic PL lines to their previous intensity. Qualitatively different behavior is observed in p-type crystals [see Fig. 3(b)] where the characteristic PL emission after being eliminated by 1200 °C annealing cannot be brought back again. An important observation is that even if the absolute intensity of both lines in n-type material changes as a result of annealing, their ratio remains the same. This behavior again implies a direct relationship between the two levels.

The results of photoluminescence, DLTS and ODLTS measurements clearly show the difference between the behavior of n- and p-type crystals. As far as n-type crystals are concerned, all observed experimental characteristics of both levels, i.e., the stoichiometry and excitation intensity dependencies of two PL lines, and the ratio of ODLTS peak heights can be explained in terms of one double-acceptor defect, most likely, Ga_{As}.

The first systematic DLTS measurements on p-type crystals also showed the presence of both traps, however, the concentration of the $H2$ level was roughly an order of magnitude smaller than that of $H1^*$. The different activation energy, namely 68 meV in p-type crystals versus 77 meV in an n-type crystal of the level $H1^*$ has also to be noted. This,

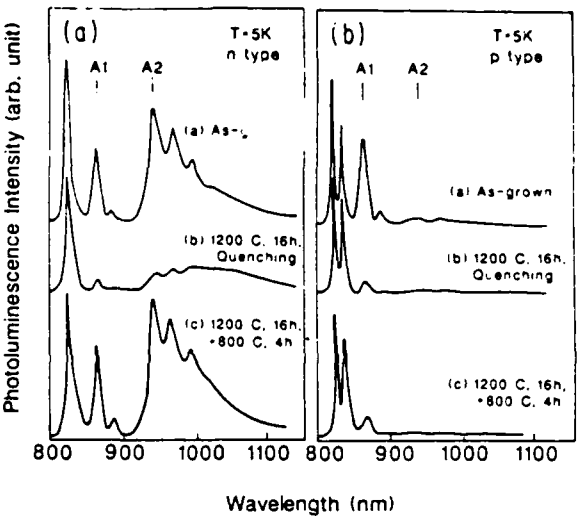

FIG. 3. Photoluminescence spectra of thermally annealed Ga-rich (a) n-type crystal and (b) p-type crystal. In both cases $\delta = 0.43$; $n,p \simeq 10^{15}$ cm^{-3}.

together with PL results showing a similar difference in integrated intensity of the $A1$ and $A2$ lines, as well as qualitatively different annealing behavior, apparently rules out the widely accepted interpretation. We conclude that the dominant defects giving rise to the levels in n-type crystals are different than those in p-type crystals. Both defects are enhanced by Ga-rich conditions, however, only those found in n-type material are likely to be due to gallium antisite double acceptors. The simplest possible explanation of these experimental findings relies on the assumption that defect formation is strongly influenced by Fermi energy. We propose the following scenario of events.

In n-type crystals, the defect which is likely to form upon solidification is the V_{Ga}-Ga_{As} pair. It can be created from the crystal containing a large amount of V_{As} by a single Ga atom hop, namely, $V_{As} \rightarrow V_{Ga} + Ga_{As}$. This pair reaction represents the transformation between a strong donor V_{As} and a strong acceptor $V_{Ga} + Ga_{As}$. Thus, the dependence of the reaction rate on Fermi energy is expected. Indeed, the theoretical calculation by Baraff and Schlüter[18] shows that the formation energy of the $V_{Ga} + Ga_{As}$ pair changes from positive in p-type to negative in n-type crystals. Despite the favorable conditions for $V_{Ga} + Ga_{As}$ pair formation in n-type crystals, we expect the dominant defect to be isolated Ga_{As} due to low binding energy of the above pair in n-type crystals as opposed to p type.[17]

In the p-type crystals the total abundance of isolated Ga_{As} should be much lower than in the n type, due to the positive formation energy of the V_{Ga}-Ga_{As} pair and the fact that once the pair is formed it tends to be stable. The concentration of the $H2$ (200 meV) level, which coincides exactly with the negative charge state of Ga_{As} observed in n-type material, has been estimated to be equal to 10^{14} cm^{-3} for $\delta = 0.43$. That of the $H1^*$ (68 meV) level in the same sample equals 4×10^{15} cm^{-3}. Therefore, the corresponding peak due to the neutral charge state of Ga_{As} which occurs at a temperature only slightly higher than $H1^*$ in the p-type crys-

tal [compare Figs. 2(a) and 2(b)] can be very easily masked by the last one. The microscopic origin of the H 1* (68 meV) level in p-type material is still disputable, however, we expect it to be related to the $(-/0)$ state of the single acceptor. That would reflect the general trend which inhibits the formation of double acceptors in p-type material. Recently, Yu, Look, and Ford[19] observed an acceptor level at 69 meV above the valence band in Ga-rich GaAs and attributed it to the $(-/0)$ charge state of V_{Ga}-Ga_{As}. Although the concentration of our H 1* level in p-type material is somewhat too high for that, this assignment in general fits our proposed scenario. Finally, we would like to comment on the fact that the positions of the A 1 line in PL spectra of n- and p-type crystal are almost the same(1.443 eV). This, although surprising at first glance, does not exclude a different origin of the A 1 line in both cases. In p-type crystals the donor-acceptor (D^0,A^0) transitions should dominate, whereas n-type crystals for electron concentration in the range of $10^{16}\,cm^{-3}$, (e,A^0)-type transitions dominate. Therefore, the activation energies of the levels involved in recombination are equal to 77 meV in n-type and 72 meV in p-type crystal, the last value being sufficiently close to 68 meV observed in DLTS.

CONCLUSION

In conclusion, we have found that the dominant native defects giving rise to the levels in n-type crystals are different than those in p-type crystals. Both defects are enhanced by Ga-rich conditions, however, only those found in n-type material are likely to be due to the gallium antisite double acceptor.

ACKNOWLEDGMENTS

The authors are grateful to the National Aeronautics and Space Administration and the Air Force Office of Scientific Research for financial support.

[1] P. W. Yu, D. E. Holmes, and R. T. Chen, Inst. Phys. Conf. Ser. No. 63, 209 (1982).
[2] P. W. Yu and D. C. Reynolds, J. Appl. Phys. 53, 1263 (1982).
[3] P. W. Yu, W. C. Mitchel, M. G. Mier, S. S. Li, and W. L. Wang, Appl. Phys. Lett. 41, 532 (1982).
[4] K. R. Elliott, Appl. Phys. Lett. 42, 274 (1983).
[5] W. J. Moore, B. V. Shanabrook, and T. A. Kennedy, in *Semi-Insulating III-V Materials*, Kah-nee-ta, 1984, edited by D. C. Look and J. S. Blakemore (Shiva, Nantwich, UK, 1984), p. 453.
[6] S. G. Bishop and B. V. Shanabrook, in *Semi-Insulating III-V Materials*, Kah-nee-ta, 1984, edited by D. C. Look and J. S. Blakemore (Shiva, Nantwich, UK, 1984), p. 302.
[7] S. G. Bishop, B. V. Shanabrook, and W. J. Moore, J. Appl. Phys. 56,1785 (1984).
[8] D. W. Fischer and P. W. Yu, J. Appl. Phys. 50, 1952 (1986).
[9] J. Wagner, M. Ramsteiner, and R. C. Newman, Solid State Commun. 64, 459 (1987).
[10] W. C. Mitchel, G. J. Brown, D. W. Fischer, P. W. Yu, and J. E. Lang, J. Appl. Phys. 62, 2320 (1987).
[11] B. V. Shanabrook, W. J. Moore, and S. G. Bishop, J. Appl. Phys. 59, 2535 (1986).
[12] B. V. Shanabrook, W. J. Moore, and S. G. Bishop, Phys. Rev. B 33, 5943 (1986).
[13] L. B. Ta, H. M. Hobgood, and R. N. Thomas, Appl. Phys. Lett. 41, 1091 (1982).
[14] P. Dansas, J. Appl. Phys. 58, 2212 (1985).
[15] D. E. Holmes, R. T. Chen, R. K. Elliott, C. G. Kirkpatrick, and P. W. Yu, IEEE Trans. Electron Devices ED-29, 1045 (1982).
[16] K. R. Elliott, D. E. Holmes, R. T. Chen, and C. G. Kirkpatrick, Appl. Phys. Lett. 40, 898 (1982).
[17] J. Lagowski, H. C. Gatos, C. H. Kang, M. Skowronski, K. Y. Ko, and D. G. Lin, Appl. Phys. Lett. 49, 892 (1986).
[18] G. A. Baraff and M. Schlüter, Phys. Rev. B 33, 7340 (1986).
[19] P. W. Yu, D. C. Look, and W. Ford, J. Appl. Phys. 62, 2960 (1987).

PHYSICAL REVIEW B VOLUME 39, NUMBER 8 15 MARCH 1989-I

Unification of the properties of the $EL2$ defect in GaAs

M. Hoinkis, E. R. Weber, and W. Walukiewicz
Center for Advanced Materials, Lawrence Berkeley Laboratory, Department of Materials Science, University of California, Berkeley, California 94720

J. Lagowski, M. Matsui, and H. C. Gatos
Massachusetts Institute of Technology, Cambridge, Massachusetts 02139

B. K. Meyer and J. M. Spaeth
Fachbereich Physik, University of Paderborn, Warburger Strasse 100a, 4790 Paderborn, Federal Republic of Germany

(Received 20 October 1988)

We provide experimental unification of the properties of $EL2$ in GaAs, linking the measurements of optical absorption, deep-level transient spectroscopy, electron paramagnetic resonance (EPR), magnetic circular dichroism (MCD), and optically detected electron-nuclear double resonance (ODENDOR). Results show that the $EL2$ defect has two energy levels, gives rise to the zero-phonon line in the neutral charge state, and gives rise to the EPR quadruplet, MCD, and ODENDOR signals in the singly ionized state. These manifestations disappear when $EL2$ is transferred to the metastable state. Any discussion of the properties of the $EL2$ defect must be consistent with these unified characteristics.

The midgap donor level $EL2$ in GaAs (Ref. 1) dominates the compensation mechanism in semi-insulating GaAs used for integrated circuits. This feature has generated an enormous practical interest in the $EL2$ defect. On the other hand, basic research has been attracted by the mystery of $EL2$ metastability which has been a driving force for many state-of-the-art theoretical calculations.[2-6] In a continuing search for the atomic structure of the $EL2$ defect in GaAs, models have been chosen considering at least one of the following $EL2$ features: (1) electronic levels, (2) optical transitions, (3) electron paramagnetic resonance signal (EPR), (4) magnetic circular dichroism (MCD) and connected with it optically detected electron-nuclear double resonance (ODENDOR) signals, and (5) the existence of normal and metastable states of the defect.

The total set of features mentioned above [(1)–(5)] should, in general, provide a unique means for linking experiment and theory. This has not become the common practice. Apparently conflicting interpretations of different experiments, many pitfalls and ambiguous results, combined with the equivocal character of the family of $EL2$-like defects,[7] and the family of paramagnetic arsenic antisite defects,[8,9] has generated uncertainty and raised a question as to which are the real features of the $EL2$ defect. As a result, many $EL2$ models are proposed considering only selected features while neglecting others.

Analysis of optical transitions, especially the 1.039 eV zero-phonon line (ZPL), provided the very first information on the tetrahedral symmetry of the occupied $EL2$ defect,[10] while a photo-EPR study linked ionized $EL2$ and the arsenic antisite EPR quadruplet signal.[11] The structurally most powerful MCD-detected ODENDOR technique identified a ⟨111⟩ distortion and C_{3v} symmetry of the paramagnetic state, and assigned the $EL2$ defect to the pair As_{Ga}-As_i.[8,12] The different $EL2$ defect symmetries, namely T_d and C_{3v}, as observed from the optical absorption ZPL and the combined MCD-ODENDOR technique, respectively, have generated the following questions. (1) Are these different experimental techniques probing the same defect? (2) What are the unified experimental features of the $EL2$ defect?

It is the intent of this work to provide the experimental evidence which unifies the properties of the $EL2$ defect as observed with optical absorption, EPR, deep-level transient spectroscopy (DLTS), and MCD-ODENDOR. However, it is not the intent of this work to assess the validity of previous conclusions, as to the exact microscopic structure of the $EL2$ defect, based on the interpretations of individual techniques reported previously.[8,10-12]

In 1987 we initiated a collaborative study designed to clarify existing uncertainties and verify relationships among the five features and their association with $EL2$. Preparation of special samples with properties tailored to the demands of different techniques was performed at MIT. The measurements of electronic levels and the zero-phonon absorption line were also made at MIT. An EPR and photo-EPR study, including quantitative determination of the spin concentration, was performed at the University of California, Berkeley, while MCD measurements were made at the University of Paderborn.

In undertaking the research, we realized the importance of the following experimental conditions: (a) the samples investigated should contain $EL2$ rather than other midgap levels occasionally present in melt-grown GaAs, (b) the concentration and the occupancy fraction must be varied and must be measured, (c) material incompatability between EPR and DLTS (which require high- and low-resistivity samples, respectively) must be overcome, and (d) the problem of the very low intensity of the EPR quadruplet in as-grown semi-insulating (SI) GaAs and the potential contributions from the family of arsenic

antisite-related defects had to be resolved for a reliable determination of the spin concentration and a comparison between absolute concentrations of EPR centers and the $EL2$ defect.

To satisfy these conditions we employed a series of n-type, p-type, and semi-insulating thermally treated GaAs crystals. These crystals were annealed at 1200 °C for 12 h in an equilibrium As-ambient followed by a rapid quench to room temperature and then reannealed between 700 and 1000 °C. The 1200 °C annealing-quenching procedure [also referred to as the inverted thermal conversion (ITC) treatment] produces GaAs virtually free of the $EL2$ defect.[13] Such crystals contain deep acceptorlike native defects frozen in during the quenching. Subsequent annealing eliminates native acceptors and leads to controlled formation of $EL2$ at a concentration dependent on the annealing temperature and time. The formation rate has a maximum at about 850 °C, roughly corresponding to 10^{14} cm^{-3} $EL2$ defects formed per second at the initial annealing stages.

Optical absorption experiments were performed with a dual beam spectrometer with a liquid-helium cold-finger cryostat allowing for variable temperature operation between 4 and 300 K. EPR measurements were carried out using an X-band spectrometer interfaced to a computer. The sample temperature was controlled and varied between 4 and 300 K with a helium-gas-flow cryostat. The apparatus had provisions for illumination of the sample in the cavity with either monochromatic or white light. The EPR quadruplet spin concentrations were determined by comparing the area under the microwave absorption curve (doubly integrated quadruplet) with the area under the microwave absorption curve of phosphorus-doped silicon samples with known phosphorus concentration. Signal intensity versus microwave power characteristics were performed to insure that saturation effects were negligible during spin-concentration determinations. MCD measurements were done at 1.6 K with a K-band computer controlled spectrometer; the experimental procedure is discussed in Refs. 8 and 12.

DLTS measurements on n-type GaAs samples which have been annealed at 1200 °C and rapidly quenched to room temperature and then reannealed at 800 °C for 1 h and rapidly quenched to room temperature (this annealing sequence is hereafter referred to as ITC+800) have shown that this thermal treatment produces only one midgap level with the electron emission rate $e_n(s^{-1}) = [T^2(3.53\times10^{-8})]\exp[-0.815(\text{eV})/kT]$ and a characteristic 1.039-eV zero-phonon line. The electron-capture cross section of $EL2$ is thermally activated with an activation energy of 66 meV, so that the energy level as measured by Hall effect is at $E_c - 0.75$ eV.[1] Both features are signatures of the true $EL2$ defect[7,10] in its filled, neutral charge state (i.e., $EL2^0$). DLTS measurements on similarly treated p-type GaAs showed that the $EL2$ formation was manifested by the formation of a trap at 0.54 eV above the valence band which corresponds to the second level of the $EL2$ defect.[7,11] Thus, the levels at $E_c - 0.75$ eV and $E_v + 0.54$ eV, respectively, seem to be the only levels of the $EL2$ defect in the GaAs energy gap.

In semi-insulating as-grown and ITC+800 GaAs samples, the EPR quadruplet and the MCD signal (previously assigned[12] to the As_{Ga}-As_i defect) were examined. Both features were measured in exactly the same as-grown and ITC+800 samples. Results are given in Table I. The relative intensities of the MCD and EPR signals indicate that both techniques are sensing one and the same defect. Detailed analysis of the MCD lines has shown that the strong signal in the ITC+800 samples corresponds to only one defect. No other MCD signals were found in this sample. We therefore infer that the EPR quadruplet signal in the ITC+800 samples examined in these studies does not contain any hidden components. This conclusion is very important since it eliminates ambiguities related to the "family of arsenic antisite defects" occasionally found in as-grown liquid-encapsulated Czochralski- (LEC) grown GaAs. As conclusively demonstrated below, the defect which gives rise to both the EPR quadruplet and the MCD signal in the samples employed in these investigations is the ionized charge state of $EL2$. Though there is no unambiguous experimental determination of the total charge states involved in the midgap level at $E_v + 0.75$ eV and the level at $E_v + 0.54$ eV, we follow common practice and call the filled midgap level $EL2^0$.

Quantitative measurements correlating the ZPL and EPR quadruplet were performed on a series of ITC+800 samples. The experimental approach was to obtain quantitative changes brought about by low-temperature optical illumination and recovery cycles, in both the EPR quadruplet concentration and optical absorption ZPL. The quantitative relationship between the ZPL and DLTS $EL2$ signal was previously demonstrated by Skowronski, Lagowski, and Gatos[14] using n-type GaAs. In n-type GaAs, all $EL2$ defects are occupied and are therefore neutral (i.e., $EL2^0$). This previous work thereby provided calibration for determining the $EL2^0$ concentrations from ZPL intensities in semi-insulating GaAs. Thus, high-resolution ZPL measurements performed on conducting as well as semi-insulating material were used as a common element linking $EL2$-related DLTS and EPR measurements. The ITC+800 samples were particularly suitable for quantitative correlations between the ZPL and the EPR quadruplet since they exhibited a high EPR quadruplet concentration before illumination with only a small ZPL absorption, while after illumination and recovery there was a small quadruplet concentration and a large ZPL. In other words, large changes in both the EPR quadruplet and ZPL absorption were brought about by the illumination and thermal recovery cycles. Special attention was placed on making the experimental conditions of EPR measurements (at Berkeley) and optical ab-

TABLE I. Comparison of MCD and EPR signal intensities measured on the same as-grown and ITC+800 GaAs samples.

Sample	Signal intensity (arbitrary units) MCD	EPR
As-grown	1	1
ITC+800°, 1 h	5	5

sorption measurements (at MIT) as similar as possible.

Quantitative results are given in Table II. They were also used to construct and plot the intensity of the EPR quadruplet signal versus the intensity of the ZPL. This plot shown in Fig. 1 demonstrates the one-to-one correlation between a decrease in spin concentration and an increase in the concentration of the neutral $EL2$. The data in Table II show that the correlation remains valid during the photoionization of $EL2$ (0.9-μm illumination), during the photopopulation of $EL2$ by photoexcitation of holes to the valence band (1.3-μm illumination), as well as upon recovery of $EL2$ from the metastable state. It is also seen that the transfer of $EL2$ to a metastable state (by white-light illumination) eliminates both the ZPL and EPR quadruplet, confirming that the metastable state is not paramagnetic and is not optically active. With the exception of steps (2) and (6), the concentration of the $EL2^0$ (determined from the ZPL) plus the EPR quadruplet concentration remains constant; $N_{EL2^0}+N_{\text{quad}} = (2.5 \pm 0.4)\times 10^{16}\ \text{cm}^{-3}$. The experimental uncertainty of $\pm 0.4\times 10^{16}\ \text{cm}^{-3}$ originates from uncertainties of about $2\times 10^{15}\ \text{cm}^{-3}$ for N_{EL2^0} and about 20% for the spin concentration.

The complementary behavior of the concentration of the EPR quadruplet and the $EL2^0$ concentration (determined from the ZPL) indicates that the entire EPR signal arises from the singly ionized charge state of $EL2$, i.e., $EL2^+$. There is, however, the possibility that a fraction of the EPR quadruplet in these ITC+800 samples arises from paramagnetic arsenic centers which do not exhibit typical $EL2$ properties as observed for instance in plastically deformed GaAs.[15] This possibility is most unlikely since both the EPR quadruplet and the ZPL are totally quenched upon white-light illumination, which is not the case in plastically deformed GaAs.[15] Furthermore, the relationship, $N_{EL2^0}+N_{\text{quad}} = 2.5\times 10^{16}\ \text{cm}^{-3}$ remains valid after $EL2$ is brought back out of the metastable state after warming to 150 K. Therefore, if such paramagnetic arsenic centers are present in these ITC+800 samples which are not $EL2$, they must therefore be optically quenchable and also return from the metastable state at 150 K along with the quadruplet signal component which is related with $EL2^+$. In consideration of these factors, we conclude that all of the quadruplet in the ITC+800 samples arises from only the $EL2^+$ defect.

Thus, the optical absorption ZPL and the DLTS $EL2$ signal had previously been quantitatively correlated by Skowronski, Lagowski, and Gatos.[14] In this work, the

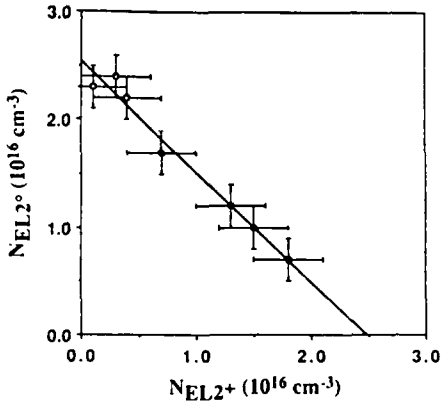

FIG. 1. The concentration of $EL2^0$, determined from the ZPL absorption coefficient, is plotted against the concentration of $EL2^+$, determined from the EPR quadruplet spin concentration.

TABLE II. Sequence of illumination and thermal recovery steps employed for quantitatively correlating the ZPL absorption coefficient with the EPR quadruplet concentration. The ZPL detects $EL2^0$ while the EPR quadruplet detects $EL2^+$. $\alpha_{\text{ZPL}} = 1.0\times 10^{-2}\ \text{cm}^{-1}$ corresponds to 0.9×10^{16}-cm^{-3} $EL2^0$ defects as determined previously (Ref. 13).

Sequence of experiment steps	Optical absorption 1.039-eV ZPL α_{ZPL} (10^{-2} cm^{-1})	Optical absorption 1.039-eV ZPL N_{EL2^0} (10^{16} cm^{-3})	EPR quadruplet N_{EL2^+} (10^{16} cm^{-3})	$N_{EL2^0}+N_{EL2^+}$ (10^{16} cm^{-3})
(1) Cooled from 300 K in the dark	0.75	0.7	1.8	2.5
(2) White-light illumination transfer to metastable state	0.0	0.0	0.0	· · ·
(3) 10-min recovery at 150 K transfer out of metastable state	1.9	1.7	0.7	2.4
(4) 30 min of 0.9-μm illumination $EL2$ photoionization	1.3	1.2	1.3	2.5
(5) 10-min recovery at 150 K	1.1	1.0	1.5	2.5
(6) White-light illumination transfer to metastable state	0.0	0.0	0.0	· · ·
(7) 10-min recovery at 150 K transfer out of metastable state	2.6	2.4	0.3	2.7
(8) Illumination with 2.5-μm light	2.4	2.2	0.4	2.6
(9) Illumination with 1.3-μm light	2.5	2.3	0.1	2.4

ZPL has been quantitatively correlated with the EPR quadruplet. In addition, the EPR quadruplet has been correlated with the MCD signal. This MCD signal is the identical signal which has previously been used in ODENDOR studies. The significance of these correlations is that they bridge together the experimental results of optical absorption, DLTS, EPR, MCD, and ODENDOR in regards to the $EL2$ defect in GaAs.

Based on these observations, the following unified view on $EL2$ properties can be deduced:

(1) The $EL2$ defect has two levels in the gap at $E_c-0.75$ eV and $E_v+0.54$ eV, respectively.

(2) The $EL2$ defect in the normal state has the following manifestations: a 1.039-eV ZPL, an EPR quadruplet (with the hyperfine splitting constant the same as that of the $As_{Ga}+$ signal reported previously[16]), and the MCD and ODENDOR signals described in Ref. 12. The ZPL corresponds to neutral $EL2$ (i.e., $EL2^0$), while the EPR quadruplet and the MCD signal originate from the ionized $EL2^+$ defect.

(3) None of the above features is observable when the $EL2$ defect is in the metastable state. It is probable that other defects in GaAs (such as antisite related defects) can have manifestations similar to some of the above features. We are, however, unaware of any other defect having all these manifestations.

At present there seems to be an important inconsistency in the unified $EL2$ properties. Namely, different $EL2$ manifestations indicate different symmetries. The ZPL implies tetrahedral symmetry[10,17] while ODENDOR clearly shows a trigonal symmetry.[12] This inconsistency may be an indication that the symmetries of $EL2$ in the neutral and ionized states are different. More difficult to reconcile is the discrepancy between the charge states of $EL2$ (0/+ for $E_c-0.75$ eV and +/++ for $E_v+0.54$ eV) and the presence of an arsenic interstitial as a constituent of the defect, for which the midgap level should be of +/++ double donor character.[2] Further studies, both experimental and theoretical, are evidently needed to solve the continuing $EL2$ puzzle.

M.H., E.R.W., and W.W. are supported by the Director, Office of Energy Research, Office of Basic Energy Sciences, Materials Science Division of the U.S. Department of Energy under Contract No. DE-AC03-76-SF00098. J.L., M.M., and H.C.G. are grateful to the U.S. Air Force Office of Scientific Research for financial support.

[1]G. M. Martin and S. Makram-Ebeid, in *Deep Centers in Semi-Conductors*, edited by S. T. Pantelides (Gordon and Breach, New York, 1986), p. 399.

[2]G. A. Baraff, M. Lannoo, and M. Schluter, Mater. Res. Soc. Symp. Proc. **104**, 375 (1988).

[3]G. A. Baraff and M. Schluter, Phys. Rev. Lett. **55**, 2340 (1985).

[4]C. Delevue, M. Lannoo, D. Stievenard, H. J. von Bardeleben, and J. C. Bourgoin, Phys. Rev. Lett. **59**, 2875 (1987).

[5]D. J. Chadi and K. J. Chang, Phys. Rev. Lett. **60**, 2187 (1988).

[6]J. Dabrowski and M. Scheffler, Phys. Rev. Lett. **60**, 2183 (1988).

[7]H. C. Gatos and J. Lagowski, Mater. Res. Soc. Symp. Proc. **46**, 153 (1985).

[8]J. M. Spaeth, A. Gorger, D. M. Hofmann, and B. K. Meyer, Mater. Res. Soc. Symp. Proc. **104**, 363 (1988).

[9]E. R. Weber and P. Omling, in *Festkörperprobleme: Advances in Solid State Physics*, edited by P. Grosse (Vieweg, Braunschweig, 1985), Vol. 25, p. 623.

[10]M. Kaminska, M. Skowronski, and W. Kuszko, Phys. Rev. Lett. **55**, 2204 (1985).

[11]E. R. Weber, H. Ennen, U. Kaufmann, J. Windscheif, J. Schneider, and T. Wosinski, J. Appl. Phys. **53**, 6140 (1982).

[12]B. K. Meyer, D. M. Hofmann, J. R. Niklas, and J. M. Spaeth, Phys. Rev. B **36**, 1332 (1987).

[13]J. Lagowski, H. C. Gatos, C. H. Kang, M. Skowronski, K. Y. Ko, and D. G. Lin, Appl. Phys. Lett. **49**, 892 (1986).

[14]M. Skowronski, J. Lagowski, and H. C. Gatos, J. Appl. Phys. **59**, 2451 (1986).

[15]P. Omling, E. R. Weber, and L. Samuelson, Phys. Rev. B **33**, 5880 (1986).

[16]R. J. Wagner, J. J. Krebs, G. H. Strauss, and A. M. White, Solid State Commun. **36**, 15 (1980).

[17]Tetrahedral symmetry has recently been confirmed by uniaxial stress ZPL measurements by K. Bergmann, P. Omling, L. Samuelson, and H. G. Grimmeis, in *Proceedings of the Fifth Conference on Semi-Insulating III-V Materials, Malmö, Sweden, 1988*, edited by G. Grossmann and L. Ledebo (Hilger, Bristol, 1988), p. 397.

Assessment of oxygen in gallium arsenide by infrared local vibrational mode spectroscopy

J. Schneider, B. Dischler, H. Seelewind, and P. M. Mooney[a)]
Fraunhofer-Institut für Angewandte Festkörperphysik, Eckerstrasse 4, D-7800 Freiburg, West Germany

J. Lagowski and M. Matsui[b)]
Massachusetts Institute of Technology, Cambridge, Massachusetts 02139

D. R. Beard and R. C. Newman
J. J. Thomson Physical Laboratory, University of Reading, Box 220, Whiteknights, Reading RG6 2AF, United Kingdom

(Received 15 November 1988; accepted for publication 5 February 1989)

Two infrared local vibrational mode (LVM) absorption lines occurring at 715 and 845 cm^{-1} shift to 679 and 802 cm^{-1} in gallium arsenide doped with ^{18}O, proving that the lines arise from the vibrations of oxygen impurities. The 715 cm^{-1} line exhibits a triplet $^{69,71}Ga$ isotope fine structure consistent with that expected from a quasi-substitutional V_{As}-O center. The 845 cm^{-1} line appears as a closely spaced doublet expected for a bonded interstitial oxygen atom.

The role of oxygen as a key impurity in semiconductor materials has been recognized since the earliest times and has stimulated an enormous volume of research. In silicon, work in the 1960s showed that there are two ways in which a single oxygen atom may be incoporated into the lattice:

(1) The stable, electrically inactive location is the interstitial site, in which the oxygen impurity forms bonds with two equivalent silicon neighbors, forming a localized Si_2O molecule, with a bond angle of $2\theta \approx 160°$. This defect is readily detected by its characteristic infrared local vibrational mode (LVM) spectrum, which has been investigated in great detail.[1]

(2) Substitutional, electrically active oxygen is created during fast particle irradiation, by the trapping of vacancies by interstitial oxygen atoms. The defect thus formed, (V-O), acts as a net acceptor, with a level at $E_c - 0.18$ eV, and is thermally stable only below 300 °C. It gives rise to a characteristic electron spin resonance spectrum in its $(V\text{-O})^-$ state ("A center")[2] and to a different infrared LVM spectrum.[3,4] In relation to the later discussion, it is important to note that the LVM frequency of the A center depends on its charge state[4]: $\tilde{\nu}(V\text{-}^{16}O)^0 = 835$ cm^{-1} while $\tilde{\nu}(V\text{-}^{16}O)^- = 885$ cm^{-1}, at 10 K. The LVM spectrum of the $(V\text{-O})^0$ defect can again be analyzed in terms of a localized Si_2O molecule, now having C_{2v} symmetry.

The role played by oxygen in III-V semiconductors has remained much less well understood over the decades, in spite of much effort. Oxygen in gallium phosphide is of course a notable exception: here, the strongly luminescent oxygen impurity occupies the substitutional P site, where it acts as deep donor, with a level at $E_c - 0.896$ eV, which can also bind a second electron.[5] However, there is also evidence from LVM spectroscopy[6] for the occurrence of interstitial oxygen or oxygen clusters in GaP.

Research related to the electrical activity of oxygen in gallium arsenide (GaAs) started quite early, after it was discovered that oxygen doping, under certain conditions, may render the material semi-insulating.[7] Below band gap near-infrared absorption studies[8,9] revealed the presence of deep impurity states in GaAs:O, but their microscopic structure remained unclear. More recently, it was shown by deep level transient spectroscopy (DLTS)[10] that GaAs grown in oxygen enriched ambients contains a midgap level with an activation energy for thermal emission of an electron of 825 meV, very close to that of the dominant midgap level EL2, with 815 meV. The first direct identification of an oxygen-related point defect in GaAs was reported by Akkerman *et al.*[11] It was found that oxygen (As_2O_3)-doped GaAs gives rise to a LVM absorption line at 836 cm^{-1} (300 K) while another line at 790 cm^{-1} was detected[1] in samples doped with ^{18}O-enriched As_2O_3. The closeness of the ratio of 790/836 = 0.9450 to the ratio $\sqrt{16/18} = 0.9428$ proves definitively that oxygen is the major constituent of the defect in question. Its detailed structure could not be determined at that time, but a bonded interstitial oxygen position is suggested for the defect because of the high frequency of the mode compared with those for known substitutional atoms such as ^{12}C(As) which has a frequency of only 582 cm^{-1} in spite of the lower atomic mass.[12]

Recently, Song *et al.*[13] and Zhong *et al.*[14] reported two new LVM absorption lines observed in high-resistivity GaAs grown either from melts contained in a quartz crucible or a quartz boat. The lines at 729 and 714 cm^{-1} were labeled A and B, respectively. Both lines showed a characteristic $^{69,71}Ga$ triplet isotope splitting, indicative of two equivalent gallium ligands nearest to the vibrating defect. Furthermore, below band gap *in situ* illumination of the samples led to photointerconversion processes $A \Leftrightarrow B$ at temperatures below 200 K, reminiscent of the similar characteristic behavior of the EL2 defect. However, the direct assignment of the A and B lines to EL2 has been questioned.[15] Instead, it has been suggested[14] that the defect causing the 729/714 cm^{-1} LVM lines should be identified with the analogous silicon A center.[2-4] Thus the defect would be an electrically active V_{As}-O pair, with the oxygen preferentially bound to two gallium ligands, forming a localized Ga_2O molecule with C_{2v} symmetry.

[a)] Permanent address: IBM T. J. Watson Research Center, Yorktown Heights, NY 10598.
[b)] Permanent address: Sumitomo Metal Mining, Tokyo, Japan.

 0003-6951/89/151442-03$01.00

In this letter we demonstrate the validity of this model, by reporting the ^{18}O-isotope shift of the B line. In addition, we have resolved a $^{69,71}Ga$ doublet isotope splitting of the 845 cm^{-1} LVM line, expected for interstitial oxygen in GaAs.

Two oxygen-doped samples of GaAs were used for our experiments. Sample No. 1 was grown by the horizontal Bridgman method from a quartz boat enclosed in a quartz ampoule filled with $^{18}O_2$ gas to a pressure of 240 Torr at room temperature. During the growth process the $^{18}O_2$ gas may become diluted with $^{16}O_2$ due to chemical interactions with the ampoule walls.[16] After completion of the growth, tne ampoule was water quenched to room temperature in order to minimize formation of oxide precipitates. Capacitance-voltage (C-V) measurements indicated that the crystal was n-type with $(N_D - N_A) = 1.6\times10^{16}\,cm^{-3}$ at 300 K. Deep level transient spectroscopy measurements showed an EL2 concentration of $1.2\times10^{16}\,cm^{-3}$. The defect labeled EL0 was not observed in this sample, indicating that the concentration was in the low $10^{15}\,cm^{-3}$ range. Sample No. 2 was grown by the liquid encapsulation Czochralski (LEC) method with the melt doped with Ga_2O_3 (not ^{18}O enriched).

Infrared absorption spectra were obtained with Fourier transform spectrometers (Bruker IFS-113v) with the samples at either 77 or 4.2 K. An overall spectrum for sample No. 1 is shown in Fig. 1. Four LVM absorption lines occur at 679, 715, 802, and 845 cm^{-1}. The broadband near 780 cm^{-1} arises from third-order lattice phonons of GaAs. In sample No. 2 (not enriched in ^{18}O) the lines at 679 and 802 were not observed. The expected frequency ratio $\nu(^{18}O)/\nu(^{16}O) \simeq \sqrt{16/18} = 0.943$ is observed for both the 679/715 and the 802/845 cm^{-1} pairs of lines. Thus, conclusive evidence is found that these four LVM lines are due to oxygen. This is an important result because the line at 715 cm^{-1} was initially claimed to be related to an arsenic interstitial, forming part of the EL2 center.[13] It should be added that line A [13,14] at 730 cm^{-1} was not observed in sample No. 1, even after photoexcitation similar to that reported in Ref. 13. The absorption at 715 and 679 cm^{-1} did not decrease and no new lines appeared.

Under higher resolution the much smaller frequency shifts caused by the $^{69,71}Ga$ ligand isotopes can be observed as shown in Fig. 2 for sample No. 2. The absorption near 715 cm^{-1} consists of three components each with a half-width of 0.18 cm^{-1} and a separation of 0.48 cm^{-1}. A similar triplet structure was observed from the line at 679 cm^{-1} due to ^{18}O. The absorption near 845 cm^{-1} consists of two components with a half-width of 0.30 cm^{-1} and a separation of 0.37 cm^{-1}. This is the first report of fine structure on the 802/845 cm^{-1} lines.

The fine structure occurs because for GaAs the natural isotopic abundances are $^{69}Ga(60.4\%)$, $^{71}Ga(39.6\%)$, and $^{75}As(100\%)$. For interstitial oxygen, which is bonded to one Ga and one As atom, there should be two components with intensities 40%:60%. This is indeed observed for the lines at 802 and 845 cm^{-1}, which supports the assignment. In the (V_{As}-O) pair, the oxygen is bonded to two equivalent Ga ligands, and the fine structure should have three equally spaced components with intensities 16%:48%:36% or 1.3:4:3. This is in good agreement with our observed fine structure of the lines at 679 and 715 cm^{-1} and also with the previously reported[13] fine structure for the lines at 715 and 730 cm^{-1}. (We have observed the 730 cm^{-1} triplet structure in a semi-insulating LEC crystal grown from a boron nitride crucible but have not so far observed optically induced interconversion with the 715 cm^{-1} line). Additional support for the assignments comes from the exact agreement between the observed line positions and those calculated from fitting parameters by the usual procedure.[3,4,17] For interstitial oxygen we find a substantial asymmetry in the force constants, i.e., $f(\text{As-O})/f(\text{Ga-O}) = 2.3$, which causes the relatively small overall splitting of the 845 cm^{-1} line (see Fig. 2).

To obtain an estimate of the concentration of the oxygen centers, we inserted the integrated absorption into the theoretical equation for infrared absorption[4]:

$$N = \frac{ncm}{2\pi^2\eta^2}\int \alpha d\omega. \qquad (1)$$

Here $n = 3.57$ is the refractive index of GaAs, c is the velocity of light, m is the oxygen mass, and η is the apparent charge. We obtain $N = 8.6\times10^{14}\,cm^{-3}$ for each of the inter-

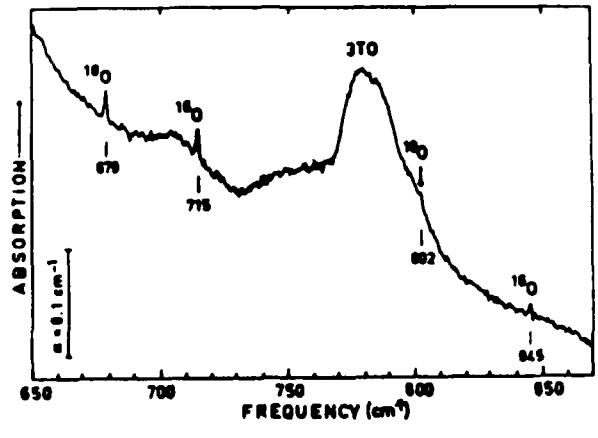

FIG. 1. LVM absorption spectrum (77 K) of the GaAs: $^{16,18}O$ sample No. 1. The broad peak near 780 cm^{-1} arises from intrinsic three-phonon absorption.

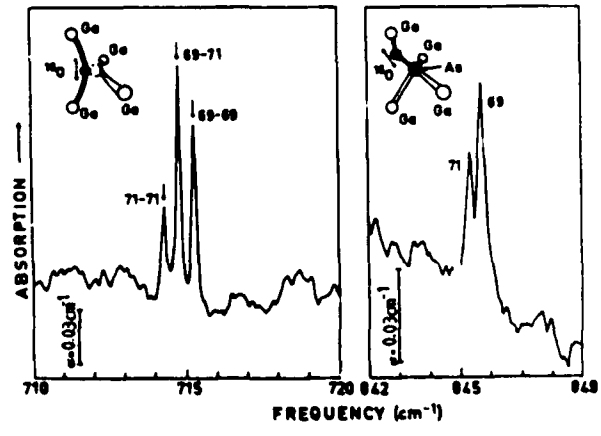

FIG. 2. Fine structure of the LVM absorption of the GaAs: ^{16}O sample No. 2, taken at 4.2 K with 0.1 cm^{-1} resolution. Suggested models, which explain the $^{69,71}Ga$ ligand isotope splittings are shown as inserts.

stitial $^{16,18}O$ bands and $N = 3.2 \times 10^{15}$ cm^{-3} for each of the (V_{As}-$^{16,18}O$) bands for sample No. 1, if we take $\eta = e_0$, as measured for other impurities in various crystals.[4] The equal amount of ^{16}O and ^{18}O is interesting in view of the doping mechanism, i.e., the sample contained as much ^{16}O derived from the SiO_2 container as ^{18}O from the enriched ambient gas. For sample No. 2, the concentrations are $N = 3.3 \times 10^{15}$ cm^{-3} for interstitial oxygen and $N = 6.1 \times 10^{15}$ cm^{-3} for (V_{As}-O). Thus the total oxygen content of $\simeq 10^{16}$ cm^{-3} would be greater than that measured previously for other crystals doped with Ga_2O_3. However a larger value of η, as found for oxygen in silicon, where $\eta = 3.8e_0$ for both the 9 μm band[18] and the 836 cm^{-1} LVM line from the O-V pair,[19,20] would reduce the estimated oxygen content by more than an order of magnitude. It is not possible to improve the precision of the estimate. Measurements of oxygen concentrations in the 10^{15} cm^{-3} range are difficult to make using secondary-ion mass spectroscopy (SIMS) and that is why we used charged particle activation analysis in our earlier work.[20]

Additional absorption measurements were made in the near-infrared region (4000–12 500 cm^{-1}, or 0.5–1.55 eV). Sample No. 1 was cooled in the dark to 10 K and a "dark" spectrum was taken. Then the EL2 absorption was bleached with an additional white-light source after which an "illuminated" spectrum was recorded. We observed a nonbleachable absorption spectrum with an onset at 0.75 eV and a steady increase up to the band edge. The difference between the two spectra was typical of the EL2 spectrum. From these measurements we derived[21] an EL2 concentration of $1.4 \pm 0.2 \times 10^{16}$ cm^{-3} in good agreement with the DLTS result for this sample, namely, 1.2×10^{16} cm^{-3}. The corresponding value for sample No. 2 was $1.0 \pm 0.2 \times 10^{16}$ cm^{-3}. The fact that the infrared absorption lines at 715 and 679 cm^{-1} do not respond to photoexcitation even though EL2 is photoexcited into the metastable state in these samples demonstrates that the oxygen defect is unrelated to EL2.

In summary, we have identified, for the first time, two types of oxygen-induced LVM absorption lines in GaAs. Their assignment to quasi-substitutional (V_{As}-O) oxygen and to interstitial oxygen is suggested, but further confirmation of the models is required. The electrical activity of the (V_{As}-O) center and the presumed electrical inactivity of the interstitial oxygen defect also remain to be investigated.

Technical assistance of B. Matthes (Freiburg) is gratefully acknowledged. J. L. and M. M. are indebted to the Air Force Office of Scientific Research for financial support D. R. B. and R. C. N. thank R. Murray (Reading) for helpful discussions and the Science and Engineering Research Council for financial support.

[1] D. R. Bosomworth, W. Hayes, A. R. L. Spray, and G. D. Watkins, Proc. R. Soc. London Ser. A 317, 133 (1970).
[2] G. D. Watkins and J. W. Corbett, Phys. Rev. 121, 1001 (1961).
[3] J. W. Corbett, G. D. Watkins, R. M. Chrenko, and R. S. McDonald, Phys. Rev. 121, 1015 (1961).
[4] R. C. Newman, *Infrared Studies of Crystal Defects* (Taylor & Francis, London, 1973).
[5] For a review on oxygen in GaP see: P. J. Dean, in *Deep Centers in Semiconductors*, edited by S. T. Pantelides (Gordon and Breach, New York, 1986), pp. 185–347.
[6] A. A. Barker, Jr., R. Berman, and H. W. Verleur, J. Phys. Chem. Solids 34, 123 (1973).
[7] C. H. Gooch, C. Hilsum, and B. R.Holeman, J. Appl. Phys. Suppl. 32, 2069 (1961).
[8] M. D. Sturge, Phys. Rev. 127, 768 (1962).
[9] A. L. Lin, E. Omelianovski, and R. H. Bube, J. Appl. Phys. 47, 1852 (1976).
[10] J. Lagowski, D. G. Lin, T. Aoyama, and H. C. Gatos, Appl. Phys. Lett. 44, 336 (1984).
[11] Z. L. Akkerman, L. A. Borisova, and A. F. Kravchenko, Sov. Phys. Semicond. 10, 590 (1976).
[12] R. C. Newman, F. Thompson, M. Hylands, and R. F. Peart, Solid State Commun. 10, 505 (1972).
[13] C. Song, W. Ge, D. Jiang, and C. Hsu, Appl. Phys. Lett. 50, 1666 (1987).
[14] X. Zhong, D. Jiang, W. Ge, and C. Song, Appl. Phys. Lett. 52, 628 (1988).
[15] U. V. Desnica, M. Skowronski, and C. Cretella, Appl. Phys. Lett. 52, 760 (1988).
[16] M. Kaminska, J. Lagowski, J. Parsey, K. Wada, and H. C. Gatos, Inst. Phys. Conf. Ser. No. 63, 197 (1981).
[17] B. Pajot and B. Cales, Mater. Res. Soc. Symp. Proc. 59, 39 (1986).
[18] Value of η derived from ASTM procedure F121-83 for oxygen in silicon.
[19] A. S. Oates and R. C. Newman, Appl. Phys. Lett. 49, 262 (1986).
[20] M. R. Brozel, J. B. Clegg, and R. C. Newman, J. Phys. D 11, 1331 (1978).
[21] G. M. Martin, Appl. Phys. Lett. 39, 747 (1981).

Gettering of donor impurities by V in GaAs and the growth of semi-insulating crystals

K. Y. Ko, J. Lagowski, and H. C. Gatos
Massachusetts Institute of Technology, Cambridge, Massachusetts 02139

(Received 8 May 1989; accepted for publication 19 June 1989)

Vanadium added to the GaAs melt getters shallow donor impurities (Si and S) and decreases their concentration in the grown crystals. This gettering is driven by chemical reactions in the melt rather than in the solid. Employing V gettering, we were able to grow reproducibly semi-insulating GaAs by horizontal Bridgman and liquid-encapsulated Czochralski techniques, although V did not introduce any midgap energy levels. The compensation mechanism in these crystals was controlled by the balance between the native midgap donor EL2 and residual shallow acceptors. Vanadium gettering contributed to the reduction of the concentration of shallow donors below the concentration of acceptors. The present findings clarify the long-standing controversy on the role of V in achieving semi-insulating GaAs.

I. INTRODUCTION

The use of vanadium for producing thermally stable semi-insulating (SI) GaAs was initiated several years ago.[1,2] It was suggested that vanadium introduced a midgap compensating level and that the diffusivity of V in GaAs was one order of magnitude lower than that of Cr. The latter characteristic of V was considered promising for limiting out-diffusion and improving GaAs device-processing characteristics. SI GaAs was indeed obtained with V doping by a variety of growth techniques[3–6] in different laboratories. However, in other laboratories V doping was shown to produce low-resistivity crystals.[7,8] Midgap energy levels originating from substitutional vanadium[1–3] or vanadium-related complexes[5,6] were proposed to explain the high resistivity of GaAs crystals grown by V doping. However, a direct identification of any V-related midgap level in GaAs was clearly lacking. Subsequent deep-level transient spectroscopy and optical absorption studies have established a substitutional vanadium acceptor level (V^{3+}/V^{2+}) at 0.15 eV below the conduction-band edge and a vanadium donor level (V^{4+}/V^{3+}) within the valence band.[9–12] No other vanadium-related levels were found within the GaAs energy gap. Since SI behavior arises from the compensation of shallow residual impurities by a midgap-level, the lack of a V-related midgap level raised questions concerning the role of V doping in the growth of SI GaAs.

In this paper we present experimental results and discuss a model of gettering of shallow donor impurities by V in the growth melt, which offers a new explanation of the role of V in achieving SI GaAs and involves no vanadium midgap levels. We show that V gettering helps to maintain the concentration of shallow donors below that of acceptors and facilitates the reproducible growth of high-resistivity crystals with a standard compensation mechanism based on the native midgap EL2 donor.

II. EXPERIMENTAL PROCEDURES

GaAs crystals doped with V were grown in our laboratory by the horizontal Bridgman (HB) and the liquid-encapsulated Czochralski (LEC) techniques. HB growth was carried out in quartz boats placed in quartz ampules employing the three-temperature-zone apparatus described in Ref. 13. Arsenic source temperature was kept at 617 ± 1 °C, which corresponds to the growth of stoichiometric GaAs. In LEC growths the crystals were pulled from stoichiometric melts enclosed in pyrolytic boron nitride (pBN) crucibles and encapsulated by an about 1-cm-thick layer of dry B_2O_3.

Vanadium doping was realized by adding ultrahigh-purity elemental V (99.9995%) to polycrystalline GaAs so that the initial V concentration in the growth melt ranged from 3×10^{19} to 3×10^{20} cm^{-3}. The V distribution coefficient in GaAs is very small (see Sec. III B); thus the vast majority of V atoms remain in the melt, and during growth the V concentration in the melt and in the solid increases. The enrichment of the melt with V leads to polycrystalline growth in the tail region of the ingots. Analysis of V-related properties was limited to the single-crystalline portions of the ingots (about 80% of the ingot for the highest initial V concentration).

Some of the V-doped crystals were intentionally co-doped with Si or Zn, in order to determine the efficiency of V gettering or to establish the range of conditions leading to the growth of SI GaAs. Reference V-free crystals were also grown employing otherwise the same growth conditions. All crystals used in the present study are listed in Table I.

Standard electrical characterizations included Hall-effect measurements in the van der Pauw configuration, Schottky barrier deep-level transient spectroscopy (DLTS), infrared optical absorption spectroscopy, and low-temperature (5-K) photoluminescence (PL) spectroscopy. Experimental apparatus and details of the approaches were the same as those described in our previous publications.[9–11] Compositional analysis by secondary-ion mass spectroscopy (SIMS) was performed by commercial laboratories.

The concentration of substitutional V in conducting n-type GaAs was determined from DLTS measurements of the V acceptor at 0.15 eV below the conduction-band edge. In high-resistivity crystals (whereby DLTS is not readily applicable) the optical method described in Ref. 11 was found especially valuable. This method relies on low-temperature (5-K) measurements of the V intracenter absorption after

 0021-8979/89/193309-08$02.40

TABLE I. Doping conditions of GaAs crystals.

Growth methods and crystal No.	Concentration of dopants in the melt (cm^{-3}) V	Si	Zn	Conductivity of grown crystal
HB-129	···	···	···	n;SC[a]
HB-123	3.5×10^{19}	···	···	n;SC
HB-133	7.3×10^{19}	···	···	n;SC
HB-138	5.0×10^{19}	1×10^{18}	···	n;SC
HB-139	5.0×10^{19}	1×10^{19}	···	n;SC
HB-140	···	1×10^{18}	···	n;SC
HB-141	···	1×10^{19}	···	n;SC
HB-142[b]	···	···	···	n;SC
HB-143	3.0×10^{19}	···	1×10^{16}	SI[c]
HB-144	3.0×10^{19}	···	2×10^{16}	SI
HB-145	···	···	1×10^{16}	n;SC
LEC-1	···	···	···	n;SC
LEC-2	1.0×10^{20}	···	···	SI
LEC-3	3.0×10^{20}	···	···	SI

[a]Semiconducting.
[b]Vanadium powder placed in the growth ampule outside the melt.
[c]Semi-insulating.

optical bleaching of the background EL2 absorption. Quantitative calibration makes possible the determination of V concentration and charge state in high-resistivity crystals from the $V^{2+}(3d^3)$ and the $V^{3+}(3d^2)$ intracenter absorptions.

III. EXPERIMENTAL RESULTS AND DISCUSSION

A. Vanadium gettering of donor impurities

Undoped GaAs grown by the HB method is typically n type. Silicon donors are the dominant impurities present at concentrations exceeding $10^{16}\,cm^{-3}$. Contamination with Si is due to the reaction of quartz material (the ampule and the boat) with Ga vapor:

$$[SiO_2]_{solid} + [2Ga]_{gas} \rightarrow [Ga_2O]_{gas} + [SiO]_{gas}. \quad (1)$$

SiO gas formed by this reaction supplies Si to the GaAs melt. The concentration of Si increases with increasing temperature of the SiO_2 and with increasing of the ratio of the free volume in the ampule to the volume of the GaAs melt; on the other hand, Si concentration decreases with increasing partial pressure of Ga_2O (addition of oxygen gas or oxides to the growth ampule.

Results of SIMS analysis of typical undoped and V-doped HB crystals are given in Table II. Both crystals were grown without the addition of oxygen. The undoped crystal exhibits a high Si concentration of about $8\times10^{16}\,cm^{-3}$ near the seed and $2\times10^{17}\,cm^{-3}$ near the tail. This behavior is consistent with the Si contamination process discussed above and Si distribution during the solidification. It is also seen from Table II that the addition of V to the growth melt decreased the Si concentration in the grown crystal significantly, i.e., to about 1×10^{16} and $4\times10^{15}\,cm^{-3}$ near the seed and the tail, respectively. The Si concentration in the V-doped crystal decreased from the seed to the tail in contrast to the Si behavior in a V-free crystal. Vanadium added to the growth melt decreased also the concentration of sulfur in GaAs crystals (see second column of Table II). It is thus apparent that V removes certain donor impurities during GaAs growth. This "vanadium gettering" has profound effects on the electrical properties of the resulting crystals.

TABLE II. The effect of V doping on Si and S concentration determined by SIMS.

Crystal		Impurity concentration (cm^{-3}) Si	S
Undoped			
HB-129	seed	8×10^{16}	1×10^{16}
	tail	2×10^{17}	2×10^{16}
V-doped			
HB-123	seed	1×10^{16}	3×10^{15}
	tail	4×10^{15}	7×10^{15}

B. Effects of vanadium on the free-carrier concentration and mobility

Results of Hall-effect measurements on HB GaAs crystals for different solidified fraction are given in Figs. 1 and 2. It is seen that V doping has two profound effects: (1) It decreases the free-electron concentration n by as much as $(5–8)\times10^{16}\,cm^{-3}$ (Fig. 1), and (2) it increases the electron mobility μ (Fig. 2).

The electron concentration in n-type semiconducting GaAs is defined as the difference between the total concentrations of ionized donors, N_D^+, and acceptors, N_A^-, $n = N_D^+ - N_A^-$. On the other hand, the electron mobility (free-carrier scattering by ionized impurities) increases as the sum $N_D^+ + N_A^-$ decreases. Thus the increase of n and decrease of μ requires that

$$(N_D^+ - N_A^-)\searrow \text{ and } (N_D^+ + N_A^-)\searrow. \quad (2)$$

This condition permits no interpretation other than a decrease in N_D^+, i.e., a decrease of the ionized donor concentration upon V doping. Gettering of shallow donor impurities Si and S is consistent with this conclusion.

The present results regarding V gettering may seem to be in conflict with the mobility decrease previously reported for V-doped LEC GaAs; that decrease was attributed to the

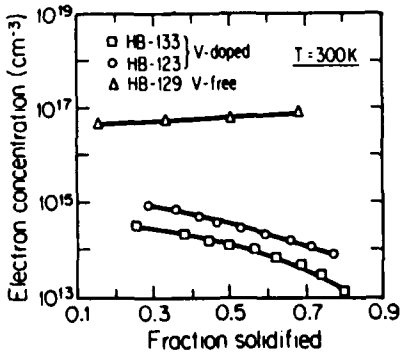

FIG. 1. Free-electron concentration along HB V-free and V-doped crystals.

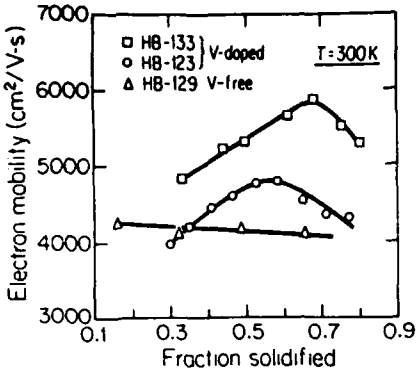

FIG. 2. Free-electron mobility of HB V-free and V-doped crystals.

ionized V acceptors at $E_c - 0.15$ eV.[9] The conflict is only an apparent one. In general, V may cause both effects; the relative magnitude of the gettering and the compensation of V acceptors depend on the donor concentration and the position of the Fermi level. The V-doped samples in Figs. 1 and 2 are from ingots HB-123 and HB-133 (see Table I). The distribution of the V acceptors in these crystals is shown in Fig. 3. The concentration of V acceptors is below about 1×10^{16} and 2×10^{16} cm^{-3}, respectively. An estimation of the occupation fraction of the V acceptors showed that only a fraction ($<20\%$) of the V acceptors were ionized. These values are small as compared to the decrease in electron concentration caused by V doping, i.e., $n = (5\text{–}8)\times10^{16}$ cm^{-3}. We can thus conclude that the role of the V acceptor in the results of Figs. 1 and 2 is insignificant.

The gettering effect of V is very similar to the established effects of oxygen on GaAs growth, i.e., the classic data on the effect of oxygen doping on the carrier concentration and carrier mobility. Figure 1 in Ref. 14 resembles the plot in Fig. 4. In both cases the electron concentration decreases and the mobility increases as a result of doping. A significant difference, however, should be pointed out between oxygen and V gettering: The reactions involving oxygen take place in the gas phase, while V gettering occurs in the GaAs melt. Vanadium in contact with the gas phase has an effect opposite to that of oxygen. In a series of experiments, V powder was placed on a small pBN tray in the quartz ampule beside

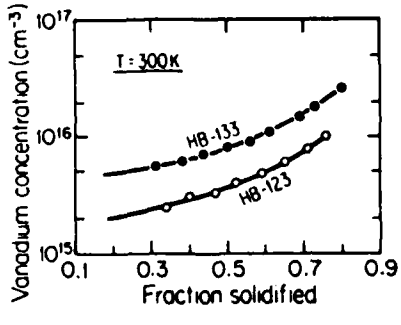

FIG. 3. Concentration of V acceptors along two HB V-doped crystals determined by the optical method described in Ref. 11. The effective segregation coefficient of V in GaAs determined from these curves is about 5.2×10^{-5}.

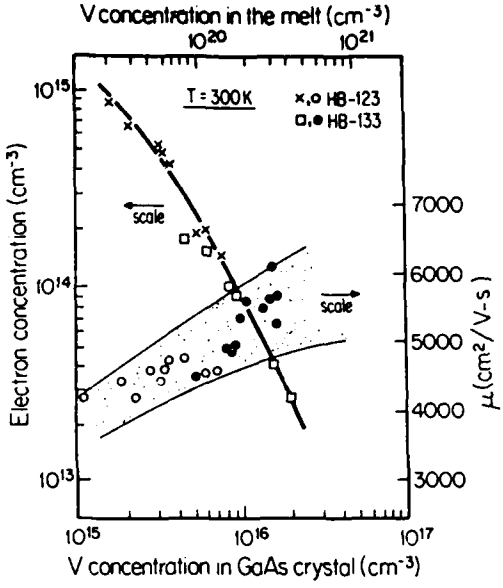

FIG. 4. Free-electron concentration and electron mobility as a function of V concentration.

the boat containing the GaAs charge. The Si concentration in the crystals was found to be greater that in the V-free crystals. Typical results are shown in Fig. 5. The enhancement of Si contamination can be explained in terms of reaction (1). Oxidation of the V powder reduces the partial pressure of Ga_2O in the growth ampule as follows:

$$[2V]_{\text{powder}} + [5Ga_2O]_{\text{gas}} \rightarrow [10Ga]_{\text{gas}} + [V_2O_5]_{\text{powder}} \cdot \quad (3)$$

Consequently, reaction (1) is driven from left to right. Mass spectroscopic analysis indeed revealed that the V powder after the growth process contained several per cents of oxygen.

The experiments with V powder were originally considered as conclusive in distinguishing between V interactions in the melt and in the gas phase. In a recent study,[15] however, we found that boron nitride can also promote Si contamination during HB growth. The contamination enhancement took place when boron was added to the GaAs melt. In experiments with V powder the pBN tray was not in contact with the melt, and thus chemical interactions involving bo-

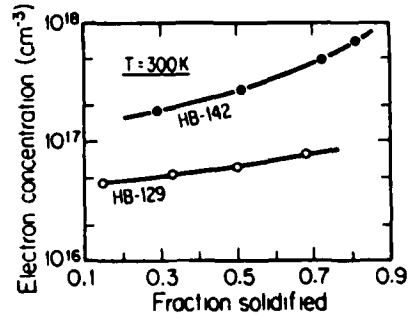

FIG. 5. Free-electron concentration in GaAs crystal HB-142 grown with V powder outside the boat in the growth ampule. Crystal HB-129 is V free.

ron nitride should be less effective. Still, it is possible that the contaminating effect of V powder contains a certain contribution from the pBN tray.

C. Effects of vanadium on heavily Si-doped crystals

Four crystals (HB-138, 139, 140, and 141 in Table I) were grown from the melt doped intentionally with Si at concentration $[Si]_{melt} = 1\times10^{18}$ cm^{-3} for HB-138 and 140, and $[Si]_{melt} = 1\times10^{19}$ cm^{-3} for HB-139 and 141. These concentrations exceed the contamination level brought about by the decomposition of the quartz ampule (reaction 1). For crystals HB-138 and 139 the melts were codoped with V in the same amount, while HB-140 and 141 served as V-free reference crystals. The electron concentrations versus fraction solidified of these crystals are shown in Fig. 6. The reference crystals exhibited a room-temperature electron concentration value of about 2×10^{17} cm^{-3} (HB-140) and 2×10^{18} cm^{-3} (HB-141) near the seed end and higher values toward the crystal tail. These results are in agreement with the "electron concentration segregation coefficient" in Si-doped GaAs ($k_{eff}^{(n)} n/[Si]_{melt}$), which for our typical growth condition is about 0.2.[13] As seen in Fig. 6, V added to the melt decreases appreciably the free-electron concentration in both crystals. [The relative decrease is about 5 for crystal HB-140, but it becomes smaller (1.5 to 2) for the crystal with higher Si doping.]

It is important to point out that the V acceptor concentration in crystals HB-138 and HB-139 was similar and ranged from about 3×10^{15} cm^{-3} near the seed to about 2×10^{16} cm^{-3} near the tail. These values are lower by an order of magnitude or more than the decrease in carrier concentration values. Thus V gettering clearly dominates over the compensation effect of V acceptors.

D. Effects of vanadium gettering on photoluminescence

Further evidence of the gettering of shallow donor impurities by V has been obtained from low-temperature photoluminescence (PL) measurements. Figure 7 presents the sub-band-gap 5-K PL spectra of the HB V-free and V-doped crystals. The broadband peaked at 1.18 eV originates from shallow donor impurity-vacancy complexes,[16] and it is present only in V-free crystals. A rough estimate of the band intensity normalized to the band-gap emission indicated at least one order of magnitude reduction of the defect concentration in comparison to the V-free crystal. A very similar effect has been reported for oxygen-doped GaAs,[17] whereby the 1.18-eV PL band was eliminated by the addition of oxygen to the HB growth ampule.

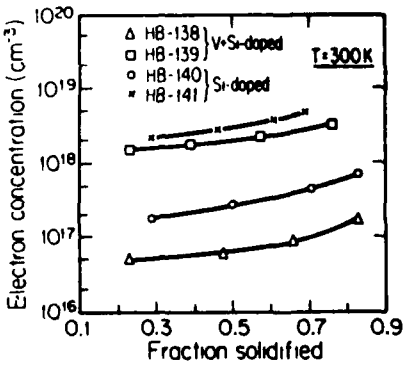

FIG. 6. Effects of V on heavily Si-doped crystals.

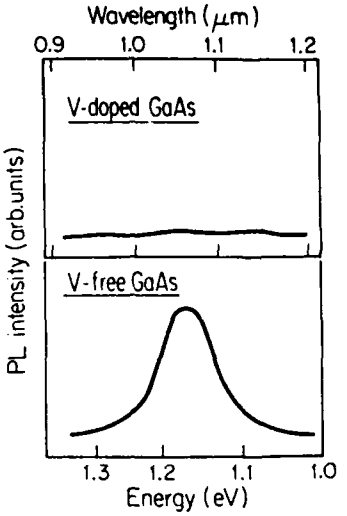

FIG. 7. Photoluminescence spectra at 5 K at around 1.18 eV for V-doped and V-free crystals. The broadband is due to donor-vacancy complexes.

E. Vanadium-doped semi-insulating GaAs

Undoped GaAs crystals grown in our HB apparatus were typically *n* type with a free-electron concentration in the mid-10^{16}-cm^{-3} range. Doping with V reduced this concentration to $\leqslant 10^{15}$ cm^{-3}. However, V doping alone was not sufficient to produce SI material with room-temperature resistivity exceeding 10^7 Ω cm and free-carrier concentration below 10^8 cm^{-3}. Crystals with such characteristics (HB-143 and 144), however, were obtained by doping simultaneously with V and Zn. The concentration of Zn required to obtain SI GaAs was about 10^{16} atoms/cm^3 in the melt. The corresponding concentration of zinc acceptors in the solid was in the low 10^{15}-cm^{-3} range, consistent with the Zn distribution coefficient of about 0.4.[18] This result is in agreement with the common consensus that the difficulty in growing SI GaAs by the HB method stems from a too high concentration of residual acceptors. Thus V doping reduces the concentration of residual donors to values below the concentration of zinc acceptors in these V + Zn doped crystals; compensation of these residual acceptors by EL2 leads to SI crystals.

SI LEC crystals (LEC-2 and 3) were reproducibly grown in our laboratory without the addition of Zn acceptors, but using V doping only. V was definitely helpful, since the V-free LEC-1 crystal (grown under identical conditions as V-doped LEC-2 and LEC-3) was *n*-type conducting. 5-K PL analysis identified Si as the major residual donor in this V-free crystal. The PL and far-infrared localized vibration-mode spectroscopy also revealed the presence of a carbon acceptor in all our LEC crystals at concentration exceeding 10^{15} cm^{-3}. Furthermore, a native 77-meV acceptor was also detected in the PL study. The presence of these acceptors

apparently eliminated the need for the acceptor codoping encountered in the case of HB GaAs.

IV. MODEL OF VANADIUM GETTERING

A. Basic relationships

The effects of V on the properties of GaAs are summarized in Table III. The first effect, i.e., the compensation of shallow donors, is well understood. It is due to the substitutional vanadium acceptor level (V^{3+}/V^{2+}) at 0.15 ± 0.01 eV below the bottom of the conduction band. Two other effects are reported here for the first time. They are indirect in the sense that they are related to V in the growth system rather than in the GaAs crystal. The enhancement of Si contamination by V powder contacting the ambient in the HB growth ampule has a plausible explanation by means of chemical reactions (1) and (3) which affect the decomposition of the quartz ampule. This phenomenon is somewhat similar to the enhancement of Si contamination by boron recently reported and studied in conjunction with problems in growing SI GaAs by the HB method using a pBN boat.[15]

The third vanadium effect listed in Table III is the most complex one. We discuss a possible explanation of this "vanadium gettering" in terms of a two-step process: (1) formation of the vanadium-silicon (or vanadium-sulfur) complexes in the melt, and (2) subsequent rejection of complexes to the melt at the solidification front. From the available data on the binary Si-V system we can expect the formation of V_3Si, V_5Si_3, and VSi_2 complexes[19–21]; in the presence of an S impurity, VS, V_2S_3, and VS_4 complexes can be expected.[22] For most V-doped crystals the initial V concentration in the melt was significantly larger (by at least two orders of magnitude) than the concentrations of Si and S. This fact has the following consequences: First, the V concentration in the melt can be treated as an independent variable changing during the growth according to normal freezing, and second, chemical reactions can be simplified by considering only V_3Si and VS prevalent under V-rich conditions. The growth melt will be approximated by a dilute solution containing Si, S, V, V_3Si, and VS at concentrations $X_{Si}, X_S \ldots$ (in units of mole fraction per cm^3) much lower than the concentration of the solvent molecules. The reactions in the melt are

$$3V + Si = V_3Si , \tag{4}$$

$$V + S = VS , \tag{5}$$

with the corresponding reaction constants

$$K_1 = X_{V,Si}/X_V^3 X_{Si} , \tag{6}$$

$$K_2 = X_{VS}/X_V X_S . \tag{7}$$

Mass conservation equations for V, Si, and S in the melt prior to solidification are

$$X_V^0 = X_V^* + 3X_{V,Si}^* + X_{VS}^* X_V^* , \tag{8}$$

$$X_{Si}^0 = X_{Si}^* + X^* V_{3Si} , \tag{9}$$

$$X_S^0 = X_S^* + X_{VS}^* , \tag{10}$$

where X^0 denotes the originally added quantities, while X^* denotes equilibrium quantities prior to growth. From Eqs. (6)–(9) it follows that

$$X_{Si}^* = X_{Si}^0/[1 + K_1(X_V^0)^3] , \tag{11}$$

$$X_S^* = X_S^0/(1 + K_2 X_V^0) . \tag{12}$$

Concentrations of silicon X_{Si} and sulfur X_S in the crystal near the seed end become

$$[X_{Si}]_{solid} \approx k_{Si}^{eff} X_{Si}^* = k_{Si}^{eff} \frac{X_{Si}^0}{1 + K_1(X_V^0)^3} , \tag{13}$$

$$[X_S]_{solid} \approx k_S^{eff} X_S^* = k_S^{eff} \frac{X_S^0}{1 + K_2 X_V^0} . \tag{14}$$

Since $[X]_{solid}$ for $X_V^0 = 0$ is greater than for $X_V^0 = 0$, it is evident that the model predicts a decrease of silicon and sulfur concentrations in the crystal as a result of the vanadium addition to the melt. The magnitude of the decrease depends on the V concentration and is described by the factors $1 + K_1(X_V^0)^3$ and $1 + K_2 X_V^0$ for Si and S, respectively. Extending formulas (13) and (14) to further stages of the solidification process, two extreme cases are considered.

In the first case we use an equilibrium approximation and assume that the concentrations of Si and S in the melt adjust during the solidification process in accord with reactions (4) and (5) and the conservation equations (8)–(10). With increasing fraction solidified f, the melt becomes enriched with vanadium $[X_V(f)]_{melt} \simeq X_V^0(1-f)^{-1}$. (Note that the vanadium segregation coefficient is much smaller than 1.) The concentrations of vanadium complexes increase, while the concentrations of isolated Si and S atoms decrease. This approximation yields

TABLE III. Effects of vanadium on properties of HB-GaAs.

Effect	Origin	Manifestations Concentration: Acceptor	Donor	Electron	Mobility
(1) Compensation	Energy levels of substitutional vanadium	increase	...	decrease	decrease
(2) Enhanced contamination	V reactions in gas phase	...	increase	increase	decrease
(3) Reduced contamination	V gettering in the melt	...	decrease	decrease	increase

$$[X_{Si}(f)]_{solid} \approx k_{Si}^{eff} \frac{X_{Si}^0}{1 + K_1 (X_V)^3}$$

$$= k_{Si}^{eff} \frac{X_{Si}^0}{1 + K_1 (X_V^0)^3 (1-f)^{-3}}, \quad (15)$$

$$[X_S(f)]_{solid} \approx k_S^{eff} \frac{X_S^0}{1 + K_2 X_V}$$

$$= k_S^{eff} \frac{X_S^0}{1 + K_2 X_V^0 (1-f)^{-1}}, \quad (16)$$

A second extreme case involves an assumption that an equilibrium state is reached only during thermal equilibration of the melt prior to the growth, but not during the growth itself. In this case the role of V is to reduce the initial concentrations of the isolated Si and S atoms in the melt (by engaging most of them in V complexes) to the values given by expressions (11) and (12). The impurity segregation of them during subsequent solidification leads to concentration profiles of the type

$$[X_{Si}(f)]_{solid} \approx k_{Si}^{eff} \frac{X_{Si}^0}{1 + K_1 (X_V^0)^3} (1-f)^{k_{Si}^{eff} - 1}, \quad (17)$$

$$[X_S(f)]_{solid} \approx k_S^{eff} \frac{X_S^0}{1 + K_2 X_V^0} (1-f)^{k_S^{eff} - 1}, \quad (18)$$

A distinctive difference between the two cases is that in the former one V gettering decreases the impurity concentrations and reverses the concentration profiles along the crystal, creating an illusion of segregation coefficients larger than one. In the latter case a decrease of the impurity concentrations takes place, but the profiles remain consistent with the true values of the segregation coefficients.

B. Comparison with experimental results

The most significant experimental result obtained for all V-doped crystals was a decrease in the Si and S concentrations in comparison to V-free crystals (effect No. 3 in Table III). The SIMS data for the seed portions of crystals HB-129 and HB-123 can be used for a rough estimation of K_1 and K_2 in expressions (13) and (14). 3.5×10^{19} cm^{-3} of V atoms added to the melt (corresponds to a value of $X_V^0 \approx 1.3\times10^{-4}$ cm^{-3}) caused an eightfold decrease in Si concentration (see Table II). This yields $1 + K_1(X_V^0)^3 = 8$ and $K_1 \approx 3.2\times10^{12}$ cm^9. A threefold decrease in S concentration of the same crystal gives $1 + K_2 X_V^0 = 3$, and $K^2 \approx 1.6\times10^4$ cm^3. These values should be treated as an order of magnitude estimate only. The uncertainty of SIMS measurements at low concentrations could be as much as a factor of 2. A reference to a "typical" undoped crystal also carries a risk of uncertainty which can be as high as 50%.

Using the above K_1 and K_2 values and expressions (15) and (16), we have calculated the concentrations of Si, S, and (Si + S) versus V concentration in V-doped crystals. The results are presented in Fig. 8. The Si concentration decreases very rapidly and reaches an asymptotic $N_{Si} \sim N_V^{-3}$ behavior as expected from the formation of V_3Si complexes. The decrease in sulfur concentration is much slower as dictated by the formation of VS complexes. It is of interest to note that the dependence of the total donor concentration $N_{Si} + N_S$ on V concentration resembles very much the experimental dependence of the electron concentration on V concentration shown in Fig. 4. An exact quantitative comparison between n and $N_{Si} + N_S$ of the present model is not possible because in GaAs with a low electron concentration range ($n \lesssim 10^{15}$ cm^{-3}) the change of n does not exactly follow the change in shallow donor concentration. The presence of deep acceptors (Cu and Fe), shallow acceptors (C), as well as trapping centers (EL2, EL4, and EL6) affects the free-electron concentration and creates some unknown parameters (such as compensation ratio) for a meaningful test of the model. However, the model does predict the general trend of free-electron concentration versus V concentration for V-doped crystals.

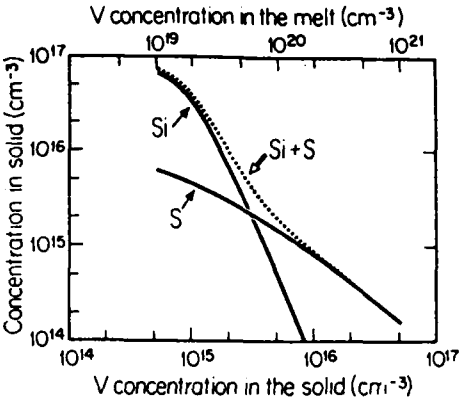

FIG. 8. Si, S, and Si + S concentrations vs V concentration calculated from Eqs. (15) and (16) of the gettering model.

The SIMS data in Table II indicate a decreasing Si concentration along the V-doped crystal. The same qualitative conclusion can be drawn from the electron concentration profile in Fig. 1. This characteristic profile is found in all V-doped crystals unintentionally codoped with Si. Its shape is consistent with the general shape of Si profile calculated from Eq. (15), which corresponds to the equilibrium approximation of the model [see Fig. 9 where results of Eqs. (15) and (16) are replotted versus the solidified fraction for

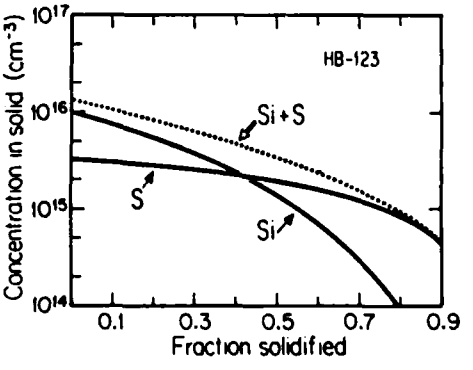

FIG. 9. Si, S, and Si + S concentrations vs V concentration vs fraction solidified calculated from Eqs. (15) and (16) using parameters corresponding to crystal HB-123.

crystal HB-123]. However, the model predicts a decreasing S concentration profile along the crystal, whereas SIMS data indicate that S concentration increases somewhat from the seed to the tail of the crystal. Nevertheless, the reduction in initial S concentration the melt is predicted correctly by the model.

A definite concentration increasing profile from seed to tail is found in intentionally Si-doped, V-free, and V-doped crystals. These profiles (see Fig. 6) are consistent with the normal freezing-type dependence [Eqs. (17) and (18)] and the effective segregation coefficient of 0.2. These results imply that for high Si concentration the V gettering is governed by the nonequilibrium condition rather than the equilibrium model.

It is of interest to note that in the nonequilibrium case the general expression of the type $[X_{Si}]_{solid} \sim G(1-f)^{k_{Si}^{eff}-1}$ (where G is a parameter with a value decreasing with V concentration added to the melt) remains valid even when the key simplifying assumptions of the model are not exactly satisfied. However, a deviation from V-rich condition and the formation of other complexes (V_5Si_3 and VSi_2) will invalidate the determination of the constant K_1. From expression (13) and the data of medium Si doping (crystals HB-138 and HB-140), we obtain $K_1 = 0.5\times10^{12}$ cm^9, while data for heavy Si doping (crystals HB-139 and HB-141) yield a still smaller value of $K_1 = 0.07\times10^{12}$ cm^9.

V. GROWTH OF SEMI-INSULATING GaAs

Vanadium gettering offers a straightforward explanation of the beneficial role of V doping in growing SI GaAs which eliminates the controversy associated with a lack of any midgap vanadium level. The presence of a midgap donor at concentration N_{DD} exceeding the difference between the net concentration of ionized acceptors and donors, $N_{DD} > (\Sigma N_A^- - \Sigma N_D^+)$, is a necessary condition for the growth of SI n-type GaAs.[23] In melt-grown GaAs the condition of having high N_{DD} is easy to satisfy owing to the omnipresent native EL2 donor with concentration exceeding 10^{16} cm^{-3}. However, the second condition required for SI material, i.e., $\Sigma N_A^- > \Sigma N_D^+$, cannot be satisfied that easily. Residual contamination with silicon donors often exceeds the concentration of acceptors, especially for HB GaAs growth in a silica boat placed in a silica ampule. Sulfur donors sometimes introduced from contaminated arsenic can also add to the problem. Improvement of the situation can be achieved by an increase in the acceptor concentration and/or a decrease of the residual donor concentration. The latter is realized via V gettering. In our HB growth experimentals 3.5×10^{19} cm^{-3} V atoms added to the GaAs melt were sufficient to reduce the donor concentration below the concentration of the codopant Zn acceptor (N_A^- at mid 10^{15} cm^{-3}) yielding SI GaAs. In our LEC experiments C impurity (concentration in the 10^{15} cm^{-3} range) and the native $E_V + 77$ meV acceptor played the role of residual acceptors so that the addition of V to the melt at concentration exceeding 10^{20} cm^{-3} consistently yielded SI material. Without V doping our LEC crystals were n-type semiconducting due to residual Si impurities.

Temperature dependence of the electrical resistivity in HB GaAs doped with V and Zn and in LEC-GaAs doped with V showed thermal activation energy of 0.78 eV. This result confirms our conclusion that the compensation mechanism in these SI V-doped crystals indeed involves the native midgap EL2 donor.[23]

VI. SUMMARY

In this work we have demonstrated the profound indirect role of V doping on the properties of melt-grown GaAs. The reduction of the concentration of Si and Si contaminants as well as the purification of melts intentionally doped with Si were correlated with the amount of added V. Electronic manifestations of these phenomena included a decrease of the free-electron concentration, an increase of electron mobility, elimination or suppression of the donor impurity-related luminescence band, and the successful reproducible growth of SI GaAs crystals using V doping. In the proposed model of V gettering, chemical interactions in the melt tie silicon (sulfur) and vanadium complexes which are not incorporated into the solid.

Vanadium gettering offered the first successful explanation of the controversial role of V in growing SI GaAs without any active involvement of V-related deep levels. According to the present results, the role of V is to decrease the shallow donor concentration below the acceptor concentration and therefore bring about the necessary condition for achieving SI GaAs with a compensation mechanism based on the native EL2 midgap donor omnipresent in melt-grown GaAs.

ACKNOWLEDGMENT

The authors are grateful to the U.S. Air Force Office of Scientific Research and to the National Aeronautics and Space Administration for financial support. We also thank Dr. A. M. Hennel and Dr. C. D. Brandt for all the fruitful discussions of the subject.

[1] W. Kutt, D. Bimberg, M. Maier, H. Krautle, F. Kohl, and E. Bauser, Appl. Phys. Lett. **44**, 1078 (1984).
[2] W. Kutt, D. Bimberg, M. Maier, H. Krautle, F. Kohl, and E. Tomzig, Appl. Phys. Lett. **46**, 489 (1985).
[3] A. V. Vasil'ev, G. K. Ippolitowa, E. M. Omel'yanovskii, and A. M. Ryskin, Sov. Phys. Semicond. **10**, 341 (1976).
[4] U. Kaufmann, H. Ennen, J. Schneider, R. Worner, J. Weber, and F. Kohl, Phys. Rev. B **25**, 5598 (1982).
[5] H. Terao, H. Sunakawa, K. Ohata, and H. Watanabe, in *Semi-Insulating III-V Materials*, Evian, 1982, edited by S. Makram-Ebeid and B. Tuck (Shiva, Nantwich, England, 1982), p. 54.
[6] M. Akiyama, Y. Karawada, and K. Kaminishi, J. Cryst. Growth **68**, 39 (1984).
[7] W. Ulrici, K. Friedland, L. Eaves, and D. P. Halliday, Phys. Status Solidi B **131**, 719 (1985).
[8] A. Mircea-Russel, G. M. Martin, and J. Lowther, Solid State Commun. **36**, 171 (1980).
[9] C. D. Brandt, A. M. Hennel, L. M. Pawlowicz, F. P. Dabkowski, J. Lagowski, and H. C. Gatos, Appl. Phys. Lett. **47**, 607 (1985).
[10] A. M. Hennel, C. D. Brandt, L. M. Pawlowicz, and K. Y. Ko, in *Semi-Insulating III-V Materials*, Hakone, 1986, edited by H. Kukimoto and S. Miyazawa (North-Holland/OHMSHA, Tokyo, Japan, 1986), p. 465.
[11] A. M. Hennel, C. D. Brandt, K. Y. Ko, J. Lagowski, and H. C. Gatos, J. Appl. Phys. **62**, 163 (1987).

[12]B. Clerjaud, C. Naud, B. Deveaud, B. Lambert, B. Plot-Chan, G. Bremond, C. Benjeddon, G. Guillot, and A. Nouailhat, J. Appl. Phys. **58**, 4207 (1985).
[13]J. M. Parsey, Y. Nanishi, J. Lagowski, and H. C. Gatos, J. Electrochem. Soc. **129**, 389 (1982).
[14]J. F. Woods and N. G. Ainslie, J. Appl. Phys. **34**, 1469 (1963).
[15]T. Kobayashi, J. Lagowski, and H. C. Gatos, in *Proceedings of 5th Conf. on Semi-Insulating III-V Materials, Malmo, Sweden, 1988* (Hilger, Bristol, England, 1989).
[16]E. M. Williams, Phys. Rev. **168**, 922 (1968).
[17]M. Kaminska, J. Lagowski, J. M. Parsey, K. Wada, and H. C. Gatos, Inst. Phys. Conf. Ser. **63**, 197 (1981).
[18]S. K. Ghandi, *VLSI Fabrication Principles* (Wiley, New York, 1983), Chap. 3.
[19]J. F. Smith, Bull. Alloy Phase Diagrams **6**, 266 (1985).
[20]H. Krautle, M.-A. Nicolet, and J. W. Mayer, J. Appl. Phys. **45**, 3304 (1974).
[21]K. N. Tu, J. F. Ziegler, and C. J. Kircher, Appl. Phys. Lett. **23**, 493 (1973).
[22]M. Hansen and K. Anderko, Eds., *Constitution of Binary Alloys*, 2nd ed., Metallurgy and Metallurgical Engineering Series (McGraw-Hill, New York, 1958).
[23]G. M. Martin, J. P. Farges, G. Jacob, and J. P. Hallais, J. Appl. Phys. **51**, 2840 (1980).